ISBN 978-82-471-1484-1 (printed ver.)
ISBN 978-82-471-1485-8 (electronic ver.)
ISSN 1503-8181

Silje Rodahl

Doctoral thesis

Doctoral theses at NTNU, 2009:55

Silje Rodahl

Adhesion of organic coatings on aluminium

NTNU
Norwegian University of
Science and Technology

Doctoral theses at NTNU, 2009:55

NTNU

NTNU
Norwegian University of
Science and Technology
Thesis for the degree of
Philosophiae Doctor
Faculty of Natural Sciences and Technology
Department of Materials Science and Engineering

NTNU
Norwegian University of
Science and Technology

Silje Rodahl

Adhesion of organic coatings on aluminium

Thesis for the degree of Philosophiae Doctor

Trondheim, March 2009

Norwegian University of Science and Technology
Faculty of Natural Sciences and Technology
Department of Materials Science and Engineering

NTNU
Norwegian University of
Science and Technology

NTNU
Norwegian University of Science and Technology

Thesis for the degree of Philosophiae Doctor

Faculty of Natural Sciences and Technology
Department of Materials Science and Engineering

ISBN 978-82-471-1484-1 (printed ver.)
ISBN 978-82-471-1485-8 (electronic ver.)
ISSN 1503-8181

IMT rapport 2009:108

Doctoral theses at NTNU, 2009:55

Printed by NTNU-trykk

Preface

The work presented in this thesis was carried out partly at the Department of Materials Science and Engineering, Norwegian University of Science and Technology, and partly at Sintef Materials and Chemistry. My work has been a part of the Light Metals Surface Science project, one program out of 8 in the national Norlight program (2000-2006). The financial support from this program (60% from the Norwegian Research Council and 40% from industrial companies) is gratefully acknowledged.

First of all I would like to thank my supervisors, Kemal Nisancioglu and Ole Øystein Knudsen, for their encouragement, assistance and supervising during these years. In addition I am forever grateful for the help of Geoff Scamans in the writing process.

The specimen preparation was performed at Sintef Materials and Chemistry and the assistance from John Erik Lein and Nils-Inge Nilsen was priceless. Without their know-how I would still whir around in the lab trying to prepare specimens properly.

The fatigue testing was performed at Hydro Aluminium Karmøy, where Roald Lilletvedt, Jan Tore Buvik Gundersen and Jan Bersaas assisted. The staff at Hydro helped out both with practical issues concerning my stay as well as on the experiments and all efforts is gratefully acknowledged.

The TEM work was performed by John Walmsley and Antonius van Helvoort at Sintef/NTNU. In addition to the work itself we had important sessions on how to interpret the data. Bjørn Steinar Tanem prepared the specimen prior to the investigations.

The XPS work was performed at the University of Surrey (UNIS), Guildford, England. In addition to the mad cow disease the village is known for its expertise in spectroscopy, by professor John Farnham Watts. He kindly allowed me to stay for 2 months, with unlimited use the XPS instrument. Steve Hinder and Marie-Laure Abel assisted in the practical issues on the lab. All staff and students at UNIS are gratefully acknowledged for making my stay as pleasant and amusing as possible and I want you to know I miss you all. The stay was financed by “NTH`s fond”.

Furthermore I would like to thank the staff at the Department of Materials Science and Engineering, especially Kjell Røkke and Martha Bjerknes, for their great support.

Finally, I would like to thank Johan, Ingeborg and Karoline for their patience with me and for their encouragement and support. Without you it would all be for nothing.

Silje Rodahl
February 2009

Summary

There is a strong increase in the use of coated aluminium alloys for construction, automotive, and transport applications. Outdoor conditions are demanding in terms of corrosion due to presence of chlorides, in addition to temperature and moisture variations. To maintain the visual appearance of a coated structure outdoors, both the coating adhesion and the corrosion resistance of the coated surface must be above a given level. Organic coatings have been successfully applied on aluminium alloys and have been used with success for outdoor applications. This is caused largely by improving the adhesion properties and corrosion resistance of the conversion coating layer used before the application of the organic coating. The conversion coating has traditionally been yellow chromating (Cr(VI)). The use of chromating has recently become restricted because of its toxicity, and this has led to the development of new chromate-free alternatives. With the exception of anodising, these alternatives have so far not proved to be as robust as chromating. The chromate-free pre-treatments has not provided the necessary adhesion or given the required protection against filiform corrosion (FFC) of the coated surface. Aluminium alloys with low copper content, if properly cleaned and etched, have shown adequate FFC resistance, although the adhesion properties in outdoor exposure have been questioned. In addition the reliability of the available test methods for assessing wet adhesion has been questioned.

Another issue, which has not been addressed in the literature, is the compatibility between the aluminium substrate, conversion coating and the organic coating. Since most organic coatings have been developed for the steel surface, which is stable in slightly alkaline environment, the applicability of these to aluminium, which is stable in slightly acidic environment, can be questioned. The success of chromating for the aluminium surface could be attributed to 1) the conversion of the naturally occurring oxide on aluminium alloys to an oxide which is more stable in alkaline environments, 2) active corrosion inhibition by the presence of Cr(VI) and 3) the hydration resistance in the oxide by the reduction product Cr(III).

The purpose of this work was, first of all, to evaluate the methods available for determining the wet adhesion properties of polymers on aluminium alloy substrates and modifying some of these for determining the wet

adhesion of organic coatings on aluminium. Another purpose was to investigate to what extent modification of the acidity of the organic coating could improve adhesion of organic coatings on aluminium, possibly without extensive chemical pre-treatment to convert the oxide.

Since the existing methods for determining adhesion of organic coatings on aluminium in humid environments were found to be inadequate, the successful fracture-mechanical methodology available for quantitatively assessing properties of adhesives on aluminium was investigated. In particular, the applicability of fracture mechanical wedge and fatigue tests, by use of double cantilever beam specimens, was studied. The tests were further used to study the durability of various pre-treatments and paint systems on extruded AA 6082-T6 aluminium alloy. Special attention was given to the compatibility of pre-treatment-paint combinations. In addition a filiform corrosion test was performed on the same coated substrates.

The wedge test, using static loading, appeared to be a reliable test to distinguish between the wet adhesion properties of different combinations of pre-treatments and paint. The Ti/Zr-treated samples suffered adhesive failure during the wedge test, and in combination with epoxy, they failed the criteria set for the corrosion test. The corrosion results for Ti/Zr pre-treated aluminium thus suggested that wet adhesion was important in controlling underfilm corrosion on pre-treated aluminium alloy surfaces. The hot AC-anodized surfaces gave good adhesion and corrosion resistance together with commercial polyester and epoxy coatings and displayed only cohesive failure, commonly regarded as acceptable adhesion. Data scatter, however, was a serious problem associated with the test and limited the information from fracture mechanical quantification of the result.

In the fatigue test the compliance of the sample was measured under cyclic loading, obtaining information about the crack growth rate as a function strain energy release rate (G). The failure mode was mainly cohesive in contrast to the wedge test results, which showed adhesive and cohesive failure modes for poor and good adhesion, respectively. Interpretation of the fatigue data was therefore not as straightforward as the wedge test data. Performance of the pre-treatments could not be distinguished statistically. The deoxidised specimen performed in a similar manner as chromated samples, which indicated that there was no effect of moisture in the test. The failure mechanisms measured by the two tests were fundamentally different. Further work is required to determine the significance of the

fatigue test for assessing wet adhesion properties of organic coatings on aluminium. The results from the two tests indicated, furthermore, that the use of chromate-free pre-treatments may require assessment of the compatibility of each combination of the modified aluminium surface and the applied organic coating. The compatibility testing will in turn require the availability of reliable test methods, taking into account specific exposure conditions of the coated product in service.

Improvement of existing commercial coating systems, possibly to an extent that substrate pre-treatment by use of conversion coatings can be eliminated in the future, requires a thorough understanding of the mechanisms concerning adhesion of coatings. Investigations by use of surface sensitive techniques are known to reveal composition and chemical state of the top monolayers of the fracture surfaces. Findings from Transmission Electron Microscope (TEM) and X-ray Photoelectron Spectroscopy (XPS) indicated that a layer of TiO_2 and ZrO_2 was incorporated in the naturally formed aluminium oxide. The mixed oxide improved adhesion to polyester coating observed in the adhesion test. TEM results revealed that both polymers entered deep into the anodised aluminium oxide structure. The enhanced adhesion properties of hot AC anodised specimens could thus be caused by stable oxide-coating bonds in addition to the mechanical interlocking effect.

The use of costly and often toxic pre-treatments could possibly be eliminated by use of strongly adhering organic coatings directly on the cleaned metal surface. The stability of aluminium oxide is enhanced in acidic aqueous environment. A more stable oxide would possibly cause bonds that are stronger and less vulnerable towards hydration. The use of a slightly acidic coating is suggested. The compatibility of a model polyester primid powder coating, pigmented with MoO_3, with a cleaned and etched AA 6082-T6 aluminium substrate, was thus investigated. Commercial polyester TGIC and epoxy DICY powder coatings were tested for comparison purposes. The pre-treatment was limited to alkaline degreasing and acidic etch. Wet adhesion properties of the coating were tested by use of a modified Boeing wedge test and the corrosion resistance was tested by use of EN 3665 filiform corrosion test. The adhesion properties of the MoO_3-pigmented coating were superior to the commercial coatings, whereas the corrosion properties were only slightly improved. It was thus demonstrated that organic coatings with improved compatibility with the

aluminium surface can be developed by introducing simple modifications to existing commercial coatings.

Contents

Preface

Summary

Contents

1. Introduction

1.1. Background

The use of a pre-treatment on a metal surface is considered necessary to maintain coating adhesion and corrosion protection in humid environments in service [1, 2]. In presence of moisture the naturally formed oxide on aluminium is believed to hydrate and swell leading to adhesive failure of the coating and eventually to filiform and underfilm corrosion attack in the presence of chloride in the environment [3-9]. A recent study of filiform corrosion on several copper-free rolled aluminium alloys concluded that proper cleaning of the surface before further chemical processing is likely to prevent filiform corrosion. However, the need for conversion coatings was emphasized especially for obtaining the necessary adhesion of the organic coatings for applications in humid environments [10].

Chromating, involving the use of chromium (VI) based chemicals, is the most commonly used conversion coating process for aluminium alloys on a world-wide basis. Chromating, which involves a short dip in a chromic acid bath, has been used extensively in the past, as it is a low cost and reliable method for adhesion promotion of organic coatings and corrosion protection [11-14]. However, chromating is becoming prohibited in many West European countries because of health and environmental hazards it poses in application and use [15]. No suitable alternatives has adequately been tested and approved by either the potential suppliers or users.

One alternative pre-treatment system for aluminium substrates is based on anodising. In the hot AC anodising process a thicker insulating anodic oxide is developed, combined with the selective removal of intermetallic particles from the surface of the substrate [16-19]. Anodising, however, is not suitable for small coating companies whose investment and expertise are based on chromating, which is based on dipping processes. Among many dipping alternatives, which have so far proved of limited success in practice, titanium and zirconium based conversion coatings offer potential replacement for chromates, especially in applications in which enhancement of the adhesion of coatings is of prime interest [20, 21].

Assessment of the adhesion properties of an organic coating on a metal substrate is not straightforward, especially in humid environments. Several tests already exist for adhesion measurement of coatings, but most of these are only suitable for the measurement of dry adhesion rather than the outdoor conditions experienced by a coated metal in service. Dry adhesion of coatings is commonly assessed by *e.g.* pull off test [22, 23] or scratch tests [22]. Under humid conditions water ingress in the coating causes degradation and swelling of the coating and hydration of the underlying pre-treatment layer, leading to a progressive loss of adhesion. There is a need to differentiate between the loss of adhesion and coating deterioration as a result of corrosion, for proper choice of organic coatings for aluminium alloys.

The compatibility of the organic coatings, which are essentially developed for steel, with the aluminium surface, can be questioned. In the absence of robust pre-treatment methods as alternative to chromating, the issue of the compatibility between the coating and substrate surface, which is not much discussed in the available scientific literature, has to be taken into consideration.

1.2. Objective and method

The primary objective of this work is to evaluate and compare methods that are suitable to assess adhesion of organic coatings on pre-treated aluminium substrates in humid environments and to be able to differentiate between potential pre-treatments considered as alternatives to chromates for the pre-treatment of aluminium.

The aluminium substrate tested in this work was extruded AlMgSi alloy AA 6082 – T6, and the organic coatings were commercial pigmented epoxy DICY and polyester TGIC powder coatings. The pre-treatments studied were commercial processes based on titanium and zirconium and hot AC anodising in sulphuric acid. For comparison a chromate based system and a simple cleaning process were used to provide reference surfaces. The adhesion tests selected were based on the Boeing wedge test [24-29] and fatigue test [26, 30, 31], both performed with double cantilever beam specimens [26, 29]. The tests are commonly used to quantify adhesion of adhesives. Filiform corrosion susceptibility of the coated surfaces was also tested by use of an accelerated standard test. In order to

find causes for the observed variations in adhesion properties of the coatings, the fracture surfaces were investigated post failure. The possibility of coating modification, in order to enhance adhesion of the coatings towards aluminium and/or chance of eliminating the pre-treatmentstep, was investigated by additions of molybdenum (VI) oxide into the coating formulation.

1.3. Structure of the thesis

Chapter 2 provides a literature survey to establish the existing knowledge at the outset of this work, along with a justification of the work in relation to this knowledge. Chapter 3 attempts to validate the Boeing wedge test procedure, originally developed for adhesive bonding [24-29], to evaluate adhesion of organic coatings on aluminium. Chapter 4 investigates the applicability of the fatigue test for adhesives [26, 30, 31] for the same purpose and compares the results to the wedge test in Chapter 3. Chapter 5 gives an investigation of the fracture surfaces from the results in Chapter 3, by use of surface analytical techniques. In Chapter 6 model coatings for improved adhesion, which are applied directly without conversion coatings, are tested by use of the method developed in Chapter 3. These chapters are followed by an overall discussion of the significance of the work and conclusions.

1.4. References

1. G. W. Critchlow and D. M. Brewis, *Int. J. of Adhesion and Adhesives*, **16**, p. 255 (1996).
2. S. M. Mirabedini, J. D. Scantlebury, G. E. Thompson and S. Moradian, *International Journal of Adhesion and Adhesives*, **25**, p. 484 (2005).
3. O. Ø. Knudsen, Bjørgum, A., Tanem, B.S., *ATB Metallurgie*, **43**, p. 175 (2003).
4. X. Zhou, G. E. Thompson and G. M. Scamans, *Corrosion Science*, **45**, p. 1767 (2003).
5. O. Negele and W. Funke, *Progress in Organic Coatings*, **28**, p. 285 (1996).
6. H. Leidheiser and W. Funke, *Journal of the Oil & Colour Chemists Association*, **70**, p. 121 (1987).
7. H. Leth-Olsen and K. Nisancioglu, *Corrosion Science*, **40**, p. 1179 (1998).
8. M. Stratmann, R. Feser and A. Leng, *Electrochimica Acta*, **39**, p. 1207 (1994).
9. J. Cognard, *International Journal of Adhesion and Adhesives*, **6**, p. 215 (1986).
10. A. Afseth, J. H. Nordlien, G. M. Scamans and K. Nisancioglu, *Corrosion Science*, **44**, p. 2491 (2002).

11. O. Lunder, J. C. Walmsley, P. Mack and K. Nisancioglu, *Corrosion Science*, **47**, p. 1604 (2005).
12. J. V. Kloet, W. Schmidt, A. W. Hassel and M. Stratmann, *Electrochimica Acta*, **49**, p. 1675 (2004).
13. J. Zhao, L. Xia, A. Sehgal, D. Lu, R. L. McCreery and G. S. Frankel, *Surface and Coatings Technology*, **140**, p. 51 (2001).
14. M. Kendig, S. Jeanjaquet, R. Addison and J. Waldrop, *Surface and Coatings Technology*, **140**, p. 58 (2001).
15. *Safety Data Sheet, Chromium (VI)*, in, Mallinckrodt Baker, Deventer, Netherlands (2007).
16. O. O. Knudsen, B. S. Tanem, A. Bjorgum, J. Mardalen and M. Hallenstvet, *Corrosion Science*, **46**, p. 2081 (2004).
17. A. Bjørgum, F. Lapique, J. Walmsley and K. Redford, *International Journal of Adhesion and Adhesives*, **23**, p. 401 (2003).
18. I. De Graeve, H. Terryn and G. E. Thompson, *Electrochimica Acta*, **52**, p. 1127 (2006).
19. B. B. Johnsen, F. Lapique and A. Bjorgum, *International Journal of Adhesion and Adhesives*, **24**, p. 153 (2004).
20. M. A. Smit, J. A. Hunter, J. D. B. Sharman, G. M. Scamans and J. M. Sykes, *Corrosion Science*, **46**, p. 1713 (2004).
21. O. Lunder, C. Simensen, Y. Yu and K. Nisancioglu, *Surface and Coatings Technology*, **184**, p. 278 (2004).
22. B. Tepe and B. Gunay, *Progress in Organic Coatings*, **62**, p. 134 (2008).
23. J. Marsh, J. D. Scantlebury and S. B. Lyon, *Corrosion Science*, **43**, p. 829 (2001).
24. (2008).
25. O. Ø. Knudsen, Rodahl, S., Lein, J.E., *ATB Metallurgie*, **45** (2006).
26. A. J. Kinloch, *Adhesion and Adhesives: Science and Technology*, Chapman and Hall, London (1990).
27. K. B. Armstrong, *International Journal of Adhesion and Adhesives*, **17**, p. 89 (1997).
28. J. P. Sargent, *International Journal of Adhesion and Adhesives*, **25**, p. 247 (2005).
29. J. Cognard, *The Journal of Adhesion*, **20**, p. 1 (1986).
30. M. M. Abou-Hamda, M. M. Megahed and M. M. I. Hammouda, *Engineering Fracture Mechanics*, **60**, p. 605 (1998).
31. M. W. Rushforth, P. Bowen, E. McAlpine, X. Zhou and G. E. Thompson, *Journal of Materials Processing Technology*, **153-154**, p. 359 (2004).

2. Adhesion of coatings on aluminium

The objective of this chapter is to review the available information about adhesion of organic coatings on aluminium alloys. The known mechanisms of adhesion and the methods used to evaluate adhesion of organic coatings are of particular interest. Furthermore the available work for understanding the effect of humidity on adhesion will be reviewed. Since the aluminium surface is usually pre-treated [1, 2], the effect of pre-treatment on adhesion will be specifically considered. As the properties of the organic coating itself are also of interest from the standpoint of investigating the compatibility of the coating with the pre-treated aluminium surface, the properties of organic coatings with emphasis on adhesion promotion is also included.

Adhesion between an organic coating and an aluminium surface is determined by chemical bonding, mechanical interlocking, electrostatic forces and interdiffusion [3, 4]. Chemical bonds are classified as the primary bonds between the metal surface and organic coating. Adsorption is an important step for chemical bonding to occur. Secondary bonds are due to van der Waals forces, dipole-dipole interactions and hydrogen bonds [5]. The primary bonds can be ionic or covalent and the binding energies of these bonds are about an order of magnitude higher than those of the secondary bonds [3, 5]. However, the secondary bonds are regarded as more important than the primary bonds in determining the adhesion of paint on a metal surface [6-8], even though these bonds break easily during exposure to moisture. Epoxy coatings are only capable of producing hydrogen bonds with hydrated aluminium oxide [9] and rely on additions of functional groups that provide stronger bonds. Some functional groups like phosphonates show evidence of acid-base interactions with hydrated oxides [8]. Evidence of primary bonds have been found for monolayers of carboxyl (–COOH) groups [10] and silanes incorporated in the organic coating [11].

In the presence of moisture in the environment, water will penetrate the coating through defects and by diffusion [4, 12-14], causing plasticization [6] and swelling [14] of the coating and disruption of secondary bonds at the coating-metal interface [4, 13]. These processes are reversible, in contrast to the irreversible processes of hydrolysis and cracking. In addition, the aluminium surface can irreversibly be damaged by hydration

and eventually by corrosion [4, 13, 15] as a result of water reaching the coating-metal interface. The processes can be interrelated, e.g., defects in the coating are typical sites for initiation of filiform corrosion [16-21]. Clearly, filiform corrosion is a cause of loss of adhesion. However, loss of adhesion can also occur in a humid environment in the absence of corrosion. A comprehensive investigation of filiform corrosion on architectural alloys without appreciable Cu content concluded that a proper cleaning of the alloy surface prevents filiform corrosion without the need for conversion coatings [22]. However, the use of conversion coatings is still deemed necessary for adhesion promotion [6].

2.1. Pre-treatment of aluminium alloys

Pre-treatment of aluminium is essentially a cleaning and conversion process designed to prepare the surface for bonding with an organic coating. The adhesion of the coating must then be maintained through all subsequent processing of the material and under extended service even in relatively extreme exposure conditions. In view of the indicated importance of pre-treatment to prevent filiform corrosion and enhance adhesion of organic coatings, the most common commercial pre-treatment methods for aluminium, along with their reported properties, deserve summarizing.

Pre-treatment includes one or more of the steps degreasing, etching and application of conversion coating. The first and/or the second step are essential for cleaning the surface from lubricants and grease remaining on the surface from thermo-mechanical processing of the alloy [18, 22]. Degreasing usually involves alkaline degreasing [23, 24] and this is often followed by a light acid etch for de-smutting and removal of any thermal oxides formed during thermo-mechanical processing [18, 22]. A deeper etch is required to remove nano-crystalline deformed layers, formed by hot rolling, grinding or machining [18, 22, 25, 26]. These active layers can promote rapid corrosion of aluminium surfaces due to their fine grain size and the content of cathodic particles, which are known to cause microgalvanic coupling. The layer should be removed to prevent filiform corrosion [17, 18, 22, 27, 28].

Conversion coatings for aluminium have traditionally consisted of chromate containing processes such as chromic acid anodising [29] and chromate dipping process [30-32]. Most chromate-free conversion

coatings, with the possible exception of anodizing [1, 33-35], has been considered to be inferior to chromating in terms of robustness and durability [2, 19, 36] based on severely accelerated corrosion tests. Pre-treatments such as chromating and anodising are known to enhance the coating performance in wet environment by increasing the resistance of the surface to hydration [21, 37].

There is some suggestion that non-chromate based pre-treatments may be less effective with the same broad range of alloy types and organic coatings that have been successfully used with chromate based systems. It is becoming apparent that the performance of the new chromate-free conversion coatings depends on the type of alloy and organic coating used [19, 38, 39], suggesting the specificity of the alloy, pre-treatment and coating combination. AA6xxx series alloys are known to activate during grinding and paint baking [40], mainly caused by segregation of alloying elements towards the surface and nucleation and growth of the precipitates in the surface layers. High Mn, Mg, Cu and Cr content in aluminium alloys contribute to the formation of electrochemically active dispersoids in the surface layers [40-42]. Copper is known to cause filiform corrosion, but with proper surface cleaning and passivation the coated aluminium should not be affected by a limited copper content [40].

Magnesium is commonly added to increase the strength of Al alloys. Mg is observed to be depleted in the outer part of the oxide films, but somewhat enhanced near the oxide-metal interface [43]. Magnesium oxides are alkaline and can therefore destabilise aluminium oxide, which is amphoteric. Adhesion problems can in general be related to the various types of oxides present in the surface, in addition to a lateral inhomogeneity of the oxides [44].

2.1.1. Chromate conversion coatings (CCC)

Chromating has been the most frequently used conversion coating on aluminium. However, it is in the process of being phased out in many countries because of its toxicity. As reviewed in detail elsewhere [30, 32, 45, 46], the process converts the original aluminium oxide into a mixed oxide consisting of a hydrophobic layer of Cr(III) oxide [31, 45], unreduced Cr(VI) oxide species, along with aluminium oxide.

The layer protects the matrix against chloride attack by a self healing mechanism. Self healing is commonly mentioned as one of the main

advantages of CCC, resulting from the reduction of the remaining Cr(VI) into Cr(III) [47] and thereby protecting against corrosion by repairing the conversion layer [31, 45]. In addition, the iron containing, cathodic intermetallic particles are coated by a thin layer of chrome-oxide, which reduces their local cathodic activity [45, 47, 48]. The beneficial action of chromate may also include improved adhesion with organic coatings caused by increased resistance to hydration [37] by the presence of Cr (III) oxide.

2.1.2. Titanium and zirconium based chemical conversion coatings

Conversion coatings based on the use of titanium and zirconium fluoroacids were originally developed for steel substrates but were found to provide good results with aluminium as a promising alternative to chromating [49-51]. These treatments lead to deposition of titanium and/or zirconium oxides on the alloy surface and at cathodic intermetallic particles [52, 53]. This process is enhanced by higher pH forming on these particles as a result of oxygen reduction and hydrogen evolution [51, 52]. However, electrochemical tests have shown that the Ti/Zr layer did not reduce the rate of reduction processes on the intermetallic particles [52]. For this reason it was suggested that these conversion coatings may be effective in enhancing adhesion rather than corrosion inhibition at cathodic sites [2].

Oxide layers deposited by coating in sol-gel treatment have improved the corrosion resistance of aluminium alloys. The utilisation of ZrO_2 in thin coating sol-gel treatment on aluminium has shown both promising barrier properties and adhesion enhancement [54]. Zr has been found to improve resistance against hydration and enhance adhesion due to formation of stable bonds [55]. Similarly, improved adhesion of epoxy coatings on aluminium by use of silanes was attributed to their resistance against hydration [56].

2.1.3. Anodising

Anodising is a method where a relatively thick, porous aluminium oxide film is grown on the metal surface by applying a voltage in an acidic electrolyte. Anodising can be carried out under DC (direct current) or AC (alternating current) conditions. DC anodising is well known for providing corrosion protection to aluminium alloy substrates [57, 58]. However, the DC method requires long processing time. AC anodising is in general faster. The hot-AC process cleans the surface simultaneous to porous film

formation, which makes separate degreasing unnecessary [33, 48, 59]. The Fe-rich intermetallic particles are also claimed to be removed [33], and this is attributed to increased corrosion resistance of the coated surface.

Anodising can be carried out in phosphoric acid (PAA), chromic acid (CAA) or sulphuric acid (SAA). For PAA, phosphate is incorporated and improves the oxide resistance to hydration [60]. Chromic acid anodising (CAA) produces a thick and more corrosion resistant oxide and the oxide strength is improved compared to PAA [60]. Sulphuric acid is the most widely used electrolyte, due to the low cost and reduced environmental hazard, even though the resistance towards hydration is lower compared to *e.g*. PAA. For adhesive bonding applications all these anodising systems are used and improved adhesion is obtained [60]. The pore size of the anodised layer depends on the type of acid used. Enhanced penetration of an organic coating into the porous structure is beneficial for the adhesion properties [37].

Hot AC anodising uses warm phosphoric or sulphuric acids (about 80°C) which result in softer, more ductile oxide layers compared to the low temperature processes [48]. Hot AC anodising is commonly used for coil coating applications due to the short anodising time [33, 48, 59]. Hot AC anodising produces a thin porous oxide of approximately 0.5 to 1 μm thickness, which is a result of the balance between simultaneous oxide production and dissolution in the anodising electrolyte [33]. The level of corrosion protection and the adhesion provided by a hot AC anodised surface has been found to be similar to a chromated surface [33, 57, 61]. Combined with the short process time and the use of inexpensive and environmentally benign anodising bath, normally sulphuric acid, hot AC anodising stands out as an interesting pre-treatment process for chromium replacement.

Anodising technology for aluminium is well-understood, and process developments are related to control of process parameters and exploiting the technology for innovative applications [62], such as by incorporating ions, e.g. molybdate [63, 64], or organic components [65] for corrosion resistance and low friction surfaces, respectively.

2.1. Organic coatings

Organic coating on a metal functions as a barrier against transport of aggressive species to the metal surface and thereby protects the metal against corrosion [66]. The properties of the coating-metal interface are closely tied to the barrier properties [66]. This means that good adhesion in humid environment is a desired property of an effective barrier coating.

The following subsections are meant as elementary background information about the major components of organic coatings; the binder, pigments, additives and solvents. These may contribute to the properties of organic coatings in different ways, which are relevant to this thesis, such as barrier, adhesion and corrosion properties.

2.2.1. Binder

The binder is the polymer, which constitutes the continuous phase and thereby the main body of the coating after it is applied on the metal surface and dried or cured. This is the material which forms the barrier seal on the surface [67, 68]. A solvent is usually present as the diluting agent that enables the coating to be applied uniformly to the surface. Cross linking of the binder reduces permeability of the coating, but too much cross linking may result in internal stresses and brittle coatings.

The most important commercial binders are alkyds, polyesters, epoxies and acrylics [67]. Alkyds are a type of polyester based on oils, fatty acids or alcohols. The main components are normally hydroxyl or carboxyl functional groups [69]. Epoxy resins contain the epoxide or oxirane group shown in Figure 2. The polymerisation reaction of the oxirane group occurs typically by ring opening and formation of new bonds by elimination of water.

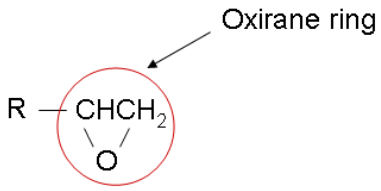

Figure 2. The oxirane group

Another important component of the epoxies is bisphenol-A, shown in Figure 3. This component, containing two functional –OH groups, is also part of many other compounds such as plasticizers and polyesters. The –OH groups at the ends of the bisphenol A molecule is involved in the polymerisation reaction, producing long chains of polymer compounds.

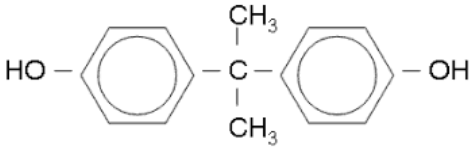

Bisphenol A

Figure 3. Bisphenol A.

Epoxy coatings are used for industrial applications due to their excellent general resistance to degradation. Epoxies are known to degrade if exposed to ultraviolet light and this results in the so-called chalking phenomenon [67, 69]. Pigmenting with TiO_2 (anastase) will prevent this.

The polyester based coatings have relatively low resistance to chemical attack compared to epoxy based formulations [69, 70]. Polyester coatings consist of polymers with an ester functional group in the main chain. Esters consist of an acid where at least one –OH group is replaced by an alkoxy group, illustrated in Figure 4.

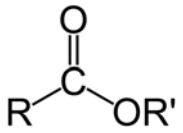

Figure 4. The alkoxy group where R and R` represent organic chains.

Esters hydrolyse and break down when exposed to moisture, becoming carboxylic acids.

Polyester coatings consist of large and branched esters, typically formed by esterification of glycerol (propane-1,2,3-triol). The curing reaction, which links the short polyester molecule with an alcohol monomer, forming long and branched 3D structures, is commonly performed by elimination of a water molecule [67] in a manner similar to that shown in Figure 2.

2.2.2. Pigment

Pigments are the discontinuous phase [67, 68] classified either as the primary pigment, which determines the visual appearance, or as fillers. Primary pigments, which can be organic or inorganic, provide opacity, colour, and anti-corrosion properties. Fillers are used for opacity and for enhancement of the mechanical properties of the coating. Fillers are generally low cost materials such as TiO_2, $BaSO_4$ and $CaCO_3$.

The pigment volume concentration, PVC, is the total volume of all pigments and fillers in the dry coating. There are upper limits for the amount of pigment that can be added to a coating, named the critical PVC [67, 68]. Too high PVC results in a porous coating with poor cohesion strength and high permeation of water and ionic species [71].

The most common white pigment in use is titanium dioxide (TiO_2). The high refractive rutile form is most commonly used, and the effect is increased opacity in addition to white colour [67]. Some of the primary pigments, such as lead chromate and other chromate containing pigments, are toxic [67]. These pigments are now replaced by less toxic ones, such as phosphates, phosphites, silicates and oxides. The beneficial effect of these pigments is mainly in their barrier capability [72] and not active corrosion inhibition [66], which is the case for *e.g* chromate containing pigments.

2.2.3. Additives

Paint additives are necessary to modify the coatings properties such as gloss, rheology, tixotrophy, adhesion, viscosity, refraction, bleeding, texture, hiding power, impact strength, and shelf life. In addition the additives limits development of defects such as pin-holes and pores [66, 68]. Benzoin is a commonly used example of an additive that prevents pore formation in powder coatings [73, 74]. Benzoin oxidises to form benzil, which is yellow [73].

2.2.4. Powder coatings

Solvents are often toxic and flammable and the use of powder coatings is beneficial since solvents are avoided. In addition excess powder can be re-used, which saves costs and waste management [67, 69].

Most powders are produced by melt mix of solid coating components by dispersing the pigments and other insoluble components, with subsequent pulverising of the formulation [75, 76]. The powder is applied by electrostatic spray or in a fluidised bed [76]. The powder is charged and attracted to the grounded sample. Curing by baking is performed immediately after powder application.

Epoxy compositions are based on bisphenol A resins cured with amines such as the dicyandiamide (DICY). Polyester powder coatings can be hydroxy functional, *i.e.*, water is released during curing by using melamine/formaldehyde curing agents. Polyesters can also be formulated from acidic polyesters cured with added epoxy resin or triglycidyl isocyanurate (TGIC). Polyester TGIC is known for its excellent durability and colour stability [67]. The DICY and TGIC molecules are shown in Figure 5

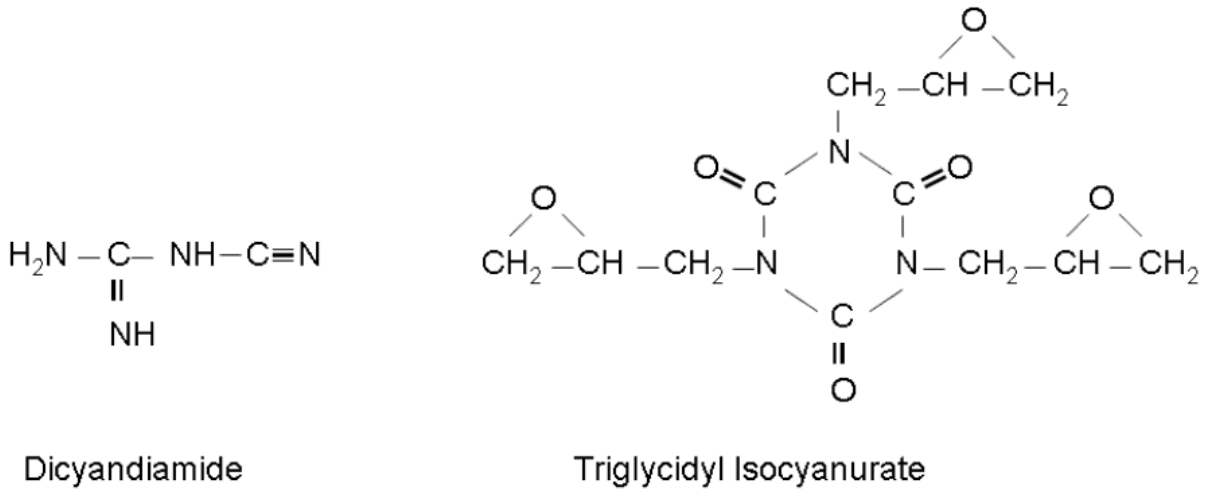

Figure 5. Typical curing agents for powder coatings [67].

The use of TGIC as curing agent for polyester powder coatings is restricted due to its mutagenic properties [69]. The component can be replaced by a primide curing agent. However, the curing reaction with primide releases water and can create pores if water is trapped inside the coating. TGIC cured coatings are known to possess excellent resistance against mechanical deformation [21] in addition to less pores since only small amounts of water is released during curing.

2.2.5. Compatibility between coatings and aluminium surfaces

Coatings are usually developed to protect steel substrates, and the same coatings are often also used for aluminium substrates. Aluminium and iron have different pH regions for the stability of their oxides [77]. Therefore, not all coatings applicable for steel, which are stable in alkaline environments, may be suitable for aluminium, which is stable in the pH range from 4 to 8 [77].

The pigments TiO_2, $BaSO_4$ and $CaCO_3$ have slightly alkaline chemistry when water is added. Amines, leaking from the epoxy coating, are known to cause an alkaline environment at the coating-metal interface [78]. This is detrimental for aluminium, suggesting the need for a slightly acidic component to stabilise the interface region [21, 79]. Inorganic pigments like vanadates, molybdates, phosphates, silicates, tungstates and chromates are acidic or amphoteric and represents possible buffers protecting the substrate under low potential and pH conditions [21].

A possible disadvantage of replacing alkaline with acid pigments is the loss of buffering effect obtained during propagation of filiform corrosion attacks. The filament heads are characterised by strongly acidic environment [17, 47], which can be neutralised by leaching of alkaline compounds from the coating. When using acidic pigments this effect is lost and more extensive filiform corrosion attacks can result.

2.3. Adhesion test methods

Wet adhesion quantification of adhesive bonds is performed mainly by lap shear, wedge and fatigue tests. The lap shear test is the most common test method for evaluating the durability of adhesive bonds [6]. The reason for using the lap shear test method is its simplicity. However, data interpretation is not straightforward, since shear forces, normally cohesive within the polymer, are measured and not the forces normal to the substrate surface.

The Boeing wedge test [3, 24, 38, 39, 80-83] and fatigue test [3, 84-87] are widely used for quantifying adhesion of adhesives. For both tests the double cantilever beam (DCB) specimen, shown in Figure 6, is commonly used. The sample geometry allows moisture to enter the fracture region

continuously as fresh surface is exposed [6]. The tapered double cantilever beam geometry has been used to obtain a strain energy release rate (G) independent of the crack length [3].

In the peel test the load increases constantly during the test [88]. In the impact wedge peel test the speed of the wedge, moving through the adhesive joint, can be varied from 0.4 m/s to 11 m/s [88]. For wet adhesion measurement the peel velocity may have to be reduced in order to obtain adequate water penetration into the debonding front.

One variant of the peel test is the blister test, where debonding occur either by a central load [89, 90] or by hydrostatic pressure [91]. The resistance in blister growth gives a quantifiable measure of adhesion. When using the blister test with a central load, often called shaft loaded blister test [89], the main uncertainty lies in yielding or creep of the polymer, caused by the low velocity of the blister expansion. Yielding and creep will lead to stretching of the polymer and thereby the applied load is relaxed through processes not related to adhesion. This will cause the calculated strain energy release rate invalid [89]. Another disadvantage is the testing time, which can be up to 4 months. In addition not all film thicknesses will allow an analytical evaluation of the strain energy release rate [90], which can limit the test usability even further. Testing of epoxy adhesives and borosilicate glass, performed by blister and DCB wedge tests, concluded that the wedge test allowed investigation of a wider range of strain energy release rates and moisture levels [89].

The pull off test has been used for wet adhesion assessment of coatings [7, 92]. The specimen is prepared by gluing a circular test dolly onto a coated specimen. The coating is then cut with a knife, following the edge of the dolly all the way around. The dolly is then pulled vertically by use of a load jig and the force required for failure is measured, followed by a *post mortem* investigation of the failure mode. Since the specimen is prepared prior to the wet exposure, the pull off test has the physical difficulty of water access to the coating/metal interface, making it hard to verify if wet or dry adhesion is being measured. Long times of wet exposure (1000 hours or more) are needed [7] to ensure water penetration into the specimen.

2.3.1. Wedge test

The wedge test [93] is based on crack growth in adhesively bonded DCB specimens [3, 80]. The main advantage of the method is that it is a relatively low cost test method. A large number of replicate specimens can be tested simultaneously. Different specimen geometries have been used [3, 94], varying in thickness and length. Figure 6 shows a typical DCB specimen geometry before and after wedge insertion.

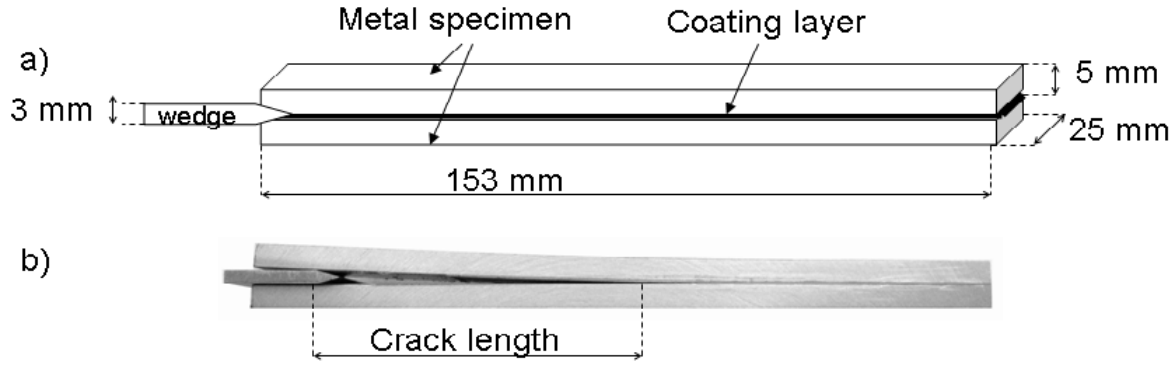

Figure 6. a) Typical DCB specimen geometry before and b) after insertion of the wedge.

In the wedge test, a constant displacement is applied at one end of the specimen. Consequently the force acting on the crack tip is reduced as the crack grows to a point where crack growth stops, determined by the adhesion strength of the interface region or the cohesion strength of the polymer. The specimen exposure can vary from total submersion in water [95] to ambient. Humid environment at elevated temperatures is often used to accelerate adhesion failure. The accelerated filiform corrosion test [96], in which a similar environment is used, the typical test conditions are 1000 hours at 40˚C and 80-90% RH. Humidity and elevated temperature are expected to enhance weakening of the interfacial bonds of the polymer [38]. Data commonly obtained are crack growth rate, total crack length and failure mode through crack surface analysis [38, 97, 98]. The reading of the crack length is normally performed on the edge of the specimen, where the crack is visible, as shown in Figure 6b. The crack opening can alternatively be monitored by use of a micrometer and displacement of fixed markers [38, 83, 99] attached to the specimen beams, to make sure no edge artefacts hinder proper crack length determination.

The most commonly noted disadvantage of the wedge test is the data scatter [35, 38] and the uncertainty of the crack length measurement. Crack

growth initiates from micro cracks [82] which can be hard to detect during the test even by use of a stereo microscope. Edge measurement may lead to an underestimate of the true crack length. The forces involved in crack growth are unevenly distributed across the specimen, giving a curved crack front, which is longer in the mid part of the specimen and retarded at the edges [98].

The fracture mechanical interpretation of the crack length data for adhesives is based on the concept of strain energy release rate, which is defined as [80, 83]

$$G = \frac{3Eh^3b^2}{16a^4} \qquad (1)$$

where E is the modulus of elasticity of the substrate, h is the specimen thickness, b is the wedge thickness and a is the crack length. G is also called the energy density in the crack tip. The use of G is controversial since the only experimental variable in equation 1 is the crack length, and the error in measuring this parameter is raised to the power of four in calculating G [80, 83, 98].

Equation 1 can be modified to correct for rotation and polymer elasticity [100]. Whether the failure mode is adhesive or cohesive can also be important in the interpretation of the results obtained by use of the equation. If the crack propagates in the adhesive layer (cohesive failure), which is expected for a good quality adhesive, the forces at the interface are not detected. If the failure is cohesive the G value calculated from the equation reveals the cohesive strength of a polymer and not the adhesive strength, which can be measured only if the failure is adhesive. The presence of mixed mode failure complicates the interpretation even further.

2.3.2. Fatigue test

Testing under a fluctuating load is a widely used and accepted method for the assessment of adhesion properties of adhesively bonded specimens [3, 95]. The fatigue strength of the adhesive is commonly measured by bending methods [101, 102] using different specimen geometries, such as lap shear. However, to investigate wet adhesion of polymers on metallic substrates, the double cantilever beam method is the common test geometry [6, 98], due to its simplicity and the constant access of water to the crack

tip. In fatigue testing the oscillation frequency can be varied, although low oscillation frequency can result in the build-up of creep strains and should be avoided [3, 103]. Oscillation frequencies of 20 Hz [104] and 5 Hz [95] have been used for testing of adhesives by use of DCB specimens. A too high oscillation frequency in corrosion fatigue is known to reduce penetration of moisture to the crack tip, and it is likely this will also be the case for fatigue tests for adhesives.

In fatigue testing the logarithm of the strain energy release rate G is plotted as a function of the logarithm of crack propagation velocity da/dN where N is the number of cycles [87]. G_0 is defined as zero crack growth and this level of growth is commonly determined at a very low crack velocity of 10^{-7} mm/cycle [95]. The G_0 values for the test specimens are then used to compare the adhesion properties.

2.3.3. Failure mode

An adhesively bonded specimen fails cohesively, adhesively or in a mixed mode [105]. Cohesive failure can occur in the bulk of the adhesive layer (Figure 7a) or in the oxide film (Figure 7c), in most cases in the adhesive. Adhesive failure can occur along interfaces between the adhesive and the oxide (Figure 7d), between the oxide and metal, or between adhesive/coating layers, *e.g.*, if a primer is used underneath an adhesive or top-coating. Figure 7 shows a sketch of the failure modes.

Near surface fracture is a cohesive failure mode characterised by crack propagation very close to the adhesive-metal substrate interface [8], as sketched in Figure 7 b). The cohesive failure mode has usually not been considered to be relevant to adhesion [106]. However, it has been claimed that the properties of the adhesive near the substrate interface may be different from that of the bulk and thereby have a certain significance on the overall adhesive properties [107]. A near surface layer was suggested to be caused by limited adhesion between the region with enhanced levels of adhesion promoters (the interphase) and the coating region with adhesion promoter depletion [104], due to a weak boundary layer occurring between these zones. The adhesion strength of the near surface region is enhanced and the weakest bonds become the coating cohesive bonds in the coating layer, close to the interface.

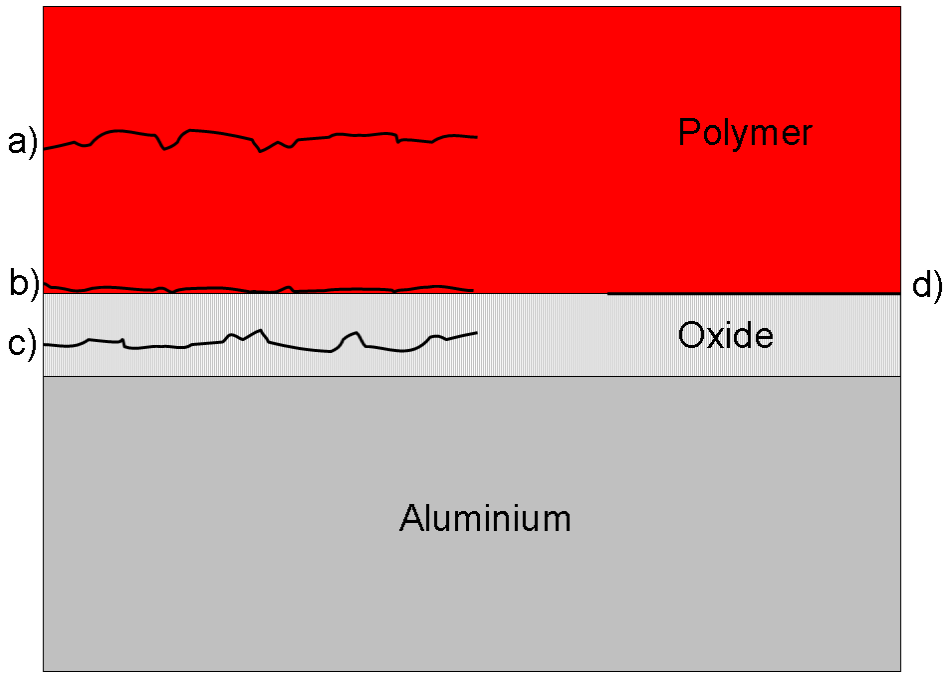

Figure 7. Sketch of failure by a) cohesive fracture in the coating b) near surface fracture c) cohesive fracture in the oxide layer and d) adhesive failure at the oxide –coating interface.

The failure mode often changes from cohesive within the polymer to adhesive at the polymer/substrate interface [3, 38] during the wet exposure for poorly adhering polymers. Metal-polymer interfaces with good wet adhesion properties almost always fail by cohesive fracture in the polymer [57, 104]. In testing of adhesives, properties of the adhesive are considered to be acceptable only if the failure mode is cohesive [6, 57], since this indicates that the adhesion strength is even larger than the cohesive strength of the polymer bulk. The crack length however, regardless the failure mode, relates to the probable service durability [98]. It appears to be important to assess adhesion both by failure mode and by crack length measurements.

Failure mode can be determined by using the naked eye, or by optical microscopes or image analysis. However, to establish the true failure mode, surface sensitive spectroscopic techniques such as X-ray Photoelectron Spectroscopy (XPS), Auger spectroscopy or high resolution electron microscopy can be used [37].

2.4. Filiform corrosion

Filiform corrosion (FFC) is the prevalent form of corrosion attack on coated aluminium surfaces that occurs in service particularly in architectural and automotive applications [21, 22, 47, 48, 108]. The corrosion attack initiates at coating defects and propagates in the form of thin filaments underneath the coating and/or conversion coating [61, 109]. Presence of electrochemically active deformed surface layers, layers created during thermomechanical processing of the alloy, enhances FFC [22].

If deformed layers are removed by etching, FFC can still occur by a successive pitting mechanism [26, 110]. The growth rate of filaments may depend on the development of stress from the growth of the voluminous corrosion products to overcome the adhesion between the coating and the substrate. Exposure of fresh metal surface in this way causes further filament growth [48, 61]. Enhanced adhesion strength of the coating-substrate interface can therefore to a certain degree hinder propagation of filiform corrosion mechanically.

Pre-treatments may interfere with cathodic sites that promote corrosion attack. For example it has been suggested that chromate inhibits filiform corrosion attack by inhibiting the oxygen reduction reaction occurring at the cathodic particles [30, 48]. A similar effect is obtained by addition of chromates to the coating itself. Alternative salts (e.g. molybdate, cerate) with a similar function may replace chromate as an additive to the coating [111].

It has been claimed that there is a relationship between adhesion and the corrosion resistance of coated aluminium surfaces [8], *e.g*, adhesion promoting additives to coating formulations inhibit corrosion attack [8]. This idea has been questioned by some authors [21, 40, 112], since the increase in adhesion forces of the coating is not a guarantee for the resistance to filiform corrosion [21].

2.5. Discussion

As discussed above the standardised adhesion tests are not suitable for wet adhesion testing. The pull off test has been used for wet adhesion [7, 92]. If

the specimen is prepared prior to the wet exposure, the pull off test has the physical difficulty of water access to the coating/metal interface, making it hard to verify if wet of dry adhesion is being measured. Depending on the coating system under investigation long times of wet exposure (1000 hours or more) is needed [7] to get complete water penetration into the specimen.

Wet adhesion quantification of adhesive bonds is performed mainly by lap shear, wedge test and fatigue test. The lap shear test is the most common test method for evaluating the durability of adhesive bonds [6], although the results of this method of testing have generally not been found to correlate with in service failure. The main drawback with the lap shear test is that it measures the shear forces, normally cohesive within the polymer, and not the level of the forces acting normal to the substrate. The wedge and fatigue tests do not pose this problem. In addition, they have the advantage of quantitative data analysis by the application of linear elastic fracture mechanics. Moreover, the use of DCB specimens allow easy access of water to the crack tip during the test, so that wet adhesion can be investigated, as is commonly done in the testing of adhesive bonding [3, 6, 36, 48, 80, 113]. The results are claimed to correlate well with service failure of adhesive bonds on aluminium alloys [98]. To investigate the use of this specimen geometry and the fracture mechanical approach for wet adhesion testing of coatings thus appears as a promising approach. Some modifications of the geometry, like specimen thickness, should be performed to compensate for the reduced stiffness of the coating compared to adhesives.

The need for more advanced test methods, in relation to the simple standardised tests, is justified also with the need to investigate less robust chromate-free pre-treatments. Recent work has indicated that the evaluation of the proposed chromate-free coatings is not as straightforward as adhesion testing of painted products using chromating [19, 39]. Assessment of differences between the performances of the chromate-free coatings has been difficult by use of the standard tests. The uncertainty resulting from this experience has necessitated looking into more quantitative techniques.

Among the chromate-free pre-treatments the commercial significance of Ti/Zr treatment is increasing because it is a dip process similar to chromating and because the corrosion resistance and adhesion properties obtained are reported to be acceptable in many applications [33, 57], comparable to that of chromating. Hot AC anodising has a commercial

significance mostly for coil coating industries [33, 35]. As a result of recent research results on its resistance to filiform corrosion [36, 57], the commercial interest for the technique has been increasing. An important advantage of the hot AC anodising process is that cleaning of the surface occurs simultaneously with anodising in a sulphuric acid bath, giving significant savings in investment and operation costs, as well as high rate of processing. Therefore, AC anodising is an interesting and promising pre-treatment method for further investigation.

The coatings selected for the present work are commercial pigmented coatings epoxy, cured with DICY, and polyester, cured with TGIC. The coatings were chosen since they are frequently used in practice, in addition to the limited release of water during the curing step. This was important since the coated specimens were prepared by curing in a hot press with possible entrapment of water and subsequent weakening of the polymer layer.

From both environmental and economical viewpoints, it is always desirable to reduce the number of steps and amount of chemicals used in chemical processing of metals. Eliminating the expensive and time consuming conversion coating step, even for outdoor applications, is therefore an attractive idea. This should be possible by using a modified organic coating to enhance the adhesion. Acid-base properties of a metal surface are important for adhesion and bond durability [114, 115] and the utilisation of an acidic additive to an organic coating appears as a possible solution to stabilise the aluminium oxide layer underneath, since aluminium oxide is stable at slightly acidic conditions [77]. An important question in connection with replacement of pigments is the possible buffering effect against initiation and propagation of localised corrosion. All forms of localised corrosion, including filiform corrosion, which is of particular interest in the present context, create strongly acidic environments locally. The acidified filament tip in filiform corrosion underneath the coating [17, 47] can be neutralised by leaching of alkaline compounds from the coating. When using acidic pigments this effect is lost and more extensive filiform corrosion attack can result, although adhesion may be improved.

To look for reasons for coating failure as well as evidence of types of bonding or changes in the oxidation state of the elements, it is necessary to use advanced surface-analytical techniques such as XPS and Auger spectroscopy. XPS provides information about the chemical states of compounds and bonding [116]. Auger spectroscopy on the other hand,

provides better lateral resolution, down to only a few nm, compared to XPS, for which the signal strength decreases rapidly for spot sizes below 100 μm. TEM provides opportunities for cross-sectional investigations of the distribution of elements at the interface, especially in the mode of energy filtering [37, 117]. The advantage of the method is the high resolution and mapping opportunities for elemental distribution across the specimen. From this discussion it seems clear that multiple techniques should be employed to discover different aspects of the adhesion of a coated specimen.

The purpose of the present study is to provide a method for assessment, possibly quantification, of wet adhesion of organic coatings on aluminium. The selected test methods used are the Boeing wedge test [93] and fatigue test [3], where the applied forces are static and dynamic, respectively. Post failure analysis of the specimen is performed to find evidence of the mechanisms causing adhesion loss. In addition to the adhesion test development, the possibility of enhancing the coating by simple pH adjustments of the coating was investigated. Model polyester primid coatings with low pH additives were tested to see if the coating can be modified to avoid conversion coatings, with the intention both to save costs and reduce environmental hazard.

2.6. References

1. G. W. Critchlow and D. M. Brewis, *International Journal of Adhesion and Adhesives*, **16**, p. 255 (1996).
2. X. F. Liu, *Corrosion Science*, **49**, p. 3494 (2007).
3. A. J. Kinloch, *Adhesion and Adhesives: Science and Technology,*, Chapman and Hall, London (1990).
4. A. Pizzi, Mittal, K.L., *Handbook of adhesive technology*, CRC Press, New York, USA (2003).
5. S. S. Zumdahl, *Chemical Principles*, DC Heath and Company, Lexington (1995).
6. B. B. Johnsen, PhD Thesis, in *Institute of Materials Science*, Norwegian University of Technology and Science (2004).
7. M. Mohseni, M. Mirabedini, M. Hashemi and G. E. Thompson, *Progress in Organic Coatings*, **57**, p. 307 (2006).
8. K. Wapner, M. Stratmann and G. Grundmeier, *International Journal of Adhesion and Adhesives*, **28**, p. 59 (2008).
9. J. van den Brand, S. Van Gils, P. C. J. Beentjes, H. Terryn, V. Sivel and J. H. W. de Wit, *Progress in Organic Coatings*, **51**, p. 339 (2004).

10. N. H. Giskeodegard, PhD Thesis, in *Institute of Materials Science*, Norwegian University of Technology and Science, Trondheim (2008).
11. A. Seth, W. J. van Ooij, P. Puomi, Z. Yin, A. Ashirgade, S. Bafna and C. Shivane, *Progress in Organic Coatings*, **58**, p. 136 (2007).
12. H. Leidheiser and W. Funke, *Journal of the Oil & Colour Chemists Association*, **70**, p. 121 (1987).
13. J. van den Brand, S. V. Gils, H. Terryn, V. G. M. Sivel and J. H. W. d. Wit, *Progress in Organic Coatings*, **51**, p. 351 (2004).
14. G. Z. Xiao and M. E. R. Shanahan, *Polymer*, **39**, p. 3253 (1998).
15. T. Nguyen, E. Byrd, D. Bentz and C. Lint, *Progress in Organic Coatings*, **27**, p. 181 (1996).
16. A. Bautista, *Progress in Organic Coatings*, **28**, p. 49 (1996).
17. H. N. McMurray, A. J. Coleman, G. Williams, A. Afseth and G. M. Scamans, *Journal of the Electrochemical Society*, **154**, p. C339 (2007).
18. G. M. Scamans, Afseth, A., Remmers, U., van der Meer, W., Hallenstvet, M., Eschauzier, F., Katzgerman, L., Nisancioglu, K., in *ECCA General Meeting, 27-30 May 2001*, B. European Coil Coating Association, Belgium Editor, Budapest, Hungary (2001).
19. O. Ø. Knudsen, Bjørgum, A., Tanem, B.S., *ATB Metallurgie*, **43**, p. 175 (2003).
20. A. T. A. Jenkins and R. D. Armstrong, *Corrosion Science*, **38**, p. 1147 (1996).
21. J. L. Delplancke, S. Berger, X. Lefebvre, D. Maetens, A. Pourbaix and N. Heymans, *Progress in Organic Coatings*, **43**, p. 64 (2001).
22. A. Afseth, J. H. Nordlien, G. M. Scamans and K. Nisancioglu, *Corrosion Science*, **44**, p. 2491 (2002).
23. G. D. Davis, J. D. Venables, M. Chaudhury and A. V. Pocius, in *Surfaces, Chemistry and Applications*, p. 947, Elsevier Science B.V., Amsterdam (2002).
24. R. P. Digby and D. E. Packham, *Int. J. of Adhesion and Adhesives*, **15**, p. 61 (1995).
25. Premendra, L. Philippe, H. Terryn, J. H. W. de Wit and L. Katgerman, *Surface and Coatings Technology*, **201**, p. 828 (2006).
26. X. Zhou, G. E. Thompson and G. M. Scamans, *Corrosion Science*, **45**, p. 1767 (2003).
27. A. Afseth, J. H. Nordlien, G. M. Scamans and K. Nisancioglu, *Corrosion Science*, **43**, p. 2359 (2001).
28. G. M. Scamans, A. Afseth, G. E. Thompson, Y. Liu and X. Zhou, *Aluminium Alloys* **519-521**, p. 647 (2006).
29. V. Moutarlier, M. P. Gigandet, L. Ricq and J. Pagetti, *Applied Surface Science*, **183**, p. 1 (2001).
30. O. Lunder, J. C. Walmsley, P. Mack and K. Nisancioglu, *Corrosion Science*, **47**, p. 1604 (2005).
31. M. W. Kendig, A. J. Davenport and H. S. Isaacs, *Corrosion Science*, **34**, p. 41 (1993).
32. J. Zhao, L. Xia, A. Sehgal, D. Lu, R. L. McCreery and G. S. Frankel, *Surface and Coatings Technology*, **140**, p. 51 (2001).
33. O. O. Knudsen, B. S. Tanem, A. Bjorgum, J. Mardalen and M. Hallenstvet, *Corrosion Science*, **46**, p. 2081 (2004).

34. A. Bjorgum, F. Lapique, J. Walmsley and K. Redford, *International Journal of Adhesion and Adhesives*, **23**, p. 401 (2003).
35. B. B. Johnsen, F. Lapique and A. Bjorgum, *International Journal of Adhesion and Adhesives*, **24**, p. 153 (2004).
36. O. Lunder, B. Olsen and K. Nisancioglu, *International Journal of Adhesion and Adhesives*, **22**, p. 143 (2002).
37. A. J. Kinloch, M. S. G. Little and J. F. Watts, *Acta Materialia*, **48**, p. 4543 (2000).
38. K. B. Armstrong, *International Journal of Adhesion and Adhesives*, **17**, p. 89 (1997).
39. O. Ø. Knudsen, Rodahl, S., Lein, J.E., *ATB Metallurgie*, **45** (2006).
40. G. Scamans, Afseth, A., Thompson, G.E., Liu, J., Zhou, X., *ATB Metallurgie*, **45**, p. 30 (2006).
41. Y. Liu, Zhou, X., Thompson, G.E., Hashimoto, T., Scamans, G.M., Afseth, A., *ATB Metallurgie*, **45**, p. 367 (2006).
42. S. Liu, R. E. Napolitano and R. Trivedi, *Acta Materialia*, **49**, p. 4271 (2001).
43. D. R. Baer, C. F. Windisch, M. H. Engelhard, M. J. Danielson, R. H. Jones and J. S. Vetrano, *Journal of Vacuum Science & Technology a-Vacuum Surfaces and Films*, **18**, p. 131 (2000).
44. W. Brockmann, O. D. Hennemann and H. Kollek, *International Journal of Adhesion and Adhesives*, **2**, p. 33 (1982).
45. M. Kendig, S. Jeanjaquet, R. Addison and J. Waldrop, *Surface and Coatings Technology*, **140**, p. 58 (2001).
46. K. Asami, M. Oki, G. E. Thompson, G. C. Wood and V. Ashworth, *Electrochimica Acta*, **32**, p. 337 (1987).
47. J. V. Kloet, W. Schmidt, A. W. Hassel and M. Stratmann, *Electrochimica Acta*, **49**, p. 1675 (2004).
48. O. Lunder, PhD Thesis, in *Institute of Materials Science and Engineering*, NTNU, Trondheim (2003).
49. E. Jaehne, S. Oberoi and H.-J. P. Adler, *Progress in Organic Coatings*, **61**, p. 211 (2008).
50. M. Poelman, M. G. Olivier, N. Gayarre and J. P. Petitjean, *Progress in Organic Coatings*, **54**, p. 55 (2005).
51. F. Andreatta, A. Turco, I. de Graeve, H. Terryn, J. H. W. de Wit and L. Fedrizzi, *Surface and Coatings Technology*, **201**, p. 7668 (2007).
52. O. Lunder, C. Simensen, Y. Yu and K. Nisancioglu, *Surface and Coatings Technology*, **184**, p. 278 (2004).
53. B. S. Tanem, O. Lunder, A. Borg and J. Mårdalen, *International Journal of Adhesion and Adhesives*, **In Press, Corrected Proof**.
54. F. Andreatta, P. Aldighieri, L. Paussa, R. Di Maggio, S. Rossi and L. Fedrizzi, *Electrochimica Acta*, **52**, p. 7545 (2007).
55. L. Fedrizzi, F. J. Rodriguez, S. Rossi, F. Deflorian and R. Di Maggio, *Electrochimica Acta*, **46**, p. 3715 (2001).
56. R. Comrie, PhD Thesis, in *Department of Pure and Applied Chemistry*, University of Strathclyde, Glasgow, UK (1998).
57. A. Bjørgum, F. Lapique, J. Walmsley and K. Redford, *International Journal of Adhesion and Adhesives*, **23**, p. 401 (2003).

58. GSB, *Quality and Test Regulations for piecework coating of aluminium building components RAL-RG 631*.
59. B. B. Johnsen, F. Lapique, A. Bjorgum, J. Walmsley, B. S. Tanem and T. Luksepp, *International Journal of Adhesion and Adhesives*, **24**, p. 183 (2004).
60. J. Bishopp and C. Philippe, in *Handbook of Adhesives and Sealants*, p. 163, Elsevier Science Ltd (2005).
61. H. Leth-Olsen and K. Nisancioglu, *Corrosion Science*, **40**, p. 1179 (1998).
62. D. R. Gabe, *Transactions of the Institute of Metal Finishing*, **78**, p. 207 (2000).
63. V. Moutarlier, M. P. Gigandet, J. Pagetti and L. Ricq, *Surface and Coatings Technology*, **173**, p. 87 (2003).
64. F. Sertcelik, A. F. Cakir, M. Urgen, D. H. Ross and D. R. Gabe, *Transactions of the Institute of Metal Finishing*, **76**, p. 179 (1998).
65. R. H. Dahm, R. J. Latham, B. Unal, D. R. Gabe and M. Ward, *Transactions of the Institute of Metal Finishing*, **81**, p. 159 (2003).
66. G. P. Bierwagen, *Progress in Organic Coatings*, **28**, p. 43 (1996).
67. R. S. Lambourne, T.A., *Paint and surface coatings. Theory and practice*, Woodhead Publishing Ltd, Cambridge, UK (1999).
68. G. K. van der Wel and O. C. G. Adan, *Progress in Organic Coatings*, **37**, p. 1 (1999).
69. R. Farrell, *Metal Finishing*, **98**, p. 135 (2000).
70. J. Marsh, J. D. Scantlebury and S. B. Lyon, *Corrosion Science*, **43**, p. 829 (2001).
71. D. G. Weldon, *Failure analysis if paints and coatings*, John Wiley and Sons, Chichester, UK (2001).
72. L. Fedrizzi, F. Deflorian, G. Boni, P. L. Bonora and E. Pasini, *Progress in Organic Coatings*, **29**, p. 89 (1996).
73. S. Jahromi, B. Mostert, A. Derks and F. Koldijk, *Progress in Organic Coatings*, **48**, p. 183 (2003).
74. B. E. Maxwell, R. C. Wilson, H. A. Taylor, D. E. Williams, W. Farnham and J. Tria, *Progress in Organic Coatings*, **43**, p. 158 (2001).
75. Z. W. Wicks, Jones, F.N., Pappas, S.P., *Journal of Coatings Technology*, **71**, p. 47 (1999).
76. J. F. Hughes, *Journal of Electrostatics*, **23**, p. 3 (1989).
77. M. Pourbaix, *Atlas of electrochemical equilibria in aqueous solutions,*, National Assocation of Corrosion Engineers, Houston Texas, USA (1974).
78. O. Lunder, F. Lapique, B. Johnsen and K. Nisancioglu, *International Journal of Adhesion and Adhesives*, **24**, p. 107 (2004).
79. W. Funke, H. Leidheiser, R. A. Dickie, H. Dinger, W. Fischer, H. Haagen, K. Herrmann, H. G. Mosle, W. P. Oechsner, J. Ruf, J. S. Scantlebury, M. Svoboda and J. M. Sykes, *Journal of Coatings Technology*, **58**, p. 79 (1986).
80. J. Cognard, *The Journal of Adhesion*, **20**, p. 1 (1986).
81. J. Cognard, *The Journal of Adhesion*, **22**, p. 97 (1987).
82. D. Plausinis and J. K. Spelt, *International Journal of Adhesion and Adhesives*, **15**, p. 143 (1995).
83. J. P. Sargent, *International Journal of Adhesion and Adhesives*, **25**, p. 247 (2005).

84. M. M. Abou-Hamda, M. M. Megahed and M. M. I. Hammouda, *Engineering Fracture Mechanics*, **60**, p. 605 (1998).
85. I. A. Ashcroft, M. M. A. Wahab, A. D. Crocombe, D. J. Hughes and S. J. Shaw, *Composites Part A: Applied Science and Manufacturing*, **32**, p. 45 (2001).
86. S. Erpolat, I. A. Ashcroft, A. D. Crocombe and M. A. Wahab, *Engineering Fracture Mechanics*, **71**, p. 1393 (2004).
87. H. Hadavinia, A. J. Kinloch, M. S. G. Little and A. C. Taylor, *International Journal of Adhesion and Adhesives*, **23**, p. 449 (2003).
88. I. Georgiou, A. Ivankovic, A. J. Kinloch, V. Tropsa, A. P. B.R.K. Blackman and J. G. Williams, in *European Structural Integrity Society*, p. 317, Elsevier (2003).
89. E. P. O`Brien, Case, S.L., *Journal of Adhesion*, **81**, p. 41 (2005).
90. C. Jin, *International Journal of Solids and Structures*, **45**, p. 6485 (2008).
91. S. Guo, K.-T. Wan and D. A. Dillard, *International Journal of Solids and Structures*, **42**, p. 2771 (2005).
92. S. M. Mirabedini, J. D. Scantlebury, G. E. Thompson and S. Moradian, *International Journal of Adhesion and Adhesives*, **25**, p. 484 (2005).
93. *ASTM 3762-03, Standard Test Method for Adhesive-Bonded Surface Durability of Aluminum (Wedge Test)*, ASTM international, West Conshohocken, USA (2008).
94. B. Johnsen, Olafsen, K., Stori, A., Vinje, K. , *Journal of adhesion Science and Technology*, **16**, p. 1931 (2002).
95. J. K. Jethwa and A. J. Kinloch, *The Journal of Adhesion*, **61**, p. 71 (1997).
96. European Standard EN 3665. Filiform corrosion resistance test on aluminium alloys, in *Test methods for paints and varnishes* (1997).
97. J. A. Marceau, *Sampe Quarterly-Society for the Advancement of Material and Process Engineering*, **9**, p. 1 (1978).
98. J. A. Marceau, Y. Moji and J. C. McMillian, *Adhesives Age*, **20**, p. 28 (1977).
99. J. Cognard, *International Journal of Adhesion and Adhesives*, **6**, p. 215 (1986).
100. T. Pardoen, T. Ferracin, C. M. Landis and F. Delannay, *Journal of the Mechanics and Physics of Solids*, **53**, p. 1951 (2005).
101. J. Oh, J. Komotori and J. Song, *International Journal of Fatigue*, **30**, p. 1441 (2008).
102. D. Muller, Y. R. Cho and E. Fromm, *Surface and Coatings Technology*, **74-75**, p. 849 (1995).
103. J. A. Harris and P. A. Fay, *International Journal of Adhesion and Adhesives*, **12**, p. 9 (1992).
104. M. W. Rushforth, P. Bowen, E. McAlpine, X. Zhou and G. E. Thompson, *Journal of Materials Processing Technology*, **153-154**, p. 359 (2004).
105. J. A. Marceau, J. C. McMillan and W. M. Scardino, *Adhesives Age*, **21**, p. 37 (1978).
106. J. Marsh, L. Minel, M. G. Barthes-Labrousse and D. Gorse, *Applied Surface Science*, **133**, p. 270 (1998).
107. A. A. Roche, J. Bouchet and S. Bentadjine, *International Journal of Adhesion and Adhesives*, **22**, p. 431 (2002).
108. G. S. Frankel, *Journal of the Electrochemical Society*, **145**, p. 2970 (1998).

109. R. Szymanski, D. N. Jamieson, A. E. Hughes, A. Mol, S. van der Zwaag and C. G. Ryan, *Nuclear Instruments and Methods in Physics Research Section B: Beam Interactions with Materials and Atoms*, **190**, p. 365 (2002).
110. H. Leth-Olsen, PhD Thesis in *Institute of materials science*, NTNU, Trondheim, Norway (1996).
111. J. Sinko, *Progress in Organic Coatings*, **42**, p. 267 (2001).
112. R. A. Dickie, *Progress in Organic Coatings*, **25**, p. 3 (1994).
113. S. Mostovoy, Crosley, P.B., Ripling, E.J, *Journal of Materials*, **2**, p. 661 (1967).
114. E. McCafferty and J. P. Wightman, *Journal of Colloid and Interface Science*, **194**, p. 344 (1997).
115. E. McCafferty, *Journal of Electrochemical Society*, **150**, p. B342 (2003).
116. J. F. Watts, Wolstenholme, J., *An introduction to surface analysis by XPS and AES*, John Wiley and Sons, Chichester, UK (2003).
117. D. J. Bland, A. J. Kinloch, V. Stolojan and J. F. Watts, *Surface and Interface Analysis*, **40**, p. 128 (2008).

3. Use of wedge test to determine wet adhesion of organic coatings on aluminium

Abstract

Applicability of the wedge test, commonly used for testing of adhesively bonded joints, was investigated in an attempt to develop a test for evaluating paint adhesion on aluminium in the presence of humidity. The test was further used, along with an accelerated laboratory test for filiform corrosion of painted aluminium, to study the durability of various pre-treatments and paint systems on extruded AA 6082-T6 aluminium alloy, with attention to the compatibility of pre-treatment-paint combinations. The hot AC-anodized surfaces gave good adhesion and corrosion resistance together with commercial polyester and epoxy coatings and displayed only cohesive failure. The chromate pre-treatment was satisfactory together with both coatings. The Ti/Zr-treated samples, in contrast, suffered adhesive failure during the wedge test, and in combination with epoxy, they failed the criteria set for the corrosion test. The results thus indicate that the use of chromate-free pre-treatments may require assessment of the compatibility of each combination of the modified aluminium surface and the applied organic coating.

3.1. Introduction

Although the effect of corrosion on the deterioration of organic coated surfaces on aluminium alloys in outdoor exposure is well investigated [1-3], relatively little information is available about the role of paint adhesion [4, 5]. This may be due to lack of reliable experimental techniques, especially those that can distinguish between the effects of adhesion and corrosion in the presence of humidity and in addition correlate to in service failure [6]. Assessment of the wet adhesion properties of organic coatings on aluminium alloys has become of increasing need because of the requirement to replace chromating with nontoxic and more environmentally friendly conversion coatings.

Most chromate-free coatings have so far proved to be inferior to yellow chromating in terms of robustness and durability [7], with the possible exception of hot AC anodizing [8-11]. It is becoming apparent that the

performance of the new chromate-free conversion coatings depends on the type of alloy and organic coating used [12-14], suggesting the specificity of the alloy, pre-treatment and coating combination. The selection of chromate-free pre-treatment and coating for a given aluminium alloy substrate is therefore not straightforward. A more detailed investigation is required to measure wet adhesion and corrosion by use of techniques, which can distinguish between these two failure mechanisms.

Dry adhesion of coatings can be assessed by pull off [15], cross-hatch tape [15], impact [5] and bending tests [16]. The pull-off test has been used by immerging the specimens in water [17]. However it is unclear how the specimen geometry could allow the penetration of water into the interface region, hindered by the attached dolly used. The other methods are difficult to modify for evaluating the coating performance in the presence of moisture, because the speed of paint removal is too fast for water to penetrate to the interface.

Non-destructive tests can contribute to the understanding of the bonds present and thereby explain the reasons for adhesion loss. Kelvin probe, which is functionalized by depositing the organic groups representative of the coating, has proven to be useful [18], with limitations related to the stability of the functionalized probe tip throughout the experiment. The method can measure the adhesive forces acting at the coating-metal interface. However, it requires flat specimen surfaces, and only microscopic areas can be investigated, which limits the utilisation to laboratory investigations of highly fundamental nature. Fourier transform infrared spectroscopy (FTIR) has been used to investigate water uptake and distribution in organic coatings [18]. However, this is not an *in situ* method. The requirement of flat surfaces limits the use for ***e.g.*** extruded specimens. Electrochemical impedance spectroscopy (EIS) is widely used to assess adhesion [15, 19] by investigating the barrier property of the coating. This is in fact considered as one of the most useful applications of the impedance technique, especially if the coating failure is a result of corrosion. Interpretation of adhesion data, however, is not straightforward, since adhesion loss does not always provide an electrical signal. Detailed models for the electrochemical interface are required for a more indirect assessment of the adhesion properties [20].

Water must enter the substrate/coating interface to measure wet adhesion. Correlation to in service failure is desirable, which means that the test

should imitate real stress and exposure as much as possible. The wedge test for adhesion assessment of adhesives is reported to be a reliable method for measuring wet adhesion of adhesives, compared to the shear and peel tests [21] in terms of correlating with outdoor exposure [6]. This might be because the slow crack opening under constant but low stress allows water to access the stressed interface during the test. The constant access of moisture to the stressed region thereby allows the effect of water to be measured. For shear or peel tests the geometry of the specimen will prevent the moisture to enter the interface and the dry adhesion only can be assessed. Another advantage of the wedge test is the inexpensive and simple equipment and sample design.

The method of interest is therefore based on crack growth on bonded double cantilever beam type specimens (DCB) [21], so called Boeing wedge test. The wedge test method [12, 21-25] is investigated because of its simplicity, which does not require a significant investment. The fatigue test is frequently used in testing the durability of adhesive bonding of aluminium alloys [21, 26], but it needs expensive testing equipment. The most frequently mentioned disadvantage of the wedge test is the data scatter [12, 21]. To deal with the scatter appropriate statistical analysis of the data is necessary to reveal the differences between the performance of the conversion and organic coating combinations.

The purpose of the present paper is to investigate the validity of a qualitative methodology based on the wedge test for determining wet adhesion of paint on aluminium. The pre-treatments selected were commercial processes for deoxidising, chromating, hot AC anodising and Ti/Zr conversion coating. The coatings selected were polyester TGIC and epoxy DICY, both pigmented commercial products. The substrate used was extruded aluminium alloy AA 6082-T6. Another objective of the work is to study compatibility between the pre-treatment methods, coatings and the aluminium substrate, and the selection of conversion and organic coating combinations was based on this consideration. In addition to the wedge test for measurement of wet adhesion, an accelerated filiform corrosion test [27] was used since it is necessary to combine adhesion and corrosion results for more complete assessment of durability of painted surfaces. The selected filiform corrosion test is frequently used based on reports about satisfactory correspondence between the results obtained from this accelerated test and the field test data [28].

3.2. Experimental

3.2.1. Surface treatment.

The substrate used in all experiments was aluminium alloy EN-AW 6082 T6 extrusions. Two promising chromate free processes, hot AC anodising [29] and Ti/Zr-treatment [30], were investigated. Samples, which were only deoxidised before application of the organic coating, were used as the worst case specimens for comparison purposes. Chromate conversion coating was used as reference.

The samples were degreased in alkaline degreaser Neutrasel 5269 (Henkel), diluted to 60 g/l, for 10 minutes at 60ºC. Deoxidising was performed in acidic 35 ml/l Alfideox 73 (CANDOR Sweden AB) for 4 minutes at ambient temperature. Approximately 0.5 μm of aluminium was removed from the surface during the surface cleaning. Samples were subsequently pretreated as specified in Table 1.

Table 1. Pre-treatment conditions.

	Ti/Zr	Chromating	Hot AC anodising
Product	Gardobond X4707/Gardolene	Alodine 6100	sulphuric acid
Time	60 seconds	2 minutes	30 seconds
Temperature	Ambient	Ambient	80ºC
Concentration	43,5 ml/l	15 ml/l	150 g/l
Conditions	pH 2,7 vigorous stirring		20 A/dm^3
Supplier	CHEMETALL GmbH	Henkel	

The paints tested were commercial epoxy DICY (dicyandiamide) and polyester TGIC (triglycidyl isocyanurate) powder coatings provided by Jotun Powder Coatings. These paints were selected based on the information that water was not supposed to be produced during their curing. Water trapped in the coating between two metal beams would be detrimental to the test results by deteriorating the coating properties by introducing pores.

3.2.2. Adhesion testing.

The starting point was the test described in ASTM D 3762-03 [31]. The metal beam dimensions were 5x25x153 mm. The bar thickness was selected with consideration of the adhesive strength of the coatings. The powders were sprayed on the bar pairs by an electrostatic spray gun and melted at about 120ºC. The bar pairs were then joined with paint facing towards each other and using 100 µm thick spacers placed at both ends of the longest dimension. Curing of paint was performed in a hot press for 20 minutes at 180ºC. The wedge was inserted 20 mm into the specimen using a programmable drilling machine with a speed of 1 mm/s. Figure 1 shows a sketch of the DCB specimen thus constructed.

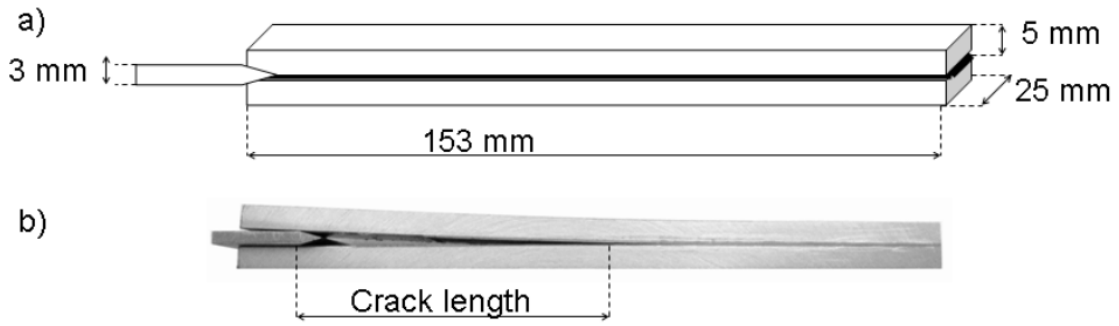

Figure 1. a) Sketch of the double cantilever beam specimen before the wedge is inserted. The black layer between the aluminium bars is the coating layer.
b) Photograph of a DCB specimen after the wedge is inserted.

After storing for 24 hours in ambient conditions, the 6 replicates of each pre-treatment - paint combination were placed in a climate chamber maintained at 40°C and 82% RH for 27 days, when the crack growth was no longer detectable for any of the specimens. The crack growth was determined by monitoring the crack length visible on the edge of the sample by use of a stereo microscope at predetermined time intervals until no further crack propagation was detectable.

3.2.3. Corrosion testing.

Filiform corrosion testing was performed on 4 replicates of each pre-treatment-coating combination according to EN 3665 [27]. A scribe was made through the coating to expose a thin stripe of bare metal surface. Corrosion was initiated by adding droplets of 16 wt% hydrochloric acid in

the scribe for ½ to 2 minutes, until corrosion reaction was visible. The excess hydrochloric acid was then carefully wiped off, and the samples were placed in a climate chamber for 1000 hours at 40ºC and 82% RH. The number of filaments per unit length of scribe (filament density) and the length of longest filament were determined to assess susceptibility to filiform corrosion.

3.3. Results

3.3.1. Adhesion test.

As described above, the wedge test was performed in two stages. The first stage involved insertion of the wedge into the DCB specimens, followed by measurement of crack growth in climate chamber for 27 days. After drying the specimens in ambient laboratory atmosphere for 7 days, the wedge was inserted further into the specimens, followed by a further 40 days of exposure and crack growth measurement in the climate chamber. This part of the experiment is referred to as Stage 2 and was performed in order to gain an extra data set from the same sample specimen.

The crack growth after wedge insertion in ambient conditions was considered as a measure of dry adhesion and crack growth in the climate chamber as a measure of wet adhesion. Figure 2 shows the crack lengths obtained during 24 hours of stabilization in ambient atmosphere after the insertion of the wedge, after the initial crack growth due to wedge insertion had stopped. The Figure indicates that from one-half to two-thirds of total crack growth in Stage 1 occurred as a result of wedge insertion in ambient atmosphere. Moreover, the crack growth during wedge insertion on deoxidised specimens was comparable to those with conversion coating, indicating similar dry adhesion properties of paint whether conversion coating was present or not.

Since a significant stress was released from all specimens as a result of Stage 1 crack growth, the Stage 2 insertion did not give a significant crack growth at all in relation to Stage 1. The scatter in the data was moreover much larger. These factors did not permit clear comparison of Stage 2 growth, although it still appeared to be quite similar for all the tested variants. Data for the deoxidized samples were not included because they cracked completely apart during Stage 1 wet adhesion measurements.

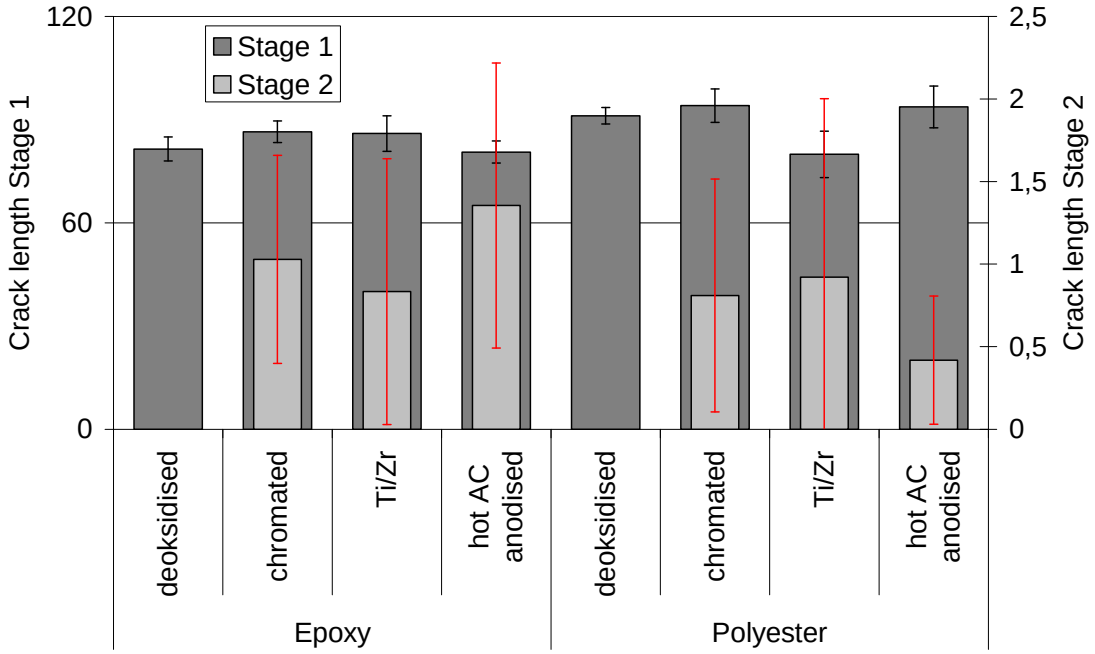

Figure 2. Crack lengths obtained during 24 hours after insertion of the wedge in ambient conditions. Stage 2 data were obtained after inserting the wedge 15 mm further into the same specimens, which were already exposed to humidity in the climate chamber for 27 days and then stored in the laboratory for 7 days. The lengths reported are only the segments grown as a result of wedge insertion.

Figure 3 shows crack growth data for Stage 1, obtained during exposure in the climate chamber, corresponding to wet adhesion. The Figure illustrates the standard way of reporting crack growth data, *viz.*, total crack length is plotted as a function of time. As can be observed readily, the crack length data in the present case was essentially dominated by the initial growth obtained as a result of insertion of the wedge. The specimens, which were only deoxidized, exhibited monotonic crack growth still after 27 days of exposure, while the crack lengths on other specimen variants more or less reached steady-state values after about 5 days of exposure. Thus, the dry-adhesion properties of the deoxidized specimens, which were not too different from the other pre-treatment variants, were misleading for assessing the overall adhesion properties, including wet adhesion, which were disclosed by exposure in the climate chamber. Wet adhesion properties of the deoxidized specimens were clearly inferior to that of the other variants.

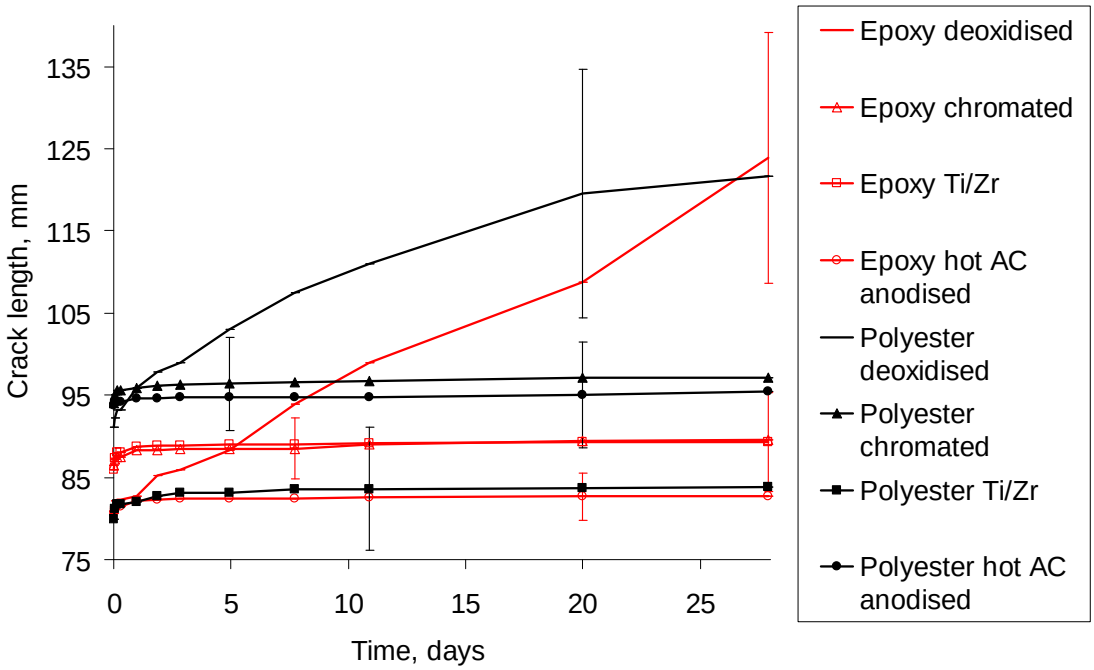

Figure 3. Average crack length vs. time obtained from the wedge test of all sample variants in Stage 1, as a result of exposure in the climate chamber. Red curves with open data points are for the epoxy coated specimen and black lines with closed points are for the polyester coated specimen. Typical error bars for the pre-treatment-paint combinations are shown at different periods of measurement to avoid overlap.

The data in Figure 3, thus, clearly demonstrated the effect of conversion coating treatment on the wet adhesion properties of painted aluminium. However, the wet growth rates of the other variants could not be clearly distinguished from one another because of rapid attainment of steady-state values. Moreover, these steady-state values were very much determined by the initial crack growth due to wedge insertion [22]. This is illustrated further in Figure 4, which compares the dry and wet crack-growth lengths separately, after steady-state lengths were obtained. With the exception of the deoxidized specimens, it is observed that the wet growth was much smaller than dry growth. As a result, Figure 3 did not provide the best means of comparing wet growth on variants other than the deoxidized.

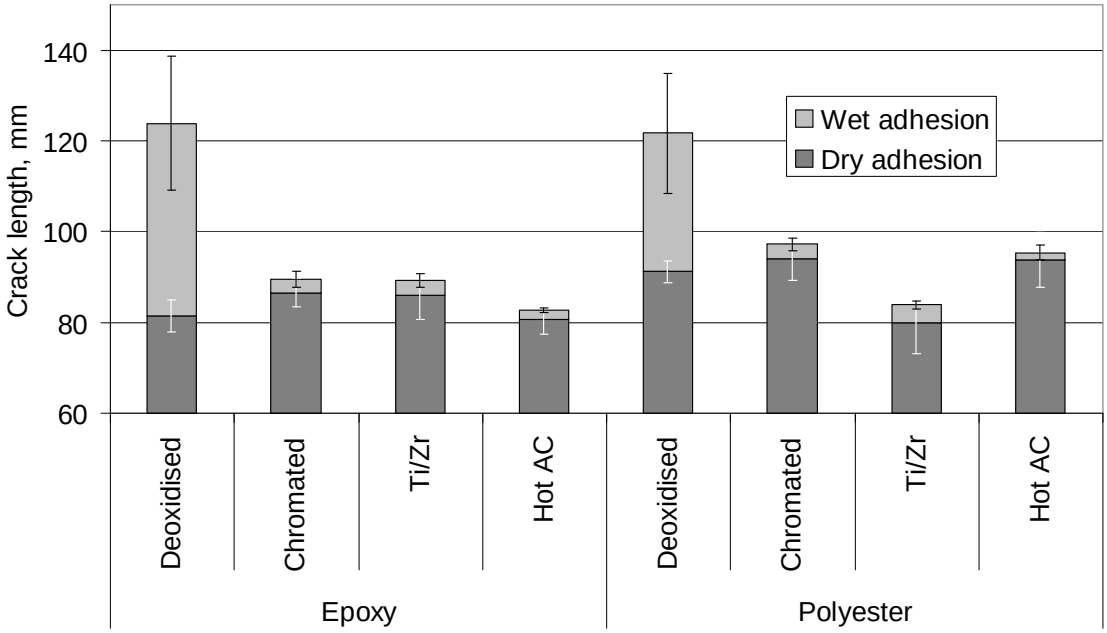

Figure 4. Steady-state crack-length segments obtained as a result of growth in ambient air after wedge insertion (dry) and as a result of further growth by subsequent exposure in the climate chamber (wet). The error bars correspond to data scatter in each phase (wet and dry) of crack growth.

In view of the foregoing discussion, crack growth during exposure in the climate chamber, which gave information about the wet adhesion properties, was normalized with respect to the initial lengths obtained before exposure in the climate chamber. That is to say, the lengths at time zero in Figure 3 were subtracted from the total crack lengths in constructing a new plot, and these results are shown in Figure 5. Thus, the Figure shows Stage 1 crack growth only during exposure in the climate chamber, and the data are relevant for the assessment of wet adhesion for each pre-treatment-paint combination, except for the deoxidized data. One typical error bar for each case is shown at a different selected time for each, in order to avoid overlap of the bars.

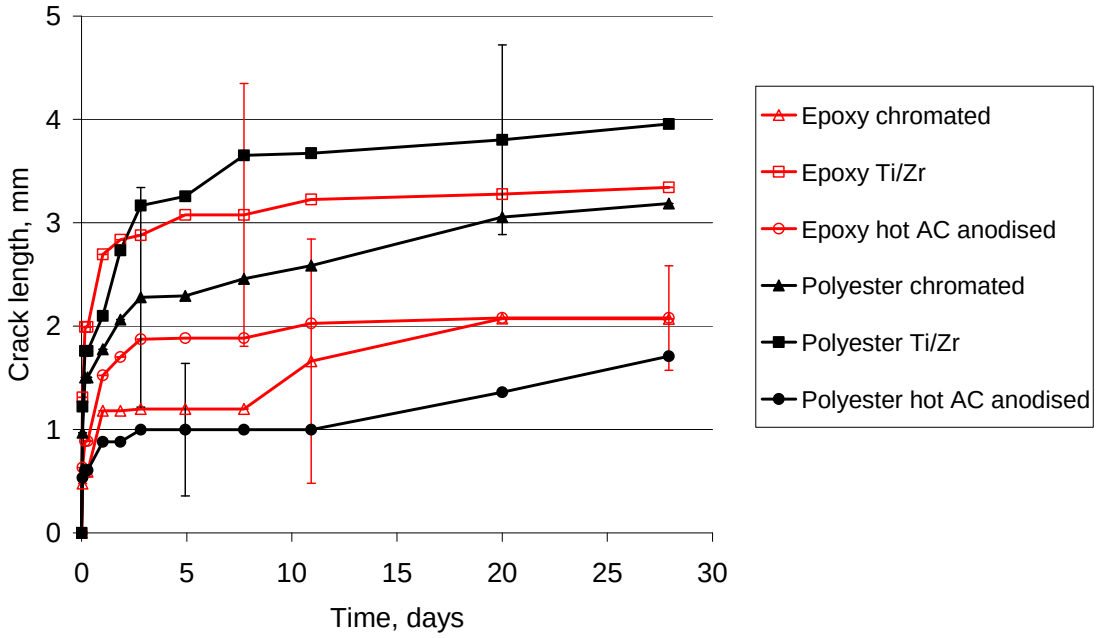

Figure 5. Average crack length vs. time obtained from the wedge test of all sample variants, except the deoxidized, after the initial dry crack length is subtracted. Red curves with open data points are for the epoxy coated specimens, and black lines with closed points are for the polyester coated specimens. Typical error bars for the pre-treatment-paint combinations are shown at different periods of measurement to avoid overlap. The error bars are based on data scatter in the replicate specimens of each variant only during crack growth in the climate chamber, *i.e.*, they exclude scatter from initial crack growth due to wedge insertion.

Since the data in Figure 5 exclude the deoxidized specimens and are normalized as explained, it is thought to be more appropriate for comparison of the pre-treatment-paint combinations, which essentially gave good wet-adhesion properties, but were difficult to compare based on a more conventional approach to data presentation (Figure 3). However, the comparison is strictly qualitative from a fracture-mechanical standpoint. Although data scatter was still significant, we believe that the statistical analysis of the data, based on the student t test reported in Appendix A, allows a limited degree of distinction between the variants. The Ti/Zr treated specimens, *e.g.*, appeared to exhibit larger crack growth than the hot-AC-treated specimens during climate chamber exposure. The crack growth on hot-AC treated specimens was at least as small as on the chromated specimens. Thus, a certain distinction of the effect of pre-treatment could be made, while no clear distinction between the organic

coatings, as regards any direct effect on the wet adhesion properties, could be achieved.

Figure 6 compares the crack lengths obtained at the end of the exposure period due to growth only during exposure in the climate chamber for all pre-treatment-organic coating combinations with the exception of the deoxidized samples. Data for both Stage 1 and Stage 2 exposures are included. The Figure does not add any new information about crack propagation in Stage 1 *per se*. The purpose of the Figure is to compare Stage 1 and Stage 2 wet propagation behaviours.

There was a significant increase in the data scatter in Stage 2 in relation to Stage 1. Crack growth obtained in Stage 2 was also in general larger than crack growth in Stage 1. This was in contrast to the smaller wedge insertion and much smaller dry crack growths (Figure 2) obtained in Stage 2 than in Stage 1. This result may indicate that the present methodology could actually distinguish between dry and wet adhesion. The wet exposure trends applicable to Stage 1 appeared to be applicable also to Stage 2. However, the only statistically allowable conclusion, based on the analysis in Appendix A was the slightly poorer wet adhesion property of the Ti/Zr-polyester combination in comparison with the other pre-treatment-organic coating combinations, which were statistically not distinguishable from one another.

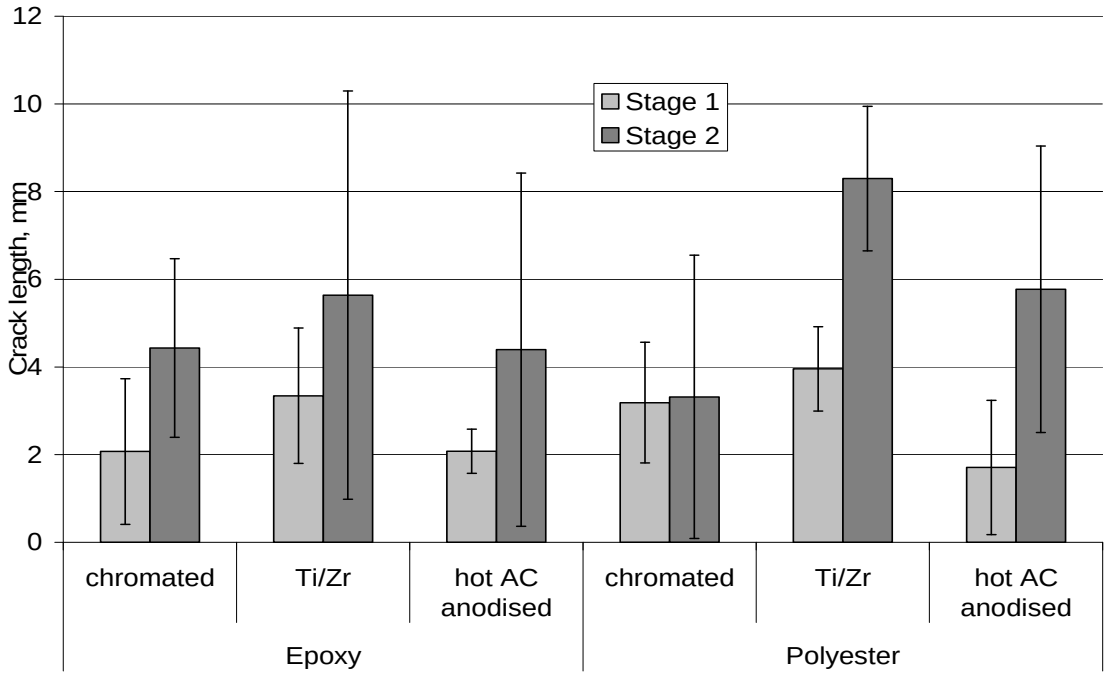

Figure 6. Comparison of the crack lengths obtained as a result of exposure in the climate chamber. These lengths correspond to the total crack segments propagated only due to exposure in the climate chamber. The results from Stage 1 and Stage 2 exposures are compared.

The method of reading the crack length from the edge of specimen is questioned since the energy release rate is not evenly distributed [32]. In Figure 7 the crack length measured from the edge of the specimen is compared to the lengths measured directly on the cracked surfaces of the separated beams in the *post mortem* investigation. The crack lengths obtained *post mortem* were approximately 0.5 cm longer than the edge measurements. However, the trends in the total crack lengths are not changed. A similar determination of each stage of crack growth would be desirable for a more accurate assessment of the adhesive failure. However, the different stages, including the dry and wet phases of growth, were not distinguishable from one another for all specimens.

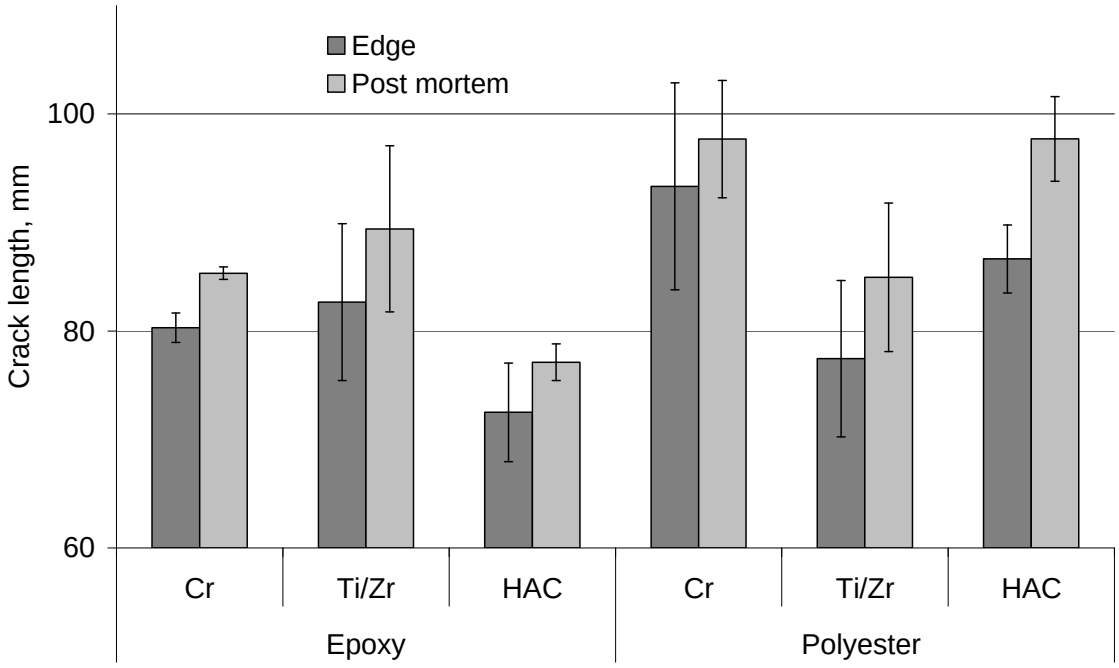

Figure 7. Comparisons of final crack lengths measured both from the edge and from the *post mortem* investigation of the specimen. The *post mortem* measurement was done directly on the crack surface of the separated specimen beams.

3.3.2. Failure mode.

Images of crack surfaces on test specimens, which were split open mechanically after the climate chamber test, are shown in Figure 8. A significant length of most of the specimens was cracked initially by insertion of the wedge the first time, as discussed above. The typical fracture types observed can be classified as a) adhesive and b) cohesive. The deoxidized specimens exhibited typical adhesive failure during climate chamber exposure (Figure 8a). Ti/Zr treated, polyester coated specimen also exhibited adhesive failure, as shown in Figure 8c. Although this occurred to a much smaller scale than that observed for the deoxidized specimen, Ti/Zr combination was the only variant among the conversion coated specimens which exhibited adhesive failure. It also appeared to give the longest crack in wet exposure among the conversion coated variants, as argued above, although all conversion-coated variants essentially indicated satisfactory adhesion properties.

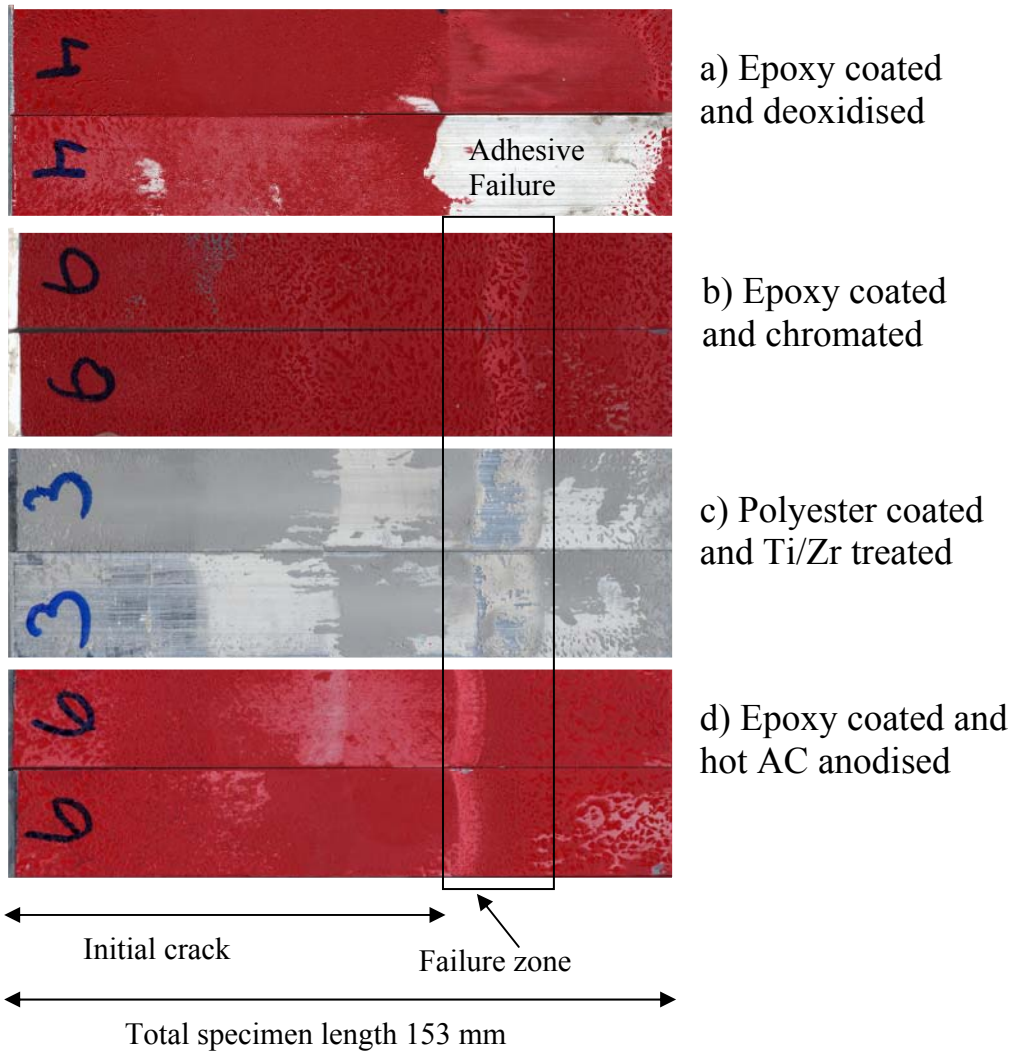

Figure 8. Examples of a) and c) adhesive and b) and d) cohesive failure modes.

Since most of the specimen variants exhibited more than one type of failure mode described above, fraction of failure mode for each variant was determined by image analysis. As illustrated in Figure 9, the coated and metallic surfaces were distinguished from one another in black and white contrast on both surfaces of the fractured DCB specimen, and the respective fractions were determined relative to the total area affected.

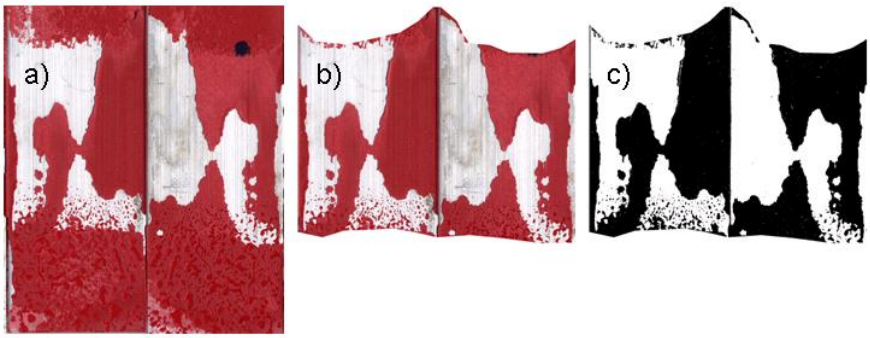

Figure 9. Illustration of image analysis procedure to establish percentage of failure mode for an epoxy coated and deoxidised specimen. a) Area of crack propagation as a result of exposure in the climate chamber. Both of the opposite surfaces of cracked DCB specimen were analysed. b) The fracture zone cropped from (a). c) The areas with and without coating are transformed into black and white areas, respectively, area fraction of which are subsequently determined by the image analysis software.

This procedure could not be used for the polyester coated specimen because of difficulty in obtaining sufficient contrast between the metallic and coated areas for the image analysis software to function. The fraction of failure mode for this case was determined by a more intuitive visual separation of the areas of different failure modes and manual area measurement. Whether the approach was manual or digital measurement, the errors incurred in determining the zones of different failure modes were significant, and the results are to be regarded as qualitative order of magnitude estimates. Figure 10 shows the average percentage of fracture modes for each pre-treatment-coating combination, based on the 6 replicate specimens for each case. The error bars indicate the average standard deviation of scatter among the replicate specimens.

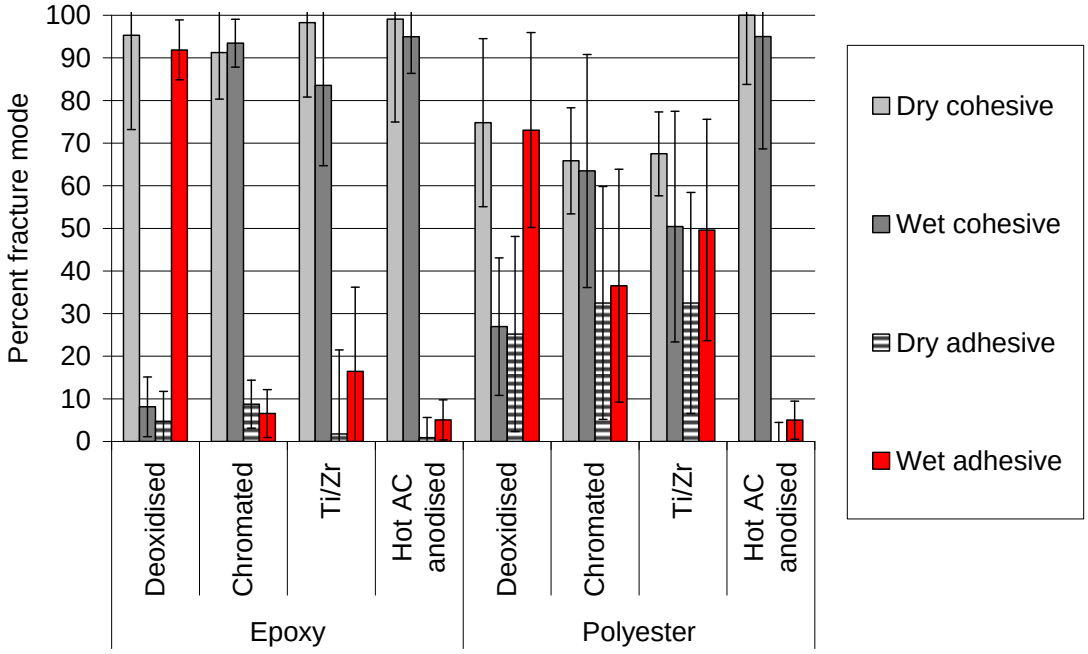

Figure 10. *Post mortem* evaluation of the fractured surfaces to determine the mode of failure during testing, showing the percentage of crack growth mode in both dry and wet phases.

The results shown in Figure 10 reconfirm that the initial dry growth phase was mainly cohesive for all specimens. During the wet phase, the deoxidised specimens exhibited mainly adhesive failure. The polyester coated specimens exhibited adhesive failure to a larger extent than the epoxy coated specimens, except for the hot-AC anodised specimens. Hot AC anodised specimens failed mostly cohesively regardless of the coating. The Ti/Zr pre-treated samples exhibited a larger extent of adhesive failure than the hot AC anodised specimens.

The data in Figure 10 demonstrates that the mode of failure for the deoxidised specimen changed from cohesive to adhesive failure when exposed to moisture. The same was also the case for the Ti/Zr treated specimen. Moreover, the polyester coated specimens exhibited a larger extent of adhesive failure than the epoxy coated specimens in general.

Inspecting the crack surfaces revealed pore formation in the paint, as shown in Figure 11. The pore area fraction in this specific example was about 30%, as determined in the same manner as the estimation of area fraction of failure modes as described above. The pores were formed as a

result of water release from the paint and its subsequent evaporation during curing. The pores may alter the adhesion result and cause the observed data scatter due to their variable action and spread. In areas with numerous pores the area of adhesion or cohesion will be reduced compared to what the outer geometry of the specimen indicates. In addition the pores may induce local stress sites in the coating, weakening the coating even further. Pores in the coating can also act as sinks for moisture and thereby act as sites where corrosion processes or coating delamination can be initiated.

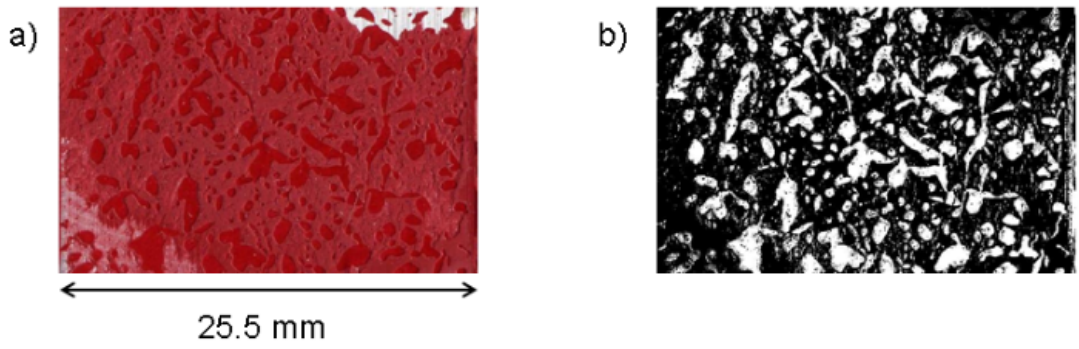

Figure 11 a) Pores in the paint revealed after separating the two beams of Ti/Zr pre-treated and epoxy coated specimen. b) Black-white rendition of the pores in Figure 10a for determination of their area fraction.

3.3.3. Corrosion test.

Corrosion test results, shown in Figure 12, indicated that all hot AC anodised samples and chromated samples were resistant to filiform corrosion regardless of the coating. Samples pre-treated with Ti/Zr showed acceptable filiform corrosion properties when coated with the polyester coating. However, when coated with the epoxy coating, the Ti/Zr treated specimens exhibited a significantly larger susceptibility to filiform corrosion, which was at the same level as the deoxidised samples. These results are in good correlation with the results obtained in summary from the evaluation of the wedge test results for wet adhesion.

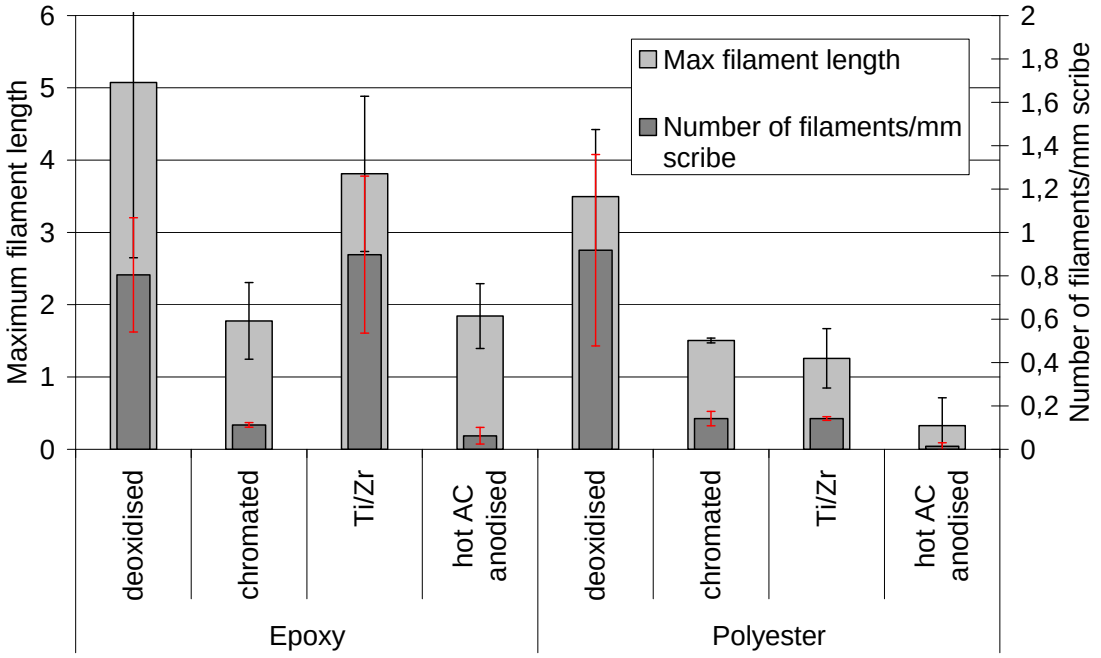

Figure 12. Results from the corrosion test in terms of filament density and maximum filament length. Maximum filament length longer than 2 mm was considered as a sign of significant susceptibility to filiform corrosion according to common procedure[14]. Error bars indicate the standard deviation in the data for 4 replicates of each coating/pre-treatment combination.

3.4. Discussion

3.4.1. Test methodology

The original purpose of the present work was to investigate whether the wedge test, often used to test the durability of adhesives [24, 25], could be used as a reliable, cost effective method to evaluate the wet adhesion properties of organic coatings on cleaned and pre-treated aluminium alloy surfaces. However, the low level of crack growth under humid conditions made quantification of the crack velocity difficult. The original intention was also to represent the results in terms of crack velocity vs. strain energy release rate (log da/dt – G) correlations [22, 25, 33]. This approach was not possible because of the large initial crack growth immediately after insertion of the wedge, which introduced a commensurate scatter to subsequently calculated G values. However, the methodology presented seems to be a reliable qualitative test, although only one of the selected specimen variants could be considered to represent unsatisfactory wet

adhesion. The rest of the variants were quite satisfactory, and for a more comprehensive validation of the method, a larger variety of pre-treatment-paint combinations should be tested.

It was demonstrated that information about both dry adhesion and wet adhesion can be obtained from the same test and furthermore that adhesion tests in dry laboratory conditions are not satisfactory if the painted surface is to be exposed to humidity during service life. This was demonstrated by the significant change in the behaviour of deoxidized specimens from exhibiting satisfactory dry adhesion to extensive adhesive failure in humid atmosphere.

Pores in the polymer layer can cause a systematic error in the results. The coatings were selected to limit pore formation. However, the porosity of the cured paints was significant as seen in Figure 11. The pores result from water released during the curing process, which becomes entrapped in the paint between the metal beams. To reduce pore formation in future work, the paint should be cured completely before the beams are glued together with a suitable adhesive. The procedure would then ensure the level of pores being low and comparable to a real coated product.

Another source of systematic error was related to the insertion of the wedge into the specimen and the resulting uncontrollable initial crack growth, as discussed earlier [25]. Improvement would be possible by introducing a shorter initial crack of controllable length, *e.g.*, by a Teflon spacer or by fatigue as used for crack initiation in stress corrosion cracking experiments with DCB specimens [6, 34]. The level of stress can be maintained by screws, holding the beams apart in one end of the specimen [6].

The Stage 2 insertion of the wedge was performed in order to obtain a second data set from the same sample specimen. The interpretation of the second data set is not straightforward, however, since the specimen for Stage 2 already had a significant pre-cracked area. When removing the contribution of the pre-cracks, both for Stage 1 and Stage 2, the effect of crack growth in wet environment becomes comparable. The growth in Stage 2 is significantly larger than Stage 1 growth, which is mainly caused by the uncontrollable crack growth when the wedge was inserted the first time. The effect of moisture was therefore less in Stage 1, as seen from Figure 6.

An important concern about the wedge test interpretation is whether the cohesive fracture mode, occurring in the coating bulk, indicates acceptable adhesion, or if the cohesive failure should also be interpreted as an indirect measure of coating adhesion failure [6]. In the present study, cohesive failure is simply interpreted as a sign of good adhesion. This view was used in interpreting cohesive failure observed in all cases of dry exposure as a measure of satisfactory dry adhesion property. The fact that introduction of moisture caused certain specimen variants, especially the ones which were only deoxidised, to change from cohesive to adhesive failure mode was interpreted as an indication of poor wet adhesion property, as also reported by others to occur for poor performing pre-treatments [21, 35]. The failure modes of chromated and hot AC anodised specimen were cohesive in this work, indicating that the conversion coatings performed satisfactorily for outdoor purposes.

3.4.2. Pre-treatment/coating combinations

Despite the large data scatter, certain distinction between different pre-treatment-coating combinations was possible based on the present results. The robustness of the hot AC treatment [8-11], even in relation to the widely acclaimed properties of chromating, was verified both as a result of the adhesion and corrosion tests employed in the present study. It can be argued that the good corrosion resistance imparted to the surface by hot AC anodizing also promotes good wet adhesion and, *vice versa,* the good adhesion obtained by the penetration of the coating into the porous oxide [22, 29] results also in good performance in a filiform corrosion test. Hot AC treatment increases the corrosion resistance of the surface by superficial dissolution or removal of the Fe-rich noble intermetallic phases[14]. Hot AC anodised aluminium oxide is porous and known for the high adsorptive power and being chemically and electrically inert [29].

While the Ti/Zr treatment-paint combinations in general gave satisfactory wet adhesion properties, Ti/Zr-epoxy combination showed more filament growth during the filiform corrosion test. Moreover, Ti/Zr-treated samples in general exhibited a larger degree of adhesive failure than the other pre-treatment-coating combinations. These results suggest that this pre-treatment may be less robust than the other pre-treatments tested and it may be necessary to test its use for each choice of paint [14, 30]. The Ti/Zr layer needs further investigation to reveal the location and action mode of crack growth. It appears that the corrosion performance of Ti/Zr treated specimen

is dependent on the coating used, since the corrosion properties are inferior when using epoxy coating (Figure 12). Uncoated specimen is known to have active surfaces similar to deoxidised specimen [30] which indicates that the bonds between polyester coating and the surface are more protective compared to the epoxy coating. One explanation of this is enhanced adhesion, however the observed difference in adhesion measurements are not statistically significant due to overlap in the results.

The general correlation noted between the wet adhesion interpretation of the wedge test data and the filiform corrosion test results may indicate a mechanistic relationship between the two phenomena. Poor corrosion resistance of the coated metal surface must certainly lead also to poor adhesion properties in practice, and *vice versa*, good adhesion of the coating may prevent filiform corrosion. As will be shown in the next Chapter, the opposite may also be the case, *i.e.*, good corrosion resistance does not always indicate good adhesion, depending on the method used in straining the metal coating interface and exposing the interface to humidity. The present correlation between adhesion and corrosion may be a pure coincidence or, conversely, an indication that the wedge test is a suitable method for investigating the adhesion properties of the coating-aluminium metal interface. The limited data presented in this work does not allow a further discussion of the possible relationship between adhesion and corrosion.

3.5. Conclusions

Wedge test appears to be a reliable test to distinguish between pre-treatment-paint combinations for indicating satisfactory or poor adhesion to the aluminium-alloy surface in humid environment. Information about dry adhesion is also simultaneously obtained. Data scatter is a serious problem associated with the test and limits the fracture mechanical quantification of failure. The DCB specimens were prepared by gluing two aluminium bars by the paint in a manner analogous to testing of adhesives for aluminium. The wet adhesion results correlated well with the data obtained from filiform corrosion test. The corrosion results of Ti/Zr pre-treated aluminium suggest that wet adhesion is important in controlling underfilm corrosion on pre-treated aluminium alloy surfaces. The hot AC anodising together with both epoxy and polyester coatings tested in this work showed promising results. The necessity of using chromate free pre-treatments will

require a closer look at the specificity and durability of new pre-treatment - paint combinations, which will in turn require the availability of reliable test methods. The absence of robust pre-treatments to replace chromating, with the exception of hot-AC anodising, requires validation of the compatibility of the selected pre-treatment with both the selected organic coating and the aluminium substrate in terms of wet adhesion and corrosion resistance.

Acknowledgements

John Erik Lein and Nils-Inge Nilsen, SINTEF, assisted in the experimental work. This work is part of a research program entitled "Light Metal Surface Science", supported by The Norwegian Research Council, Hydro Aluminium, Jotun Powder Coatings AS, DuPont Powder Coatings, Fundo Wheel AS, Norsk Industrilakkering AS and Profil-Lakkering AS.

3.6. References

1 H. Leth-Olsen and K. Nisancioglu, *Corrosion Science* **40**, 1179 (1998).
2 A. T. A. Jenkins and R. D. Armstrong, *Corrosion Science* **38**, 1147 (1996).
3 A. Bautista, *Progress in Organic Coatings* **28**, 49 (1996).
4 S. M. Mirabedini, J. D. Scantlebury, G. E. Thompson, S. Moradian., *International Journal of Adhesion and Adhesives* **25**, 484 (2005).
5 K. D. Bouzakis, A. Asimakopoulos, N. Michailidis, S. Kompogiannis, G. Maliaris, G. Giannopoulos, E. Pavlidou, G. Erkens, *Thin Solid Films* **469**, 254 (2004).
6 J. A. Marceau, Y. Moji and J. C. McMillian, *Adhesives Age* **20**, 28 (1977).
7 O. Lunder, B. Olsen and K. Nisancioglu, *International Journal of Adhesion and Adhesives* **22**, 143 (2002).
8 O. O. Knudsen, B. S. Tanem, A. Bjorgum, J. Mårdalen, M. Hallenstvet, *Corrosion Science* **46**, 2081 (2004).
9 A. Bjorgum, F. Lapique, J. Walmsley, K. Redford., *International Journal of Adhesion and Adhesives* **23**, 401 (2003).
10 G. W. Critchlow and D. M. Brewis, *International Journal of Adhesion and Adhesives* **16**, 255 (1996).
11 B. B. Johnsen, F. Lapique and A. Bjorgum, *International Journal of Adhesion and Adhesives* **24**, 153 (2004).
12 K. B. Armstrong, *International Journal of Adhesion and Adhesives* **17**, 89 (1997).
13 O. Ø. Knudsen, Rodahl, S., Lein, J.E., *ATB Metallurgie* **45** (2006).
14 O. Ø. Knudsen, Bjørgum, A., Tanem, B.S., *ATB Metallurgie* **43**, 175 (2003).
15 B. Tepe and B. Gunay, *Progress in Organic Coatings* **62**, 134 (2008).
16 A. E. Dolinko and G. H. Kaufmann, *Optics and Lasers in Engineering* **46**, 230 (2008).

[17] J. K. Jethwa and A. J. Kinloch, *The Journal of Adhesion* **61**, 71 (1997).
[18] K. Wapner, M. Stratmann and G. Grundmeier, *Electrochimica Acta* **51**, 3303 (2006).
[19] F. Andreatta, P. Aldighieri, L. Paussa, R. Di Maggio, S. Rossi, L. Fedrizzi, *Electrochimica Acta* **52**, 7545 (2007).
[20] I. Epelboin, Keddam, M., Takanouti, H., *Journal of applied electrochemistry* **2**, 71 (1971).
[21] A. J. Kinloch, *Adhesion and Adhesives: Science and Technology,* Chapman and Hall, London, (1990).
[22] R. P. Digby and D. E. Packham, *Int. J. of Adhesion and Adhesives* **15**, 61 (1995).
[23] J. P. Sargent, *International Journal of Adhesion and Adhesives* **25**, 247 (2005).
[24] J. Cognard, *International Journal of Adhesion and Adhesives* **6**, 215 (1986).
[25] J. Cognard, *The Journal of Adhesion* **20**, 1 (1986).
[26] J. A. Harris and P. A. Fay, *International Journal of Adhesion and Adhesives* **12**, 9 (1992).
[27] in *Test methods for paints and varnishes*, 1997).
[28] H. Leth-Olsen, in *Institute of materials science* (NTNU, Trondheim, Norway, 1996).
[29] A. Bjørgum, F. Lapique, J. Walmsley, K. Redford, *International Journal of Adhesion and Adhesives* **23**, 401 (2003).
[30] O. Lunder, C. Simensen, Y. Yu, K. Nisancioglu, *Surface and Coatings Technology* **184**, 278 (2004).
[31] ASTM 3762-03, *Standard Test Method for Adhesive-Bonded Surface Durability of Aluminum (Wedge Test)* ASTM international, West Conshohocken, USA, (2008).
[32] J. Schon, *Composites Science and Technology* **60**, 553 (2000).
[33] D. Plausinis and J. K. Spelt, *International Journal of Adhesion and Adhesives* **15**, 143 (1995).
[34] A. K. Roy, D. L. Fleming, D. C. Freeman, B. Y. Lum, *Micron* **30**, 649 (1999).
[35] A. J. Kinloch, M. S. G. Little and J. F. Watts, *Acta Materialia* **48**, 4543 (2000).

Appendix A.

The table shows results from student t testing of the selections tested in the wedge test. Grey areas show unacceptable overlap, with more than 5% probability of arriving from the same sample selection. Light grey areas show results acceptable within a 90% confidence interval instead of a 95% confidence interval.

Pretreatment/coating combination		Raw data %	Stage 1 dry %	Stage 1 wet %	Stage 2 dry	Stage 2 wet
Epoxy deoxidised	Epoxy chromated	0,3	5	0,1		
	Epoxy Ti/Zr	0,2	11,5	0,1		
	Epoxy hot AC	0,1	66,5	0,1		
	Polyester deoxidised	79,9	0,1	17,8		
	Polyester chromated	0,7	0,1	0,1		
	Polyester Ti/Zr	0,1	63,1	0,1		
	Polyester hot AC	0,5	0,4	0,1		
Epoxy chromated	Epoxy Ti/Zr	88,9	85,1	26,9	95,9	65,1
	Epoxy hot AC	1,1	2,9	99,4	55,8	85,5
	Polyester deoxidised	0,3	5,4	0,4		
	Polyester chromated	2,7	2	31,7	66,5	52,4
	Polyester Ti/Zr	14,5	7,7	11	86,4	2,5
	Polyester hot AC	10,1	4,4	73,9	20,4	45,1
Epoxy Ti/Zr	Epoxy hot AC	4,5	6,3	10,5	53,6	90,6
	Polyester deoxidised	0,2	6,2	0,4		

	Polyester chromated	4	2,1	85,7	71,5	74,2
	Polyester Ti/Zr	20,3	11,5	43,4	90,3	0,2
	Polyester hot AC	11,4	4,2	9,9	23,1	24,2
Epoxy hot AC	Polyester deoxidised	0,1	0	0,3		
	Polyester chromated	0,1	0	11,4	30,2	72,8
	Polyester Ti/Zr	73,2	82,9	0,4	50,1	4,2
	Polyester hot AC	0,3	0,2	59,4	6,9	41,2
Polyester deoxidised	Polyester chromated	0,7	22,6	0,4		
	Polyester Ti/Zr	0,1	0,8	0,5		
	Polyester hot AC	0,5	37,5	0,3		
Polyester chromated	Polyester Ti/Zr	0,7	0,2	29,5	85,1	1,2
	Polyester hot AC	61,4	90,7	11,3	31,3	22,3
Polyester Ti/Zr	Polyester hot AC	1,8	0,5	1,6	36,5	13,5

4. Fatigue testing for measuring adhesion between organic coatings and aluminium

Abstract

With the purpose of developing reliable and quantitative methodology for determining wet adhesion of organic coatings on aluminium, fatigue test, commonly used for testing adhesives, is used for organic coatings. Pre-treated and coated surfaces of extruded aluminium alloy AA6082-T6 sample pairs were joined together to form double cantilever beam (DCB) specimens analogous to the specimens used in testing of adhesives. The pre-treatments used were hot AC anodising and Ti/Zr conversion coating. Chromate conversion coating and deoxidised samples were used as reference. The organic coatings used were commercial polyester and epoxy coatings. By measuring the compliance of the sample under cyclic loading, the crack growth rate versus strain energy release rate G correlations were obtained from calibration data for the specimen geometry used in the conventional manner. The failure mode was mainly cohesive in contrast to the wedge test results, which showed adhesive and cohesive failure modes for poor and good adhesion, respectively. Interpretation of the fatigue data was therefore not as straightforward as the wedge test data. Performance of the pre-treatments could not be statistically distinguished. The failure mechanisms for the two tests are probably fundamentally different, and further work is required for determining the significance of the fatigue test for assessing wet adhesion properties of organic coatings on aluminium.

4.1. Introduction

Adhesion between the coating and the metal surface is determined by properties of both the organic coating and the modified metal surface. Durability of the coating during atmospheric exposure is reported to depend on good adhesion properties [1], which in turn is expected to protect against filiform corrosion, which is one of the most important causes of deterioration of coated aluminium [2, 3].

There is a general agreement that pre-treatment of the metal surface before the application of organic coating is of prime importance [4, 5] both to maintain adhesion and protect against corrosion. Chromating [4, 6-9],

chromic acid anodising [10] and addition of chromium containing pigments to polymeric coatings [11] have been widely used and proven both to enhance adhesion and prevent corrosion. However, the carcinogenic effects of chromium (VI) restrict the use of these chemicals [12, 13]. More recent work has documented the importance of surface pre-treatment, including chromate-free conversion coatings on the filiform corrosion properties [3, 4, 14, 15].

In Chapter 3, the applicability of a modified Boeing wedge test methodology to assess dry and wet adhesion properties of organic coatings on pre-treated aluminium surface was investigated. The method was applied to study adhesion of selected polyester and epoxy powder coatings on aluminium alloy AA6082 extrusions, pre-treated by Ti/Zr treatment and hot AC anodising. Hot AC anodising was shown to be a promising alternative to chromating, in agreement with earlier investigations [16, 17]. Ti/Zr treatment did not appear to be as robust as chromating and hot AC anodising. Titanium and zirconium based pre-treatments have been suggested as promising dip-processes [18-21]. However, they need to be validated for specific alloy-coating combination prior to any application [19]. The study in Chapter 3 further demonstrated that the quality of the organic coating becomes increasingly important with decreasing confidence in the robustness of the conversion coating.

This work will focus on measurements of adhesion between the modified aluminium surface and the organic coating by use of fatigue testing of double cantilever beam (DCB) specimens [5, 22-24] in continuing effort to develop a quantitative methodology to assess wet adhesion properties of organic coatings on aluminium. The results will be compared to the wedge test results reported in Chapter 3.

4.2. Theory

The fatigue test under consideration is a common method for testing the durability of adhesively bonded metal components [5]. It uses double cantilever beam (DCB) substrates which are joined together laterally with a thin layer of adhesive, as shown in Figure 1.

Figure 1 Sketch of a DCB specimen, where a is the crack length, b is the specimen width, and d is the displacement at the load point.

The test is performed in presence of water to measure crack growth rate under cyclic stress. In treating the data by application of the principles of elastic fracture mechanics, it is useful to define a strain energy release rate G [25, 26] for tensile crack opening mode,

$$G = \frac{P^2}{2b}\frac{dC}{da} \qquad (1)$$

where P is the applied load, b is the specimen width, a is the crack length, and C is the compliance, which in turn is defined by the relationship

$$d = PC \qquad (2)$$

where d is the crack displacement measured at the point where the stress is applied. Compliance and crack length are related according to the equation [23]

$$C^{1/3} = m(a+\Delta) \qquad (3)$$

where m and Δ are as described in Figure 2. This equation is used to calibrate the samples by use of specimens produced especially for this purpose. Equation 3 is analogous to the frequently used equation [27]

$$C = \frac{2}{3EI}\left((a + 0.6h)^3 + h^2 a\right) \qquad (4)$$

where E is the elastic modulus of the metal, h is the beam height and I is the moment of inertia of one half-beam ($I = bh^3/12$).

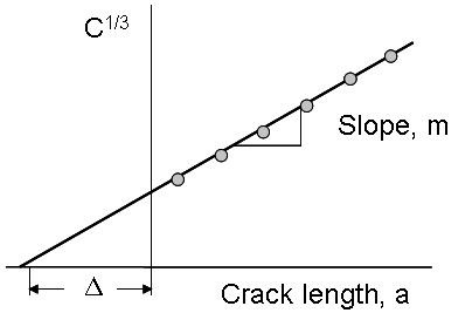

Figure 2. The relationship between compliance and crack length.

Combination of equations 1 through 3 gives [28]

$$G=\frac{3Pd}{2b}\frac{m}{C^{1/3}} \qquad (5)$$

The logarithm of G values calculated from the fatigue test data by use of the above formulation is plotted against the logarithm of crack propagation velocity da/dN, where N is the number of cycles [29], as will further be discussed in the paper. G_0 is the strain energy release rate corresponding to nearly zero crack growth rate, often assumed to correspond to 10^{-7} mm/cycle [26]. G_0 can be regarded as a fundamental parameter for quantifying the adhesion properties of metal substrate – pre-treatment – adhesive combinations.

4.3. Experimental

The substrate used in all experiments was extruded AlMgSi aluminium alloy EN-AW 6082 T6 extrusions. DCB beam dimensions used were 5x20x180 mm. The pre-treatments used were identical to those discussed in Chapter 3. The samples were degreased in alkaline degreaser Neutrasel 5269 (Henkel, Dusseldorf, Germany), diluted to 60 g/l, for 10 minutes at 60ºC. Deoxidising was performed in acidic 35 ml/l Alfideox 73 (CANDOR Sweden AB, Norrkoping, Sweden) for 4 minutes at ambient temperature. Approximately 0.5 µm of aluminium was removed from the surface during the surface cleaning. Samples were subsequently pre-treated as specified in Table 1. Two promising chromate free processes, hot AC anodising [17] and Ti/Zr-treatment [18] were investigated. Samples, which were only deoxidised before application of the organic coating, were used as the

worst case specimens for comparison purposes. Chromate conversion coating was used as reference.

The paints tested were commercial epoxy DICY (dicyandiamide) and polyester TGIC (triglycidyl isocyanurate) powder coatings provided by Jotun (Jotun Powder Coatings AS, Larvik, Norway), identical to the coatings used in Chapter 3. These paints were selected based on the information that water was not supposed to be produced during their curing. Water trapped in the coating between two metal beams would be detrimental to the test results by creating pores.

Table 1. Pre-treatment conditions.

	Ti/Zr	Chromating	Hot AC anodising
Product	Gardobond X4707/Gardolene	Alodine 6100	sulphuric acid
Time	60 seconds	2 minutes	30 seconds
Temperature	Ambient	Ambient	80ºC
Concentration	43,5 ml/l	15 ml/l	150 g/l
Conditions	pH 2,7 vigorous stirring		20 A/dm^3
Supplier	CHEMETALL GmbH	Henkel	

The powders were sprayed on the bar pairs by an electrostatic spray gun and melted at about 120ºC. The bar pairs were then joined with paint facing towards each other and using 100 μm thick spacers placed at both ends of the longest dimension and 50 mm into the end of the specimen where stress was applied. This generated a crevice in the coating layer in the sample specimen, as shown in Figure 3. Curing of paint was performed in a hot press for 20 minutes at 180ºC.

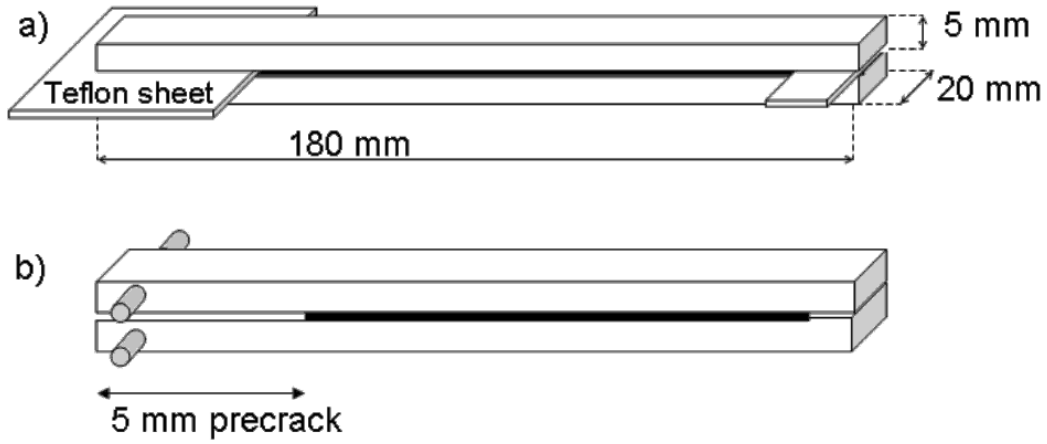

Figure 3. a) Specimen prepared for fatigue testing. A debonded zone/precrack was created with a Teflon sheet in the top end of the specimen. A 3.2 mm diameter hole was drilled in both beams. b) Teflon sheet was removed. Black area indicates the coating. 3 mm diameter pins were inserted at both upper and lower metal beam and were attached to the fatigue testing rig.

The joint was strained by cyclic tensile loading by use of MERL Mk 6 Environmental Fatigue Machine located at Hydro Aluminium Karmøy, Norway [28]. Fatigue tests were performed at 6 Hz, similar to the value used in fatigue testing of adhesively bonded DCB beams [28, 30]. A preload of 20 N was applied to maintain sufficient minimum displacement between the metal beams at the end of each cycle, as is also the usual practice in adhesive testing. The maximum peak-to-peak displacement between the beams, relative to the preload, was maintained constant at 0.9 mm at each cycle. The preload and the maximum displacement values selected in this work were lower than the values used in adhesive testing [31], due to assumed low cohesive strength of the coatings compared to the commonly used adhesives. The analysis of data according to equation 5 was based on the maximum load and displacement at each cycle.

The tests were performed in ambient conditions for a period of about 24 hours. At the end of this period the conditions were changed to 40 ºC and 95% RH. This procedure was selected to obtain information about both dry and wet adhesion from the same set of specimens. Samplings of displacement and load were made every 10 cycles the first 3000 cycles, every 100 cycles the next 3000 cycles and then every 1000 cycles for the remainder of the experiment, which lasted up to a maximum 8 days.

A calibration was performed prior to the fatigue test in order to confirm linear response of strain to applied stress and measure the parameters m and Δ in equation 3. Calibration samples were made with 50, 70, 90, 110, 130 and 150 mm spacers, giving 6 points on the calibration curve.

4.4. Results

4.4.1. Calibration

The compliance calibration curve, obtained as described above, is shown in Figure 5. For validation purposes, the measured compliance curve was compared to values calculated from equation 4 [27, 32], commonly used to estimate the compliance of DCB specimens with similar geometry. As shown in Figure 5, there was a good agreement between the measured and calculated curves.

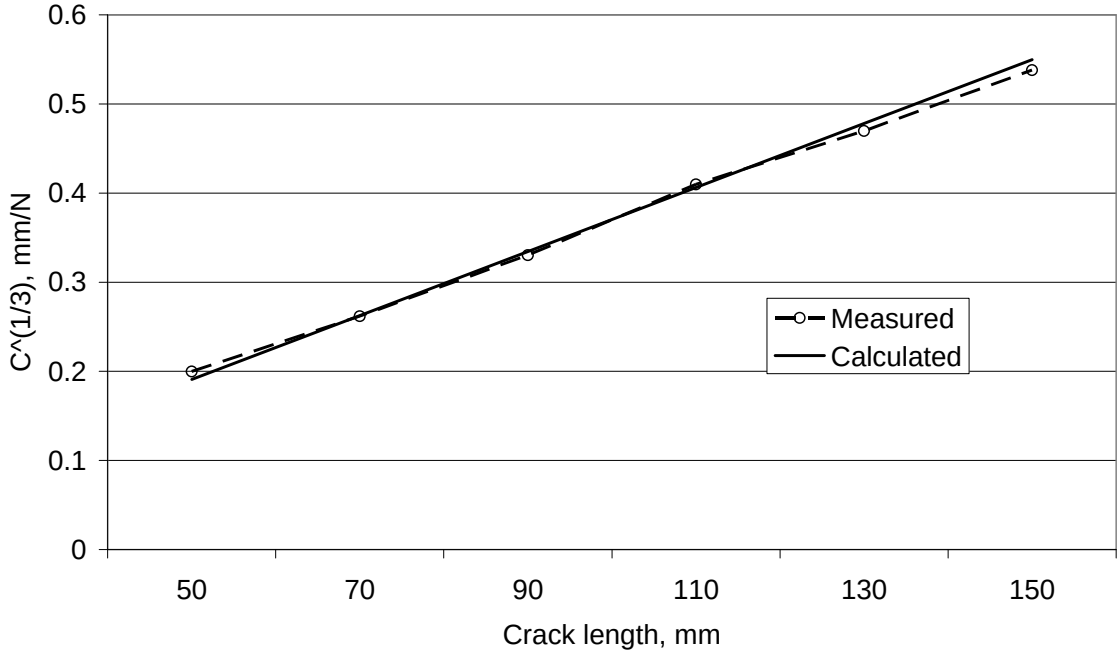

Figure 5. Comparison of measured compliance data with compliance calculated from equation 4. R^2 is 0.998.

4.4.2. Fatigue test

For demonstration purposes Figure 6a shows the measured compliance versus number of cycles for all three replicates of the hot AC-anodized

specimen. The curves were smoothed out by use of moving average statistics [33, 34] for the purpose of reducing noise during differentiation to calculate the crack velocity da/dN and G, correlation of which is given in Figure 6b. The black data points represent crack growth under ambient dry condition and the red data points after application of 40°C and 95% RH environment. The data indicate that crack growths on two of the replicates were affected by the introduction of the humid environment, and one replicate was not affected, thus exhibiting a certain scatter. The effect of humidity is deduced from a significant change in the slope of the log da/dN vs. G correlation, while the correlation for the unaffected replicate continued to follow the trend of the dry data. The threshold G_0 values obtained by extrapolating the curves to 10^{-7} mm/cycle thus indicated significant reduction of the adhesive properties of the coating in relation to the unaffected variant. A similar analysis for the three replicate specimens, which were treated with Ti/Zr conversion coating and coated with polyester paint, shown in Figure 7, indicated much smaller effect of humidity on crack growth. The da/dN vs. G correlation for the dry and wet data points converged to similar G_0 threshold values for all replicates.

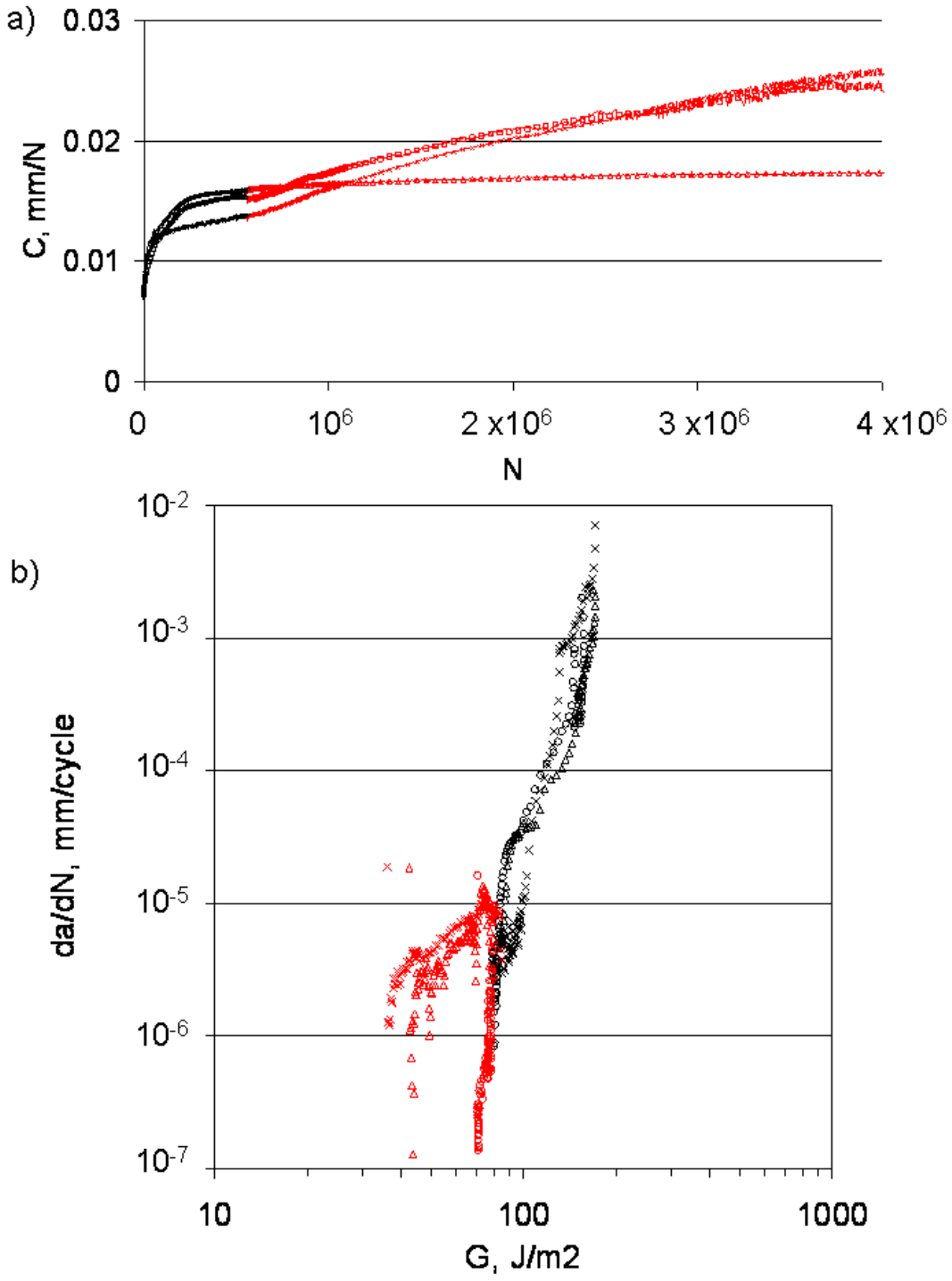

Figure 6. a) Measured compliance data for all three replicates of hot AC anodised and epoxy coated specimen. b) log da/dN vs. log G correlation obtained by moving average and fracture mechanical analysis of the compliance data. The data in black represent the dry measurements and the red after the application of the humid environment.

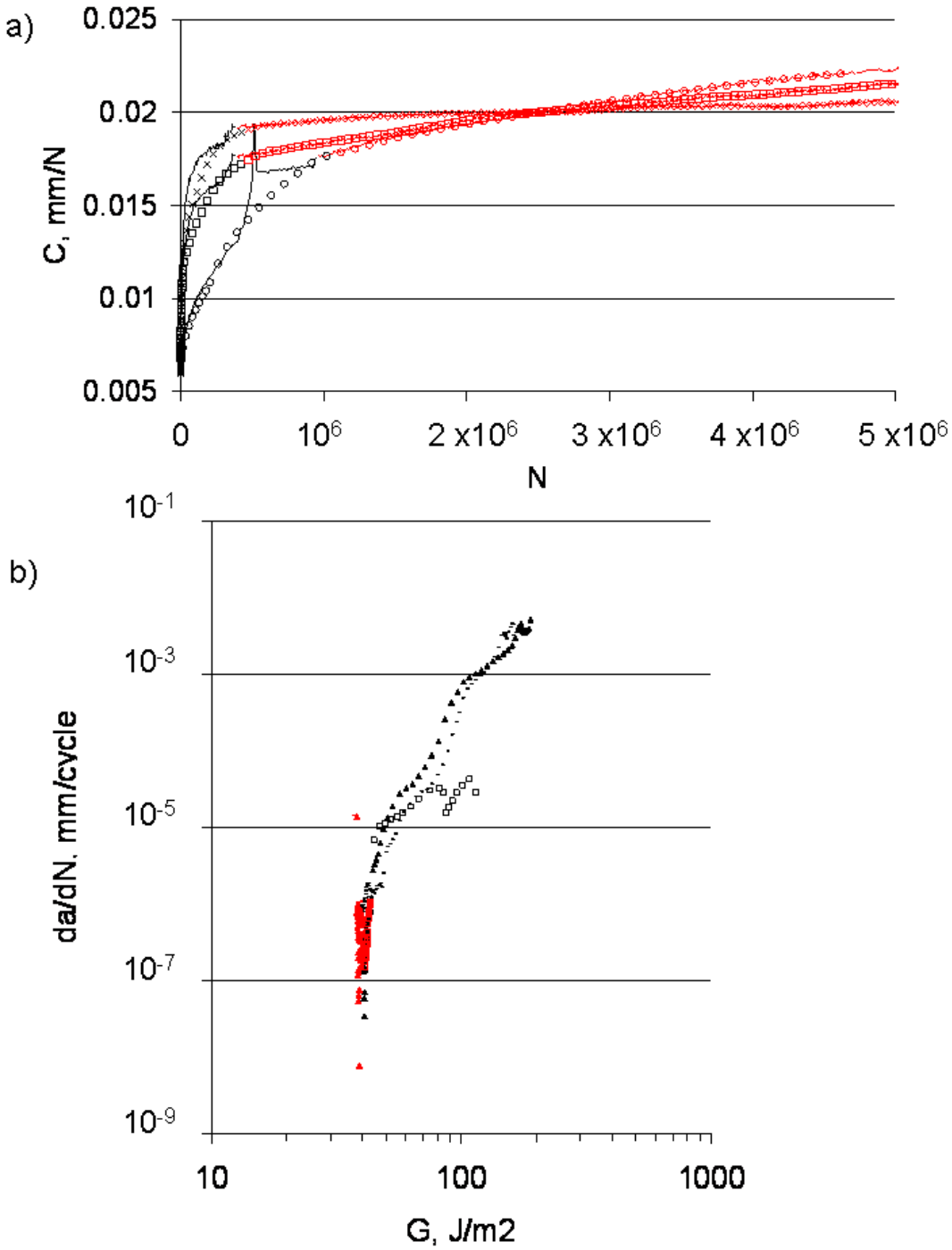

Figure 7. a) Measured compliance data for all three replicates of Ti/Zr treated and polyester coated specimen. b) log da/dN vs. log G correlation obtained by moving average and fracture mechanical analysis of the compliance data. The data in black represent the dry measurements and the red after the application of the humid environment.

Much of further data evaluation is based on the G_0 values from the da/dN – G correlations of the type shown in Figures 6 and 7. The G_0 values for all coating - pre-treatment combinations are shown in Figure 8. The error bars indicate the scatter of the data points obtained from the 2-4 replicates of each specimen type. The epoxy coated variants showed larger G_0 values than their polyester coated variants in general. The dry G_0 values were also larger than the wet values for each specimen type, although this generalization did not have a statistical basis for some of the variants based on the data scatter, especially for the polyester coated variants. For a given coating type, the difference between the G_0 values for wet exposure of the deoxidized specimens were not dramatically different from the conversion coated variants, especially for the polyester coated variant. The effect of wet exposure was not too different from that of dry exposure during the period of the test, indicating the same type of behaviour discussed for the Ti/Zr-treated variant in Figure 7. The wedge test results discussed in Chapter 3, in contrast, indicated a significant deterioration of the adhesive properties of the deoxidized specimens as a result of wet exposure, in comparison to the conversion-coated variants. In addition, the G_0 values for the hot-AC anodized and polyester coated specimens were unexpectedly lower than the G_0 values for the other variants, including the deoxidized, in contrast to the wedge test results, which indicated that the hot-AC treated specimens showed the best adhesion properties.

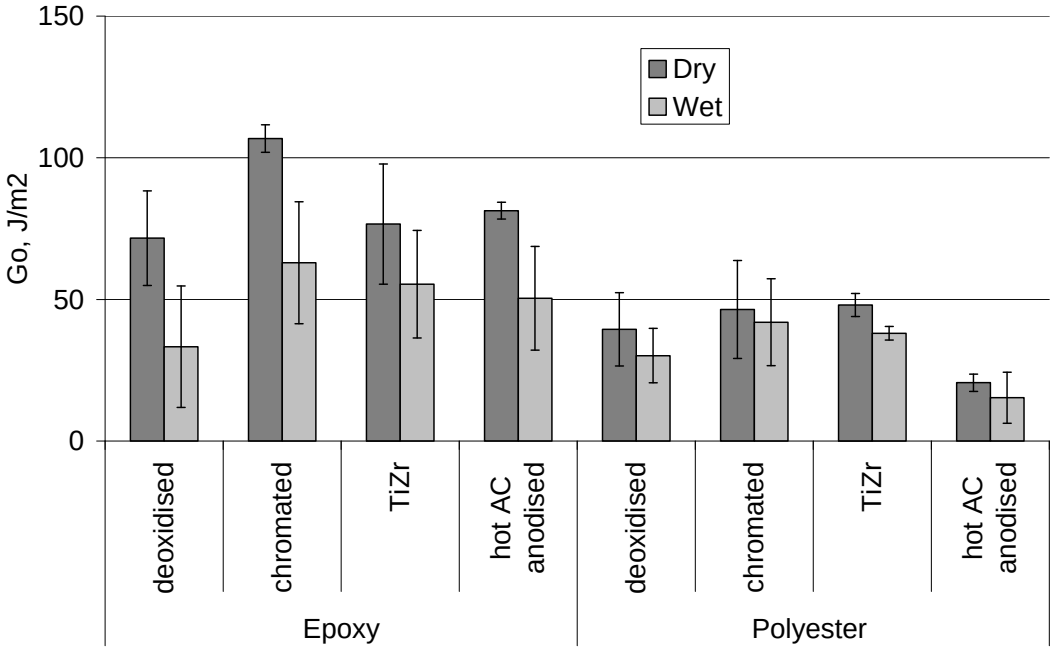

Figure 8. G_0 values for wet and dry exposure obtained from fracture-mechanical analysis of fatigue data. The error bars indicate the data scatter based on the replicate specimens used for each pre-treatment-coating combination.

4.4.3. Post-mortem analysis

The results in the foregoing Figures were based on crack lengths calculated from the compliance correlation data, rather than directly measured values. The validity of the results from Figure 8 was controlled by crack lengths measured directly from the crack surface morphologies of the beams, separated mechanically from one another after the fatigue test. The calculated and measured values indicated good agreement, as shown for the polyester coated samples in Figure 9. Comparing these results with the reciprocal of corresponding G_0 data (sum of dry and wet bars) in Figure 8 indicates also that the use of final crack length for comparison and ranging purposes must be just as valid as basing the comparison on G_0 data, although G_0 has a higher quantitative significance.

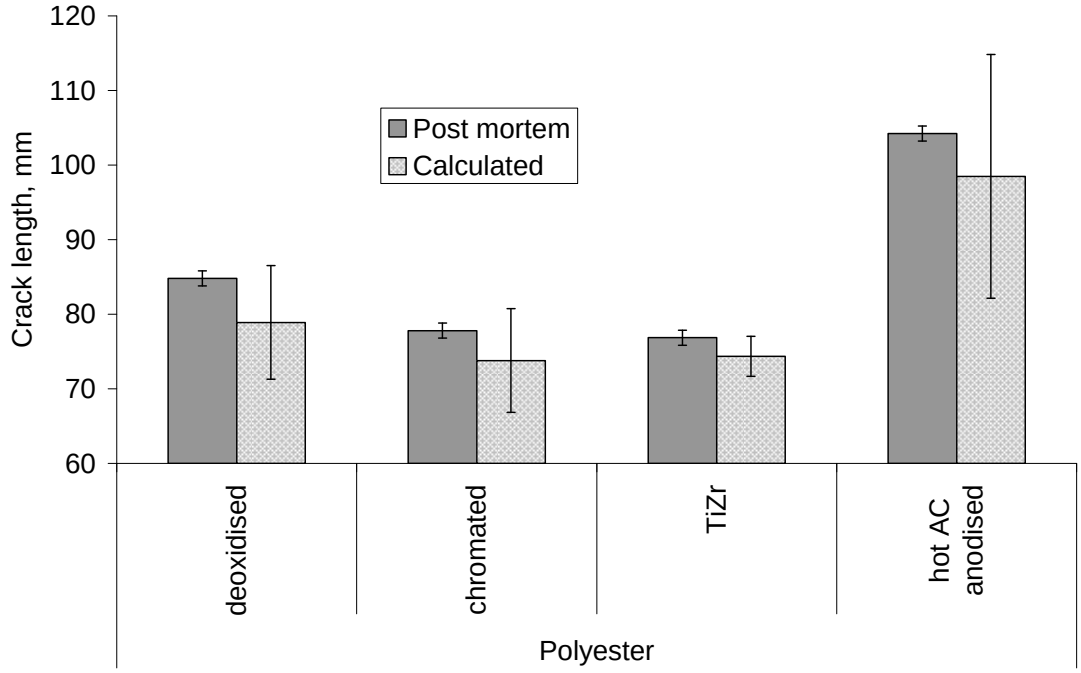

Figure 9. Crack length data obtained by *post mortem* analysis of fracture surfaces after the fatigue test compared to the corresponding crack length calculated from the compliance calibration (equation 3), based on the compliance data obtained during the fatigue test.

The *post mortem* assessment of the failure mode of samples was performed by visual inspection of the separated beam surfaces. The approximate areas of cohesive failure, near cohesive failure and adhesive failure were determined. This was based on opaque paint layer remaining on surfaces of both beams (cohesive), a translucent layer on one beam and an opaque layer on the other (near surface cohesive) and a clear metallic surface on one beam and opaque paint layer on the other (adhesive). The near surface failure mode is often observed also in fatigue testing of adhesively bonded aluminium, and it is regarded as an intermediate between adhesive and cohesive failure [35]. It was not possible to separate the wet and dry test regions. The analysis therefore included both dry and wet areas of propagation. The results, shown in Figure 10, indicated predominantly cohesive failure for the epoxy coated specimens with the exception of the deoxidized variant. Adhesive failure was more frequently observed for the polyester coated specimens, in relation to the epoxy coated specimens. However, for the deoxidized specimens, adhesive failure was clearly the more predominant failure mode for the epoxy coated samples than for the polyester coated samples. These observations are in qualitative agreement

with the wedge test data for the corresponding specimen variants, with the possible exception of the epoxy coated deoxidised values which are based on only one replicate in Figure 10.

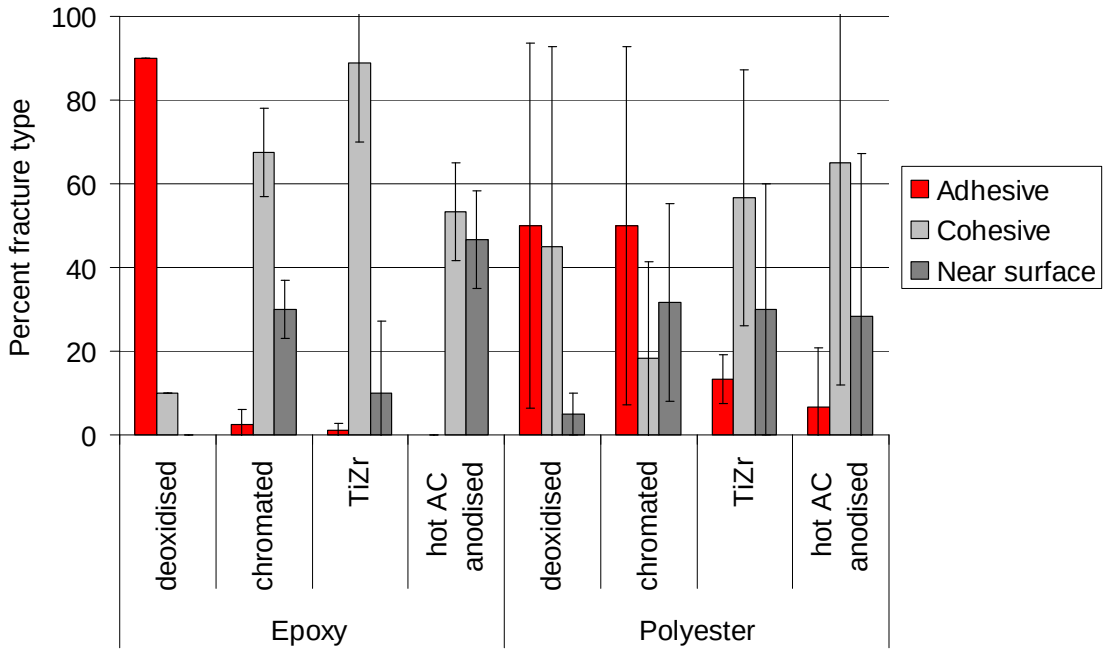

Figure 10. Failure mode of the fatigue specimens based on *post mortem* evaluation. The error bars indicate the scatter among the replicate specimens. Only one specimen of the deoxidised-epoxy combination was investigated.

4.5. Discussion: Comparison of fatigue and wedge tests

A direct comparison of wedge and fatigue tests is in principle not possible because of differences in mechanical straining and exposure of the crack tip to environment. These differences are analogous to the differences between the fracture mechanical stress corrosion cracking and corrosion fatigue testing of identical metal DCB specimens. Moreover, the wedge test data, especially crack propagation in humid conditions, could not be analysed according to the existing fracture mechanical methodology because of the error introduced during crack initiation and subsequent dry growth. Nevertheless a comparison is attempted in Figure 11 based on the final crack lengths obtained from the two tests and foregoing discussion about the validity of comparing final crack lengths instead of G_0 data. Because of the limitations indicated, the absolute crack lengths from the two tests

cannot directly be compared. However, it was still of interest to compare the crack length trends, between the pre-treatment - coating variants in one test with the corresponding trend obtained from the other test, in a qualitative manner.

The trends based on the crack length can be observed to be similar for the two tests with the possible exception of the deoxidized variants. While the wedge test indicated clearly that the deoxidized variants exhibited larger crack lengths than the conversion coated variants, the difference was less clear based on the fatigue test results. The fatigue test indicated smallest crack growth for the chromated, epoxy coated specimen, while the wedge test did not indicate a similar distinction. Another possible difference was that relatively large crack growth, indicated by the fatigue test for the hot AC-polyester combination, was not evident from the wedge test.

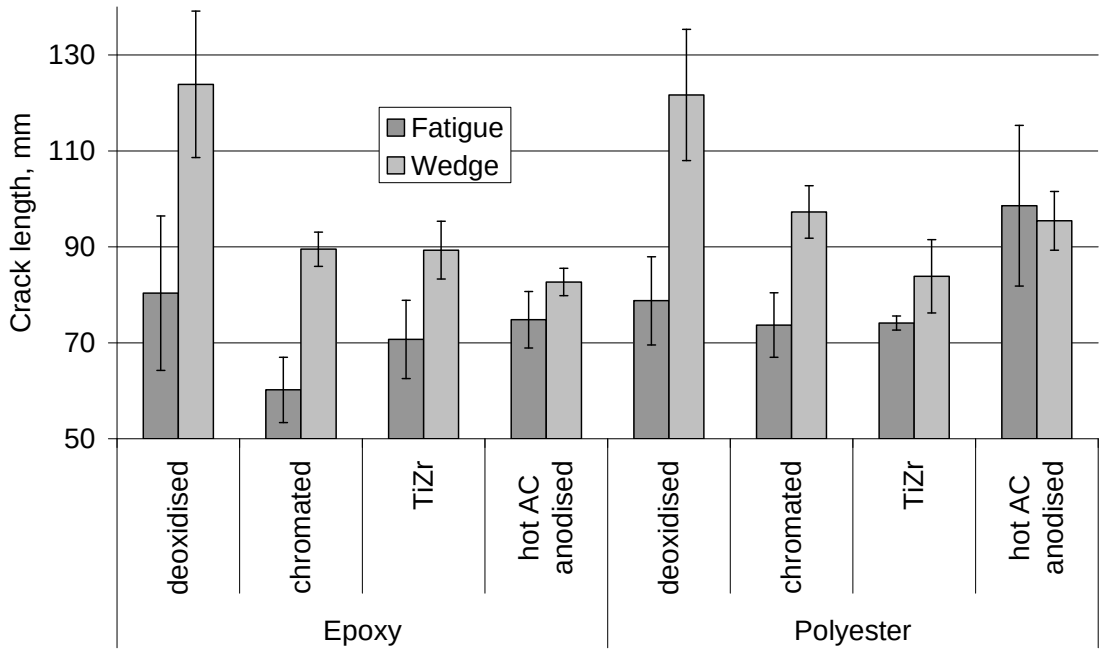

Figure 11. Comparison of the final crack lengths obtained from wedge and fatigue tests.

Additional useful information can be extracted by comparing the dry and wet crack lengths separately, as was discussed in Chapter 3 for the wedge test data. The wedge test data are obtained from the edge readings during the test and fatigue test data are calculated from the compliance calibration. A comparison of the dry data is shown in Figure 12. The wet exposure data

obtained in the similar manner are compared in Figure 13. By taking the scatter bars into consideration, it can be concluded that the trends for the fatigue and wedge test results are similar for chromated and Ti/Zr treated specimens. Both types of pre-treatments, independent of the organic coating, showed similarly favourable adhesion properties. The hot AC-anodised specimens, who showed the shortest wet crack lengths in wedge testing, exhibited longer wet crack lengths in relation to chromated and Ti/Zr-treated specimens in fatigue testing. The wet crack length obtained for the deoxidized, polyester coated specimen was unexpectedly of the same order of magnitude as the pre-treated specimens.

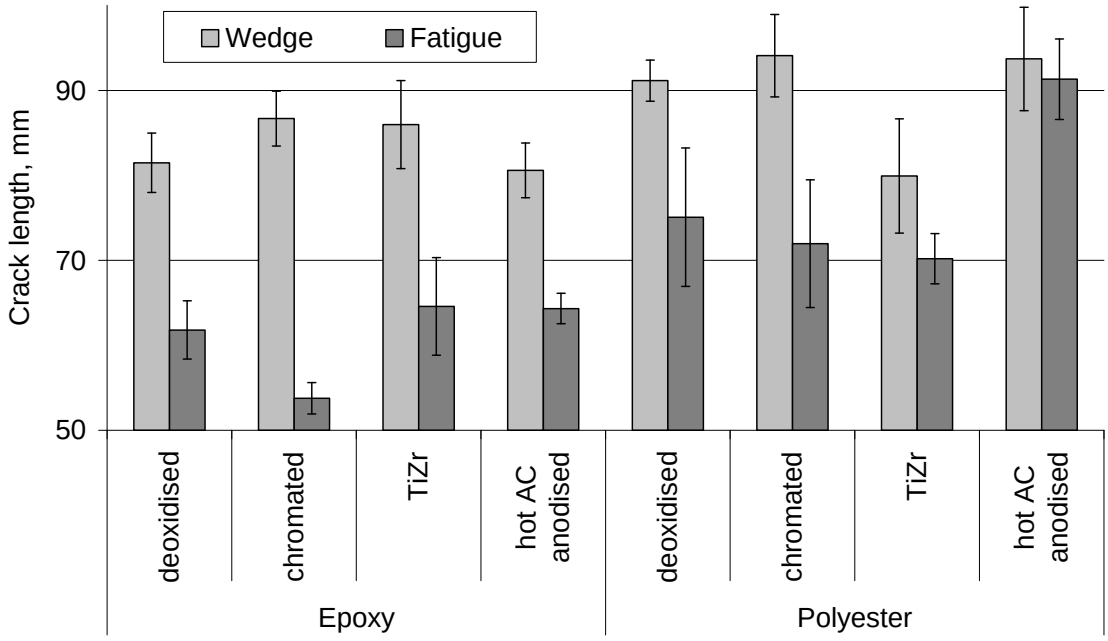

Figure 12. Comparison of crack lengths obtained by wedge and fatigue tests in dry conditions. The error bars indicate the standard deviation in the crack lengths among the replicate specimens.

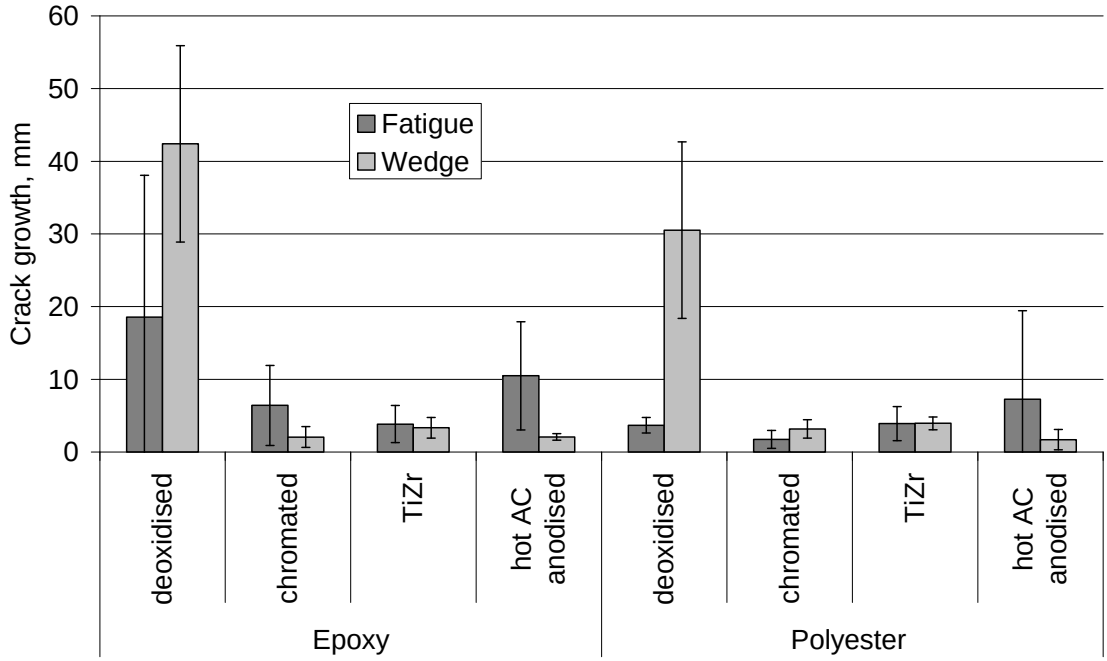

Figure 13. Comparison of crack lengths obtained by wedge and fatigue tests during exposure to the humid environment. The dry crack length is subtracted from the total crack length.

4.6. Further discussion

The fatigue test did not indicate a significant difference between any of the surface-treatment variants, including the deoxidized specimens, in contrast to more clear differences reported earlier by use of the wedge test. The G_0 values corresponding to dry exposure were in general larger than the G_0 values for wet exposure. However, the differences were not significantly large when the data scatter was taken into consideration. Crack growth during dry exposure was larger than during wet exposure, similar to the wedge test results. It is unclear whether the G reduction during wet exposure was really caused by the introduction of water. In further work submerging the specimen in water should be considered [26]. A lower dynamic load frequency can also be used. The results obtained in wet environment should be compared to separate dry measurements, to see if there is a clear effect of moisture on the adhesion threshold levels.

In most cases the failure mode was cohesive. Cohesive failure near metal substrate surface is supposed to indicate a certain weakness of the interface

[36]. However, the available information is not conclusive enough to be able to discuss the present results with reference to data available from literature. It is not clear how results based on cohesive failure should be used to discuss adhesive failure. The present results neither contribute to a better understanding of such a phenomenon. The deoxidized specimens, especially the polyester coated, did not show any worse properties than the pre-treated specimens in terms fatigue failure. Moreover, the AC-anodized samples, which showed very good adhesion properties in comparison to Ti/Zr-treated and chromated surfaces according to other tests and for adhesively bonded aluminium [17, 37], unexpectedly showed higher susceptibility to fatigue failure than the other pre-treatments in the present work. Organic coatings are also reported to adhere well on DC-anodized aluminium when evaluated by the wedge test [16, 17, 37, 38]. These results indicate that the fatigue test approach has to be investigated more thoroughly to decide about its applicability as a test method for adhesion of organic coatings on aluminium.

The epoxy-coated specimens showed higher G_0 values than the polyester coated specimens in general. Slightly better adhesion properties thus exhibited by the epoxy-coated specimens were also suggested by the crack lengths for dry exposure. However, the comparison of the wet crack lengths did not indicate any advantage for epoxy coating in relation to polyester coating. *Post mortem* observation of the crack surfaces after the fatigue test indicated largely cohesive failure for the chromated and Ti/Zr treated, epoxy coated specimens, while the polyester coated counterparts of these exhibited also partly adhesive failure.

The coatings used in this work are chosen to minimize the number of pores. However, as discussed in Chapter 3, there were significant amount of pores in the coating in DCB specimens produced in this work, which may act as stress raisers during the cyclic test. However, this problem did not appear to affect the conclusions reached in Chapters 3 and 5. The number of pores should be limited as much as possible. In further work the coatings should be cured completely and rubbed with sand paper and subsequently adhered by a suitable adhesive.

4.7. Conclusions

- Fatigue testing did not reveal reliable results for assessing the adhesion properties of organic coatings on aluminium.
- The performances of the pre-treatments during wet exposure could not be distinguished, with the possible exception of the hot AC anodising pre-treatment.
- The test parameters selected did not appear to allow sufficient water penetration into the crack area.
- The high porosity of the coating layer can induce stress raisers and enhanced crack growth.
- The failure mechanism of a coated specimen exposed to dynamic loading appeared to be fundamentally different from that subjected to a static wedge test procedure. The failure occurs faster and appears to be less sensitive towards moisture at the dynamic load frequency used in this work.
- The test method needs further development. Improvements are suggested to obtain a more reliable fatigue test. The test procedure should be designed to imitate the actual service conditions.

Acknowledgements

John Erik Lein and Nils-Inge Nilsen (SINTEF) assisted with specimen preparation. Zhiliang Zhang (NTNU) performed the nanoindenter test. Roald Lilletvedt and Jan Bersaas (Hydro Aluminium Karmøy) assisted with the fatigue test. This work was part of a Norwegian national research program entitled "Light Metal Surface Science", supported by The Norwegian Research Council, Hydro Aluminium, Jotun Powder Coatings AS and DuPont Powder Coatings.

4.8. References

1 M. Stratmann, R. Feser and A. Leng, *Electrochimica Acta* **39**, 1207 (1994).
2 A. Bautista, *Progress in Organic Coatings* **28**, 49 (1996).
3 H. Leth-Olsen and K. Nisancioglu, *Corrosion Science* **40**, 1179 (1998).
4 G. W. Critchlow and D. M. Brewis, *International Journal of Adhesion and Adhesives* **16**, 255 (1996).
5 A. J. Kinloch, *Adhesion and Adhesives: Science and Technology,* Chapman and Hall, London, (1990).

[6] O. Lunder, J. C. Walmsley, P. Mack, K. Nisancioglu, *Corrosion Science* **47**, 1604 (2005).
[7] J. V. Kloet, W. Schmidt, A. W. Hassel, M. Stratmann, *Electrochimica Acta* **49**, 1675 (2004).
[8] J. Zhao, L. Xia, A. Sehgal, D. Lu, R. L. McCreery, G. S. Frankel, *Surface and Coatings Technology* **140**, 51 (2001).
[9] M. Kendig, S. Jeanjaquet, R. Addison, J. Waldrop, *Surface and Coatings Technology* **140**, 58 (2001).
[10] G. W. Critchlow, K. A. Yendall, D. Bahrani, A. Quinn, F. Andrews, *International Journal of Adhesion and Adhesives* **26**, 419 (2006).
[11] T. Prosek and D. Thierry, *Progress in Organic Coatings* **49**, 209 (2004).
[12] T.-C. Aw, *Regulatory Toxicology and Pharmacology* **26**, S8 (1997).
[13] S. A. Katz and H. Salem, *The Science of The Total Environment* **86**, 53 (1989).
[14] O. Ø. Knudsen, Bjørgum, A., Tanem, B.S., *ATB Metallurgie* **43**, 175 (2003).
[15] K. Y. I. Oleinik S.V., *Protection of metals* **43**, 391 (2006).
[16] O. O. Knudsen, B. S. Tanem, A. Bjorgum, J. Mårdalen, M. Hallenstvet, *Corrosion Science* **46**, 2081 (2004).
[17] A. Bjørgum, F. Lapique, J. Walmsley, K. Redford, *International Journal of Adhesion and Adhesives* **23**, 401 (2003).
[18] O. Lunder, C. Simensen, Y. Yu, K. Nisancioglu, *Surface and Coatings Technology* **184**, 278 (2004).
[19] B. D. Voevodin N., Balbyshev V., Khramov A., Johnson J., Mantz R., *Materials Performance (NACE Tri-Service Conference, Orlando, Florida, USA 2005)*, 48 (2006).
[20] O. Lunder, F. Lapique, B. Johnsen, K. Nisancioglu, *International Journal of Adhesion and Adhesives* **24**, 107 (2004).
[21] B. Tepe and B. Gunay, *Progress in Organic Coatings* **62**, 134 (2008).
[22] J. A. Harris and P. A. Fay, *International Journal of Adhesion and Adhesives* **12**, 9 (1992).
[23] S. Erpolat, I. A. Ashcroft, A. D. Crocombe, M. M. Abdel-Wahab , *Engineering Fracture Mechanics* **71**, 1393 (2004).
[24] D. J. Bland, A. J. Kinloch, V. Stolojan, J. F. Watts, *Surface and Interface Analysis* **40**, 128 (2008).
[25] E. J. Ripling, Mostovoy, S.,Patrick R.L., *Materials Research and Standards*, 129 (1964).
[26] J. K. Jethwa and A. J. Kinloch, *The Journal of Adhesion* **61**, 71 (1997).
[27] S. Mostovoy, P. B. Crosley and E. J. Ripling, *Journal of Materials* **2**, 661 (1967).
[28] J. A. Harris, in *SAE VI, 6th international conference on structural adhesives in engineering*, edited by I. C. Ltd (IOM Communications Ltd, Jurys Bristol Hotel, London, UK, 2001), Vol. 2001, p. 13.
[29] H. Hadavinia, A. J. Kinloch, M. S. G. Little, A. C. Taylor, *International Journal of Adhesion and Adhesives* **23**, 449 (2003).
[30] A. J. Kinloch, M. S. G. Little and J. F. Watts, *Acta Materialia* **48**, 4543 (2000).
[31] X. X. Xu, A. D. Crocombe and P. A. Smith, *International Journal of Fatigue* **17**, 279 (1995).
[32] R. Olsson, *Composites Science and Technology* **43**, 329 (1992).

[33] D. S. Ermer and B. D. Notohardjono, *Engineering Fracture Mechanics* **20**, 705 (1984).
[34] G. P. Solomos and V. C. Moussas, *Structural Safety* **9**, 211 (1991).
[35] A. A. Roche and J. Guillemenet, *Thin Solid Films* **342**, 52 (1999).
[36] D. Arayasantiparb, S. McKnight and M. Libera, *Journal of adhesion Science and Technology* **15**, 1463 (2001).
[37] O. Lunder, B. Olsen and K. Nisancioglu, *International Journal of Adhesion and Adhesives* **22**, 143 (2002).
[38] B. Lonyuk, I. Apachitei and J. Duszczyk, *Surface and Coatings Technology* **201**, 8688 (2007).

5. Surface-analytical characterisation of adhesively failed coatings after wedge test

Abstract

Adhesion of coatings on extruded AA6082-T6 substrates, pre-treated separately by a commercial Ti/Zr system, hot AC anodising in sulphuric acid and standard chromating and coated by polyester and epoxy coatings, was investigated in Chapter 3 by use of Boeing wedge test. In this Chapter surface-analytical characterization of adhesively failed surfaces is reported. Transmission Electron Microscope (TEM) showed that both polymers were able to penetrate completely into the pores of the anodic oxide. Failed Ti/Zr-treated surfaces indicated adhesive failure by visual inspection, while characterisation by X-ray Photoelectron Spectroscopy (XPS) showed that a layer of TiO_2 and ZrO_2 was present on top of the naturally formed aluminium oxide. No change in the chemical state, compared to the originally deposited compound, had occurred which indicated the absence of any self-healing property of the coating. The failure mode was cohesive in the polyester coating, whereas with the epoxy coating the failure mode was adhesive, explaining superiority of adhesion of the Ti/Zr treatment and polyester coating combination according to the wedge and filiform corrosion tests. The failure modes of the deoxidised specimens were similar to that for Ti/Zr treated specimen, but the crack extension was significantly larger, proving deoxidised specimen to be inferior to Ti/Zr pre-treated specimen.

5.1. Introduction

In Chapter 3 a modified Boeing wedge test was used to test the dry and wet adhesion of coatings to pre-treated aluminium surfaces. The pre-treatments tested were Ti/Zr treatment, hot AC anodising and yellow chromating. Surfaces that were deoxidised alone before the application of the organic coating were also used as reference. The coatings applied were polyester TGIC (triglycidyl isocyanurate) and epoxy DICY (dicyandiamide). It was found that the Ti/Zr pre-treated specimen had the lowest final crack length of all the polyester coated specimens. The filiform corrosion resistance of this pre-treatment-coating combination, as determined by the accelerated filiform corrosion test EN-3665, was also satisfactory, similar as for hot-

AC anodised and chromated specimen. However, for the epoxy coated variants, the filiform corrosion properties of the Ti/Zr treated specimens were inferior to the chromated and hot-AC treated specimen. The corrosion resistance of Ti/Zr treated and epoxy coated specimen were similar to the deoxidised specimens. Thus, Ti/Zr treated aluminium appeared to exhibit different adhesion and corrosion behaviour depending on the type of coating used.

According to earlier results by Lunder *et al.* [1] the Ti/Zr conversion layer was inhomogeneously distributed as a thick layer on the Fe-containing cathodic intermetallic particles, reducing in thickness and becoming discontinuous on the aluminium matrix with distance away from the intermetallic particles. The layer did not significantly reduce the cathodic activity of the intermetallic particles, indicating that the Ti/Zr layer itself did not provide appreciable corrosion protection. Since compatibility between the aluminium substrate, pre-treatment and organic coating is an important subject of interest, the different behaviour with the different pre-treatment-coating combinations was worthy of further investigation. Emphasis was on the chromate free Ti/Zr and hot-AC anodising pre-treatment processes.

The failure mode is commonly assessed by visual inspection of the specimen after adhesion tests [2-5]. In wedge and fatigue tests, good adhesion is expected to be associated with cohesive failure of the organic coating in dry environment [4, 5]. However, visual inspection may lead to concluding adhesive failure for cases where cohesive failure occurs very close to the metal surface, *i.e.*, determination of the true locus of failure is not always possible by visual inspection alone. An interphase region in the polymer adjacent to the metal has been detected, where the composition of the epoxy is altered compared to the bulk composition by chemical segregation of components in the polymer interphase, such as adhesion promoters and pigment particles [6]. Such an interphase region may determine the adhesion properties of the specimen during wet exposure, *i.e.,* this region can be a preferential failure site. An important step in the determination of the effect of adhesion therefore will be to investigate the true locus of failure by use of surface sensitive techniques.

The chemical nature of fracture surfaces was investigated by X-ray photoelectron spectroscopy (XPS) to determine the locus and mode of failure [4, 5]. Although it has a limited lateral resolution, XPS has a high

depth resolution; it can give chemical characterization of nanometer thick layers at the metal surface and reveal oxidation states and bonding properties of the species present [4, 7]. Remnants of coating, pre-treatment and corrosion products on a fractured surface will reveal information, which can be helpful in determining the failure mode. Investigation of the background noise in the XPS spectra can also reveal useful information about thin composite films. A rising background at higher binding energy, relative to the peak itself, will indicate inelastic processes in the surface signal and thereby indicate coverage of the signal by a thin layer of another element [8-10].

The extent by which the coating interacts with the modified oxide, especially pore filling capability, can be assessed by transmission electron microscopy (TEM) investigation of cross-sectional foils of the surface by use of electron energy loss spectroscopy (EELS) capability [6, 11-13], also called energy filtered TEM (EF-TEM). EELS is well suited to detect specimens containing light elements such as carbon and oxygen and thereby determine the penetration depth of the coating into the oxide [13]. TEM in scanning mode, combined with EDS mode, is used to gain elemental information on the elemental composition of the interface region.

The objective of this Chapter is to determine the locus of failure along the metal - modified oxide - coating interphase region by using the surface-analytical techniques mentioned above and thereby explore the reasons for the observed differences in the performance of the pre-treatment - coating combinations found by use of the wedge test reported in Chapter 3.

5.2. Experimental

5.2.1. Surface treatment.

The substrate used in all experiments was aluminium alloy EN-AW 6082 T6 extrusions. Two promising chromate free processes, hot AC anodising [2] and a Ti/Zr-based treatment [1] were investigated. Samples, which were only deoxidised before application of the organic coating, were used as the worst case specimens for comparison purposes. Chromate conversion coating was used as reference.

The samples were degreased in alkaline degreaser Neutrasel 5269 (Henkel), diluted to 60 g/l, for 10 minutes at 60ºC. Deoxidising was performed in acidic 35 ml/l Alfideox 73 (CANDOR Sweden AB) for 4 minutes at ambient temperature. Approximately 0.5 µm of aluminium was removed from the surface during the surface cleaning. Samples were subsequently pre-treated as specified in Table 1. The paints tested were commercial epoxy DICY (dicyandiamide) and polyester TGIC (Triglycidyl isocyanurate) provided by Jotun Powder Coatings. Preparation of the DCB specimens and the wedge test was performed according the procedure described in Chapter 3.

Table 1. Pre-treatment conditions.

	Ti/Zr	Chromating	Hot AC anodising
Product	Gardobond X4707/Gardolene	Alodine 6100	sulphuric acid
Time	60 seconds	2 minutes	30 seconds
Temperature	Ambient	Ambient	80ºC
Concentration	43,5 ml/l	15 ml/l	150 g/l
Conditions	pH 2,7 vigorous stirring		20 A/dm^3
Supplier	CHEMETALL GmbH	Henkel	

5.2.2. Electron microscopy

Field emission scanning electron microscope (FE-SEM) analysis was performed using a Hitachi S-4300 SE equipped with X-ray EDS capability. Transmission electron microscopy (TEM) was used for cross section imaging of the post failure interfaces. A JEOL 2010F with an Oxford EDX system and GATAN GIF2000 for filtered imaging was used. Energy Filtered Transmission Electron Microscopy (EF-TEM) was performed to obtain maps of elemental distribution and chemical information. In addition to energy filtered TEM there were also performed scanning TEM (STEM).

The TEM specimens were prepared by gluing the fractured surfaces of the beams together, by use of an epoxy adhesive. A selected small part was cut from the fracture area, and thin foils, which were approximately 50 nm in

thickness, were prepared using a Reichert-Jung ultramicrotome with a diamond knife. The foils were gathered on Cu-grids and covered with a carbon film before analysing in the microscope.

EDS line scans were performed, and these provided elemental insight in a small area of nm scale. A 1 nm probe was used for the EDS measurement. Moving average statistics were performed to smoothen out the signal noise. The moving average procedure performed an averaging of 10 measurement points at each measurement step. The procedure smoothens out measurement noise.

5.2.3. XPS

The specimens were cut into smaller size to fit into the specimen holder of the XPS instrument, as well as to limit the air evacuation time. Approximately 25x20 mm pieces were cut from each side of the DCB specimen, as illustrated in Figure 1, for analyzing the fracture surface. The samples were taken from regions fractured during wet exposure wedge test, where adhesive failure mode was visually determined.

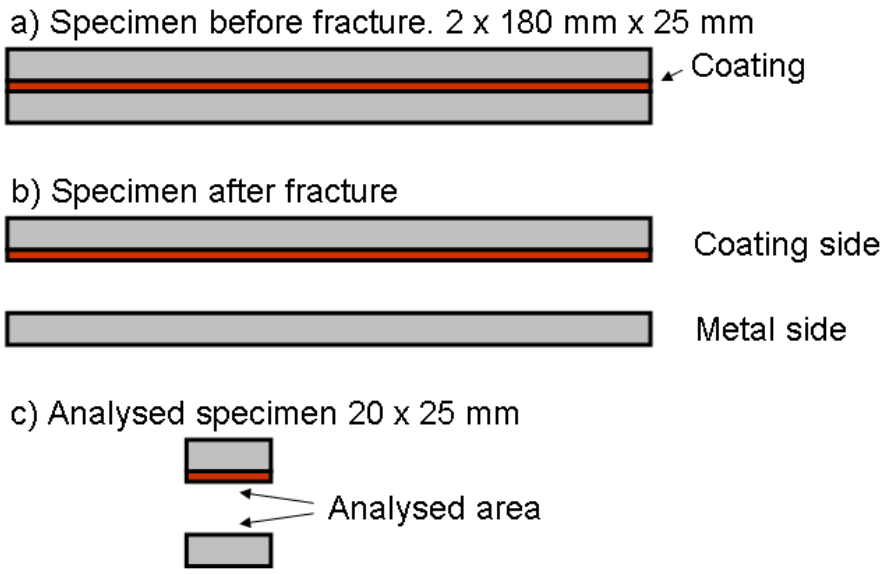

Figure 1. The wedge test specimen a) before and b) after fracture. Coating side and metal side of the specimen are indicated. Figure c) illustrates the samples that were obtained from the regions which were fractured during adhesion test. Both fracture surfaces were investigated by XPS.

XPS analyses were performed in plane view on a Thermo VG Scientific (East Grinstead, UK) Sigma Probe spectrometer. The twin anode MgKα X-

ray source (hν = 1253.6 eV) was used at 300 W. The area of analysis was ~1 mm in diameter. Pass energy was set to 150 eV for all survey spectra and 50 eV for the acquisition of high resolution, core level spectra. Acceleration voltage was 15 keV for all data acquisition. Quantitative surface chemical analyses were calculated from the high resolution, core level spectra following the removal of a non-linear (Shirley) background. The manufacturer's Avantage software was used, which incorporated the appropriate sensitivity factors and corrected for the electron energy analyser transmission function. The software also was used to perform signal smoothing for peak fitting.

The XPS experiments were performed by use of one of the 6 replicate specimen of each pre-treatment-coating combination. In addition to spot analyses, line scans were performed on the fracture surfaces. The line scans will however not be presented, since the variations along the surfaces analysed were small. These results verified the consistency of the spot analyses reported.

In addition to post failure investigations a freshly prepared Ti/Zr treated aluminium specimen was investigated, without the organic coating and exposure in climate chamber, for comparison purposes. The specimens had to be stored for 24 hours before testing due to transportation. No sputtering was conducted in order to determine the amount of airborne contamination.

5.3. Results

5.3.1. FE-SEM

FE-SEM analysis of the pre-treated surfaces before application of the organic coating was performed to verify that the surface morphology of the pre-treated specimen was in agreement with the results found by others. Intermetallic particles were still present on deoxidized samples, and a few etch-pits were observed. Chromated aluminium specimen had the characteristic porous and cracked oxide structure [14]. Ti/Zr treated aluminium specimen had, similar to deoxidised specimen, remnants of intermetallic particles and some etch-pits. No evidence of Ti or Zr could be detected by EDS. Evidence of Ti and Zr was expected on the intermetallic cathodic particles according to the findings by Lunder *et al* [1], originating from thick Ti/Zr oxide layer due to localised processes favouring Ti and Zr

precipitation [15, 16]. However, the presence of a thin Ti/Zr layer, not detectable by EDS, cannot be ruled out, as verified by TEM investigation reported below. The apparent absence of Ti/Zr on the samples may be explained by the procedure of conversion coating application, which was performed at shorter times and lower pH compared to the earlier results [1, 15], leaving a thinner layer of Ti and Zr on the specimen. In this work the application procedure specified by the supplier was followed. The absence of a porous oxide on the surface rules out mechanical interlocking as a likely adhesion mechanism for these samples. Any adhesion enhancement caused by the pre-treatment layer must therefore be due to primary or secondary bonds generated between the oxide and the polymer. Hot AC anodised aluminium, on the other hand, had a porous surface structure allowing penetration of the polymer, thereby enhancing the adhesion by mechanical interlocking effects. Small pore diameter could possibly hinder filling of the pores by the polymer, and thereby limit adhesion caused by mechanical interlocking [4] and the availability of binding sites.

Post mortem investigation of the cracked specimen by use of SEM was difficult because of charging caused by aluminium oxide and coating remains. Carbon coating was used to limit the charging problems. However, the failure during wet exposure was mainly cohesive, *i.e.*, the interface region was covered by a thick polymer coating layer, and SEM was therefore not a useful tool for investigating the interface region underneath the coating.

5.3.2. TEM

Cross sectional samples of the post failure surface was investigated by scanning TEM and energy filtering (EF-TEM). TEM investigations were performed for Ti/Zr treated and hot AC anodised specimens.

The results from TEM investigations, although not shown, indicated that Ti/Zr coating was discontinuous in agreement with the earlier studies [1]. Most of the EDS line scans across the coating-metal interphase region on cross-sectional foil samples did not detect Ti/Zr. The presence of Ti/Zr was only occasionally detected, indicating the presence of discrete Ti/Zr particles or film.

EF-TEM carbon and oxygen map and linescans of the hot AC anodised specimen with polyester coating, shown in Figure 2, indicated that the

polymer penetrated the oxide with decreasing concentration towards the metal surface. The penetration depth was probably limited by the small diameter of the pores and the high viscosity of the binder. Figure 3 shows the analysis of hot AC anodised epoxy coated interphase region with similar results. The penetration of the porous oxide indicated a very strong adhesion between the polymer and the oxide, both due to large amount of binding sites caused by the large surface area [17] and possibly also enhanced mechanical interlocking [18, 19]. Comparison of Figure 2 and 3 indicated that the penetration depth of the polyester and epoxy coatings into the pores of the hot-AC layer was similar. The adhesion test results for these coatings, reported in Chapter 3, indicated also no distinguishable difference in the adhesion properties.

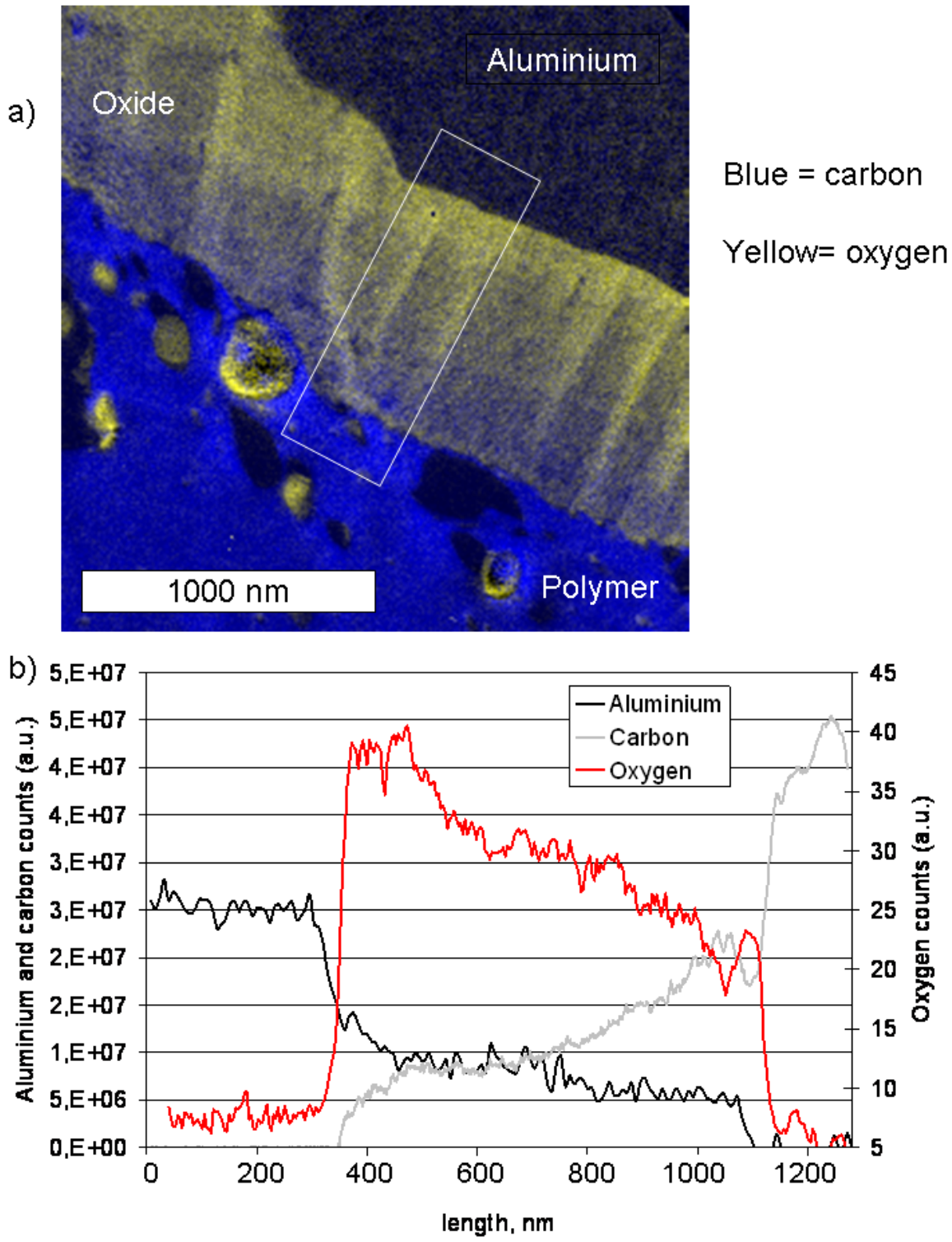

Figure 2. a) TEM cross section showing penetration of polyester coating (blue) into the porous structure of the hot AC anodized surface (yellow). b) EF-TEM elemental line scan of the analysis area marked in (a). The line scans are measured from the aluminium surface towards the polymer.

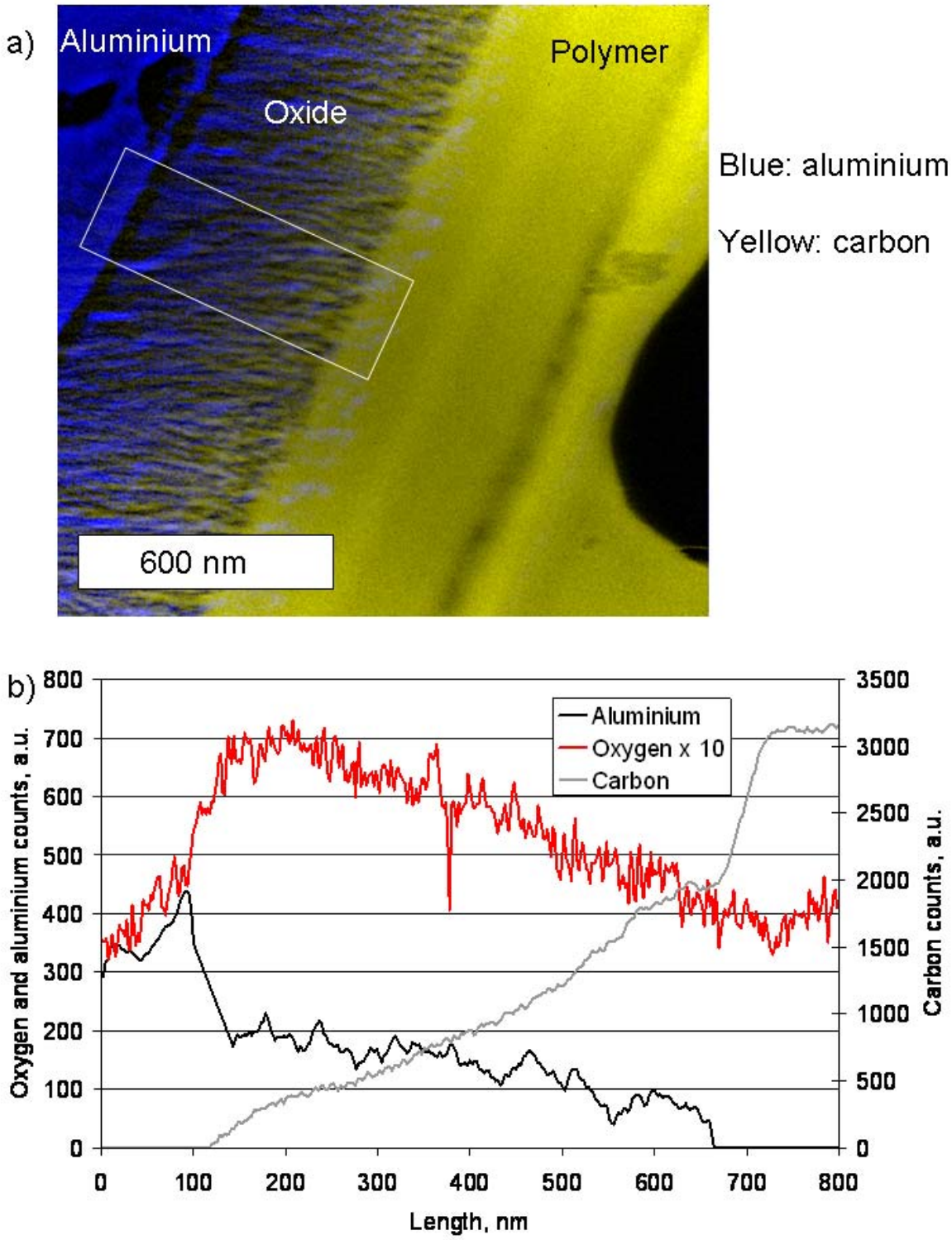

Figure 3. TEM cross section showing penetration of epoxy coating into the porous structure of the hot AC anodized surface. b) EF-TEM elemental line scan of the analysis area marked in (a). The line scans are measured from the aluminium surface towards the polymer.

5.3.3. XPS

In order to find the differences arising from remnants of organic coating on the fractured surfaces, the surface of a freshly prepared specimen with Ti/Zr conversion coating (without organic coating) is compared to the wedge-test cracked surface of a Ti/Zr-treated, coated specimen, in Figure 4. The quantification of the element concentrations on the surface is shown in Figure 4 a) and b), and the survey spectra are shown in Figure 4 c) and d). The unsputtered specimen was chosen to investigate the level of the background carbon contribution, shown in Figure 4 d). From the element percentage illustration in Figure 4 a) it is seen that the concentration of carbon increased after exposure, which is related to presence of the polymeric coating. The aluminium and oxygen signals were reduced in the presence of coating (Figure 4a). The signal for fluorine was completely absent after exposure. Silicon, titanium and zirconium were reduced significantly for the exposed specimen (Figure 4b). The source of F was HF which is present as pickling agent in the solution bath used for application of the Ti/Zr layer. The reason why the F-peak was not visible on the exposed specimen is not clear. Ti and Zr were detected both on the fresh and exposed surfaces, but in reduced amounts after exposure. In contrast, nitrogen and barium signals were detectable only after exposure. Nitrogen is present in the curing agents used, and barium sulphate is common filler for the polymeric coatings. Nitrogen from the atmosphere will not adsorb on the metal surface. Therefore, the source of nitrogen is the polymer components only. Since the N-peak is also located away from the other peaks in the spectrum, nitrogen was selected as marker for coating remains.

The carbon content on the unsputtered and freshly prepared specimen was assumed to be due to atmospheric carbon containing species, adsorbed on the sample surface. Its concentration was calculated as 33 atomic % which agreed with the concentration of carbon measured on a fresh aluminium specimen [20].

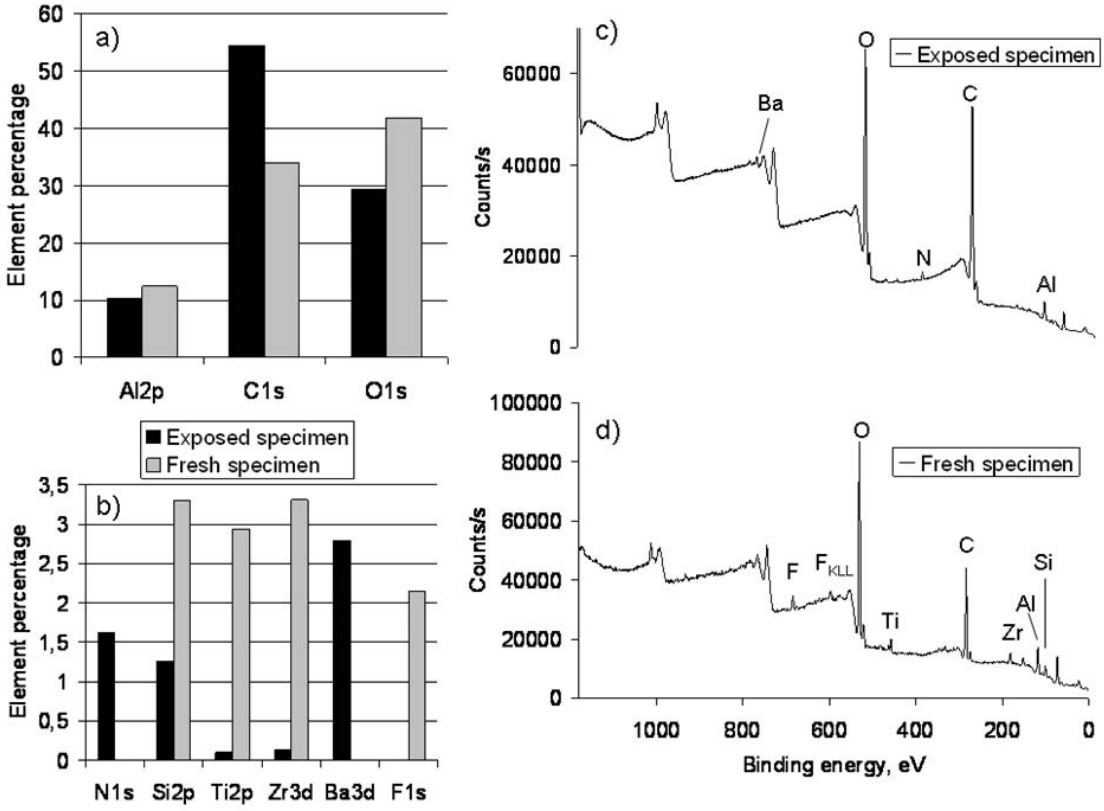

Figure 4. Comparison of the elemental composition, in atomic percent, of Ti/Zr treated specimen. Fresh specimen was characterised shortly after pre-treatment. Exposed specimen was coated with polyester TGIC. It was characterised after long term wet adhesion testing. Figures a) and b) show the differences in chemical composition of the surface of the exposed (black bars) and fresh specimen (grey bars). Figure c) and d) show the survey scan of the surfaces. Relevant peaks are marked.

The only specimens with mainly adhesive failure, judged from visual inspection, were the deoxidised specimen and some regions of the Ti/Zr treated specimen (see Figure 10, Chapter 3). XPS was performed on what appeared to be bare metal on the fracture surface, to look for coating remnants and to find any evidence of changes in the composition of the pre-treatment layer. Figure 5 shows parts of the metal side survey scans of the Ti/Zr treated specimen and the deoxidised specimen. The complete spectra for the coating and metal side of the failed surface, deoxidised metal and bulk coating are shown in Appendix A. The binding energies of the specific peaks in the spectra are listed in Table 2. Figure 5 compares the characteristic XPS peaks of the polyester coated specimen and the epoxy coated specimen in combination with the two pre-treatment methods.

Although aluminium was visible on all specimens, and the failure mode visually was determined as adhesive, the Figure showed residue of coating on all specimens, revealed by the nitrogen signal.

To decide whether the peaks related to a homogeneous layer or to patches of polymer inside cracks and other surface features, the background ratio between the carbon and aluminium peaks must be investigated. If the ratio increases with the binding energy, it indicates that inelastic scatter takes place by retardation of Auger electrons from the surface, resulting from the presence of another substance on the metal [9, 21]. In the present case such a layer must be a carbon-containing layer or an oxide. The ratio increase appeared on the polyester coated specimen in Figure 5 a) and b), but not on the epoxy coated specimen in Figure 5 c) and d). A layer therefore appeared to be present on the polyester coated specimen, at least partly. Since the surfaces compared were expected to be covered by the same type of oxides, the inelastic scattering of the Auger electrons on the polyester coated specimens was attributed to the presence of polyester on the metal surface. Moreover, the data in Appendix A indicated the absence of aluminium on the coating side of all types of fractured interfaces, which showed that the fracture did not propagate in the aluminium oxide layer in any of the specimens.

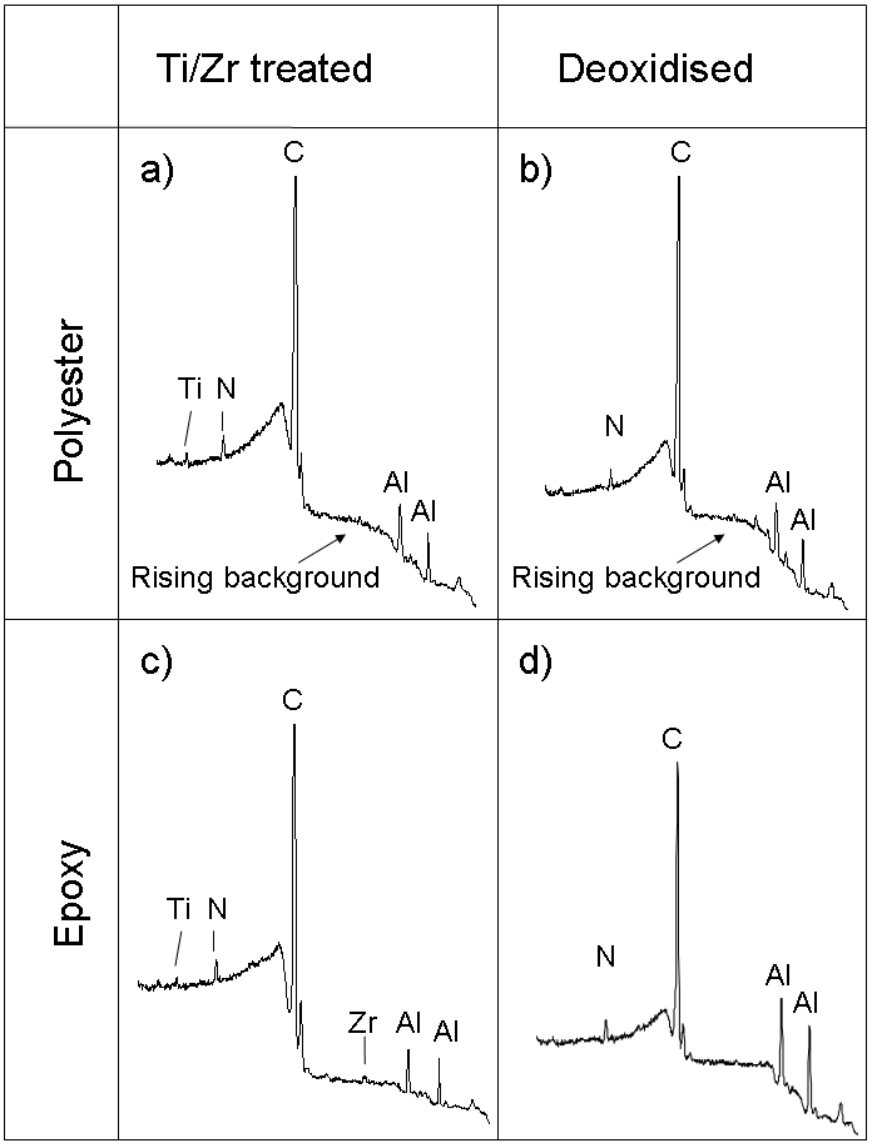

Figure 5. XPS spectra for the metal side of deoxidised and Ti/Zr treated specimens, coated with polyester and epoxy, after adhesive failure. Binding energy is on the x-axis and counts/s is on the y-axis. Specific changes of interest (see text) in the background noise are marked with arrows. The peak locations are listed in Table 2.

Table 2. The peak energies identified in this work are listed. All spectra are calibrated with respect to the carbon signal. The values are in agreement with the values reported in the literature [22]

Element	Binding Energy (eV)
Al2s	120
Al2p	74.8
Zr3d	185
N1s	401
C1s	286.4
Ti2p [23]	459

In summary, the deoxidised and Ti/Zr treated specimens, coated with polyester, showed evidence of an organic film (polyester) on the fracture surfaces after the wedge test. Whether the layer was uniform or consisted of patches could not be assessed by these investigations. An analogous film was not detected on the fracture surfaces of the epoxy coated specimens.

The magnified peaks of Ti and Zr from the coating side and metal side are shown in Figure 6 to investigate further the locus of fracture on the adhesively failed surfaces of Ti/Zr-treated specimens. These were obtained from the survey spectra shown in Figure A1 in appendix A. Both Ti and Zr peaks were resolved on the metal side of the fractures, as shown in Figure 6 a)-d). Only the Zr peak was clearly detectable on the coating side of the polyester coated sample, shown in Figure 6 f). The Ti peak on the coating side (Figure 6 e)) was not clearly resolved. No clear evidence of Ti or Zr could be seen on the polymer side of the epoxy coated specimen, as shown in Figure 6 g) and h). This suggests that fracture propagated along the interface between the coating and oxide for the epoxy coated specimen. The fracture appeared to occur partly within the oxide for polyester coated specimen. It should be emphasised that these conclusions are based on one sample of each pre-treatment-coating combination, but the results from several measurements from different locations of the same fracture surface were consistent with one another.

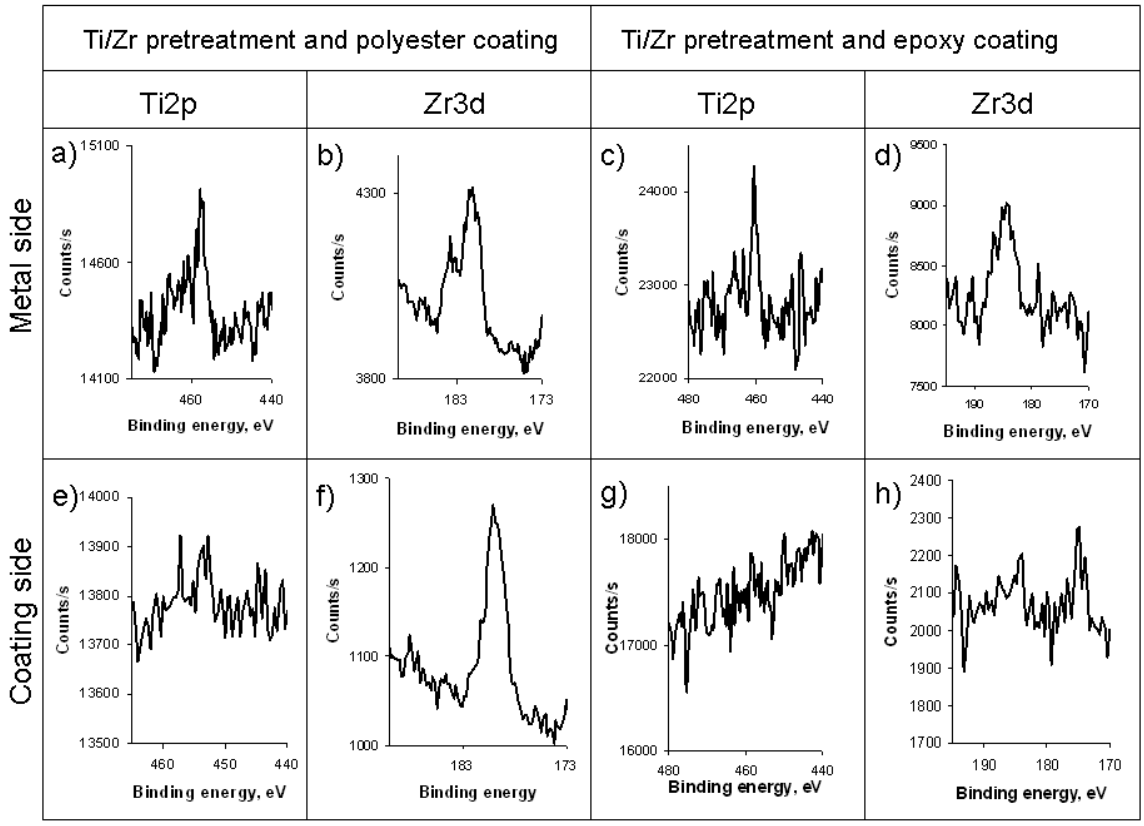

Figure 6. Ti and Zr peaks for the epoxy and polyester coated specimen on the coating and metal sides, magnified at relevant binding energies from the survey scans of the fracture region, seen in Appendix A, Figure A1 c)-f).

The Zr and Ti signals in Figure 6 a) and 6 b), respectively, which look like double peaks, were analysed in more detail in Figure 7 by use of freshly prepared specimens. The analysis was performed to find the chemical state of the Ti and Zr elements, in order to find evidence of any possible self healing mechanism. Self healing is a protection mechanism known for chromating and causes the layer to act as a corrosion inhibitor of the substrate material [14, 24, 25]. The self healing mechanism results in a negative change in the oxidation state of Cr, from +6 to +3 valences. The binding energies of the zirconium signals at 185.2 eV and 182.6 eV correspond to ZrO_2 [26]. Metallic Zr, which would appear at about 178 eV, was not observed, nor was other oxidation levels. Similarly, the titanium peaks at 464.3 eV and 458.8 eV correspond to TiO_2 [23]. Other alternatives for Ti would be Ti_2O_3 or TiO, in addition to metallic Ti [23]. The most stable states of Ti and Zr are both at oxidation level +4, which corresponds

to TiO_2 and ZrO_2. Self healing properties or reduction of the species were therefore not expected.

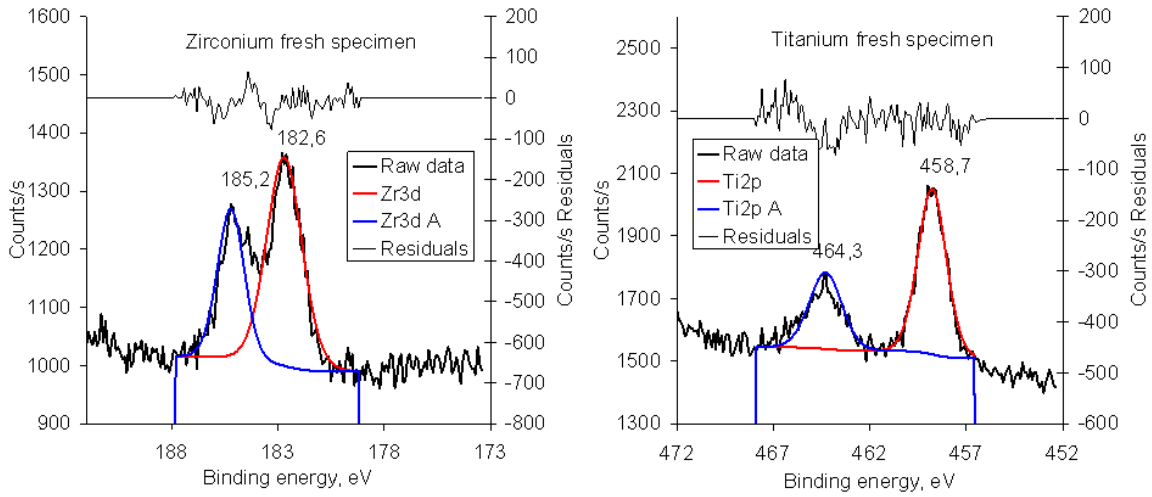

Figure 7. Titanium and zirconium high resolution peaks each consisting of two sub-peaks with distinct binding energies. The residual plot related to curve- fitting of the peaks is shown, revealing no additional structures, which validate the calculated fit.

5.5. Discussion

The Ti/Zr pre-treatment has been reported not to protect against corrosion in general [1, 15]. In this work, Ti/Zr treatment did not give acceptable filiform corrosion properties when coated with epoxy (Chapter 3), while both the adhesion and corrosion properties were satisfactory when coated with polyester. Corrosion performance of the Ti/Zr-treated surface appears therefore to depend on the compatibility between the pre-treatment and the coating. Good adhesion probably also contributes positively to corrosion resistance. The reported capability of Ti/Zr pre-treatment to prevent hydration may furthermore improve both adhesion and corrosion resistance [17]. This may be an explanation of the filiform corrosion resistance and good adhesion properties of Ti/Zr-treated and polyester coated specimens found in this work.

Ti and Zr could be detected only at a few locations along the specimen by TEM characterisation, rather than as a continuous film, in agreement with earlier work stating that the pre-treatment results in the precipitation of

discrete Ti and Zr oxide particles and not a uniform conversion layer [1]. The XPS data indicated remnants of organic coating on the metal side of the crack surface. Similar organic coating remnants were detected also on the deoxidised specimen, although deoxidised specimens showed a far more severe adhesion loss in the wedge test. Although it is likely that the organic coating layer can adhere to the surface without a Ti/Zr conversion layer, the presence of Ti/Zr oxides on the surface had a clear positive effect on wet adhesion. A thick Ti/Zr oxide layer is known to precipitate on cathodic intermetallic particles [1], which means the oxide layer is of variable thickness across the surface. It is unclear how such islands of TiO_2 and ZrO_2, without corrosion inhibiting effect, protect the coated surface against filiform corrosion, as reported in Chapter 3. It has been suggested that hydration resistance may be a factor in enhancing the adhesion properties of pre-treatments [27], and this characteristic may be applicable to Ti/Zr oxides.

Remnants of organic coating were not detected on the fracture surface of epoxy coated specimen. In addition Ti or Zr was not detected on the coating side, suggesting that the failure occurred along the organic coating - oxide interface. It should be noted, however, that the predominant failure mode (more than 80%) of the Ti/Zr treated and epoxy coated specimen was cohesive, as illustrated in Figure 10 in Chapter 3. The reason for the differences in failure mode of epoxy compared to polyester may be explained by the pH expected to develop at the surface during wet exposure, as shown in Chapter 6. Epoxy coating, which adhered strongly to the aluminium substrate when dry, deteriorated in the presence of humidity. TGIC cured polyester was found to have a slightly lower pH compared to epoxy DICY in aqueous environment (Chapter 6), suggesting that the tertiary amines provide fewer sites for hydrogen reception and thereby lower pH. Similarly, Roche *et al* [28] found that aluminium oxide was damaged by the alkaline diamine curing agent of an epoxy coating. These results demonstrate the importance of compatibility between the pre-treatment and coating in terms of chemical behaviour during wet exposure.

For deoxidised specimen the failure mode was mainly determined as adhesive from the visual inspection. A clear nitrogen signal was visible in the XPS spectra for both polymers, and this indicated remains of coating on the metal side. For the polyester coating the fracture signature indicated presence of a thin layer of coating on the metal side. Even though the thin layer indicated enhanced adhesion between the coating and the metal

surface, the extensive crack growth proved that the enhanced bond strength was not sufficient to maintain adhesion. This could be related to a limited hydration resistance of the deoxidised specimen, compared to Ti/Zr treated specimen.

5.6. Conclusions

- The location of failure on the polyester coated specimen, both deoxidised and Ti/Zr treated, was partly within the polymer but very close to the interface. The Zr signals from the coating side revealed that the adhesion failure of the Ti/Zr treated specimen occurred also partly in the deposited Ti/Zr layer.
- Both polymers penetrated into the pores of the AC anodized surface. The mechanical interlocking effect and the properties of the oxide/polymer composite formed significantly improved the adhesive properties of the interface.
- Ti/Zr oxide pre-treatment improved the adhesion and corrosion properties of the surface compared to deoxidised specimens without conversion coating. However, the improvement was not to the same degree as for the hot AC anodised surface. The Ti/Zr layer appeared to improve adhesion more for the polyester coating than for the epoxy coating.

Acknowlegdements

Professor John F Watts provided access to the XPS instrument and valuable discussion of the results obtained at the University of Surrey. Steve Hinder and Marie-Laure Abel are acknowledged for their generous assistance with the XPS work. Antonius van Helvoort and John Walmsley of SINTEF, Trondheim performed the TEM work. Bjørn Steinar Tanem (SINTEF) prepared the TEM samples.

5.7. References

1. O. Lunder, C. Simensen, Y. Yu and K. Nisancioglu, *Surface and Coatings Technology*, **184**, p. 278 (2004).
2. A. Bjørgum, F. Lapique, J. Walmsley and K. Redford, *International Journal of Adhesion and Adhesives*, **23**, p. 401 (2003).

3. M. Fernando, W. W. Harjoprayitno and A. J. Kinloch, *International Journal of Adhesion and Adhesives*, **16**, p. 113 (1996).
4. A. J. Kinloch, M. S. G. Little and J. F. Watts, *Acta Materialia*, **48**, p. 4543 (2000).
5. M. L. Abel, A. N. N. Adams, A. J. Kinloch, S. J. Shaw and J. F. Watts, *International Journal of Adhesion and Adhesives*, **26**, p. 50 (2006).
6. D. Arayasantiparb, S. McKnight and M. Libera, *Journal of adhesion Science and Technology*, **15**, p. 1463 (2001).
7. D. J. Bland, A. J. Kinloch, V. Stolojan and J. F. Watts, *Surface and Interface Analysis*, **40**, p. 128 (2008).
8. J. E. Castle, H. Chapman-Kpodo, A. Proctor and A. M. Salvi, *Journal of Electron Spectroscopy and Related Phenomena*, **106**, p. 65 (2000).
9. J. F. Watts, Wolstenholme, J., *An introduction to surface analysis by XPS and AES*, John Wiley and Sons, Chichester, UK (2003).
10. S. Tougaard, *Applied Surface Science*, **100/101**, p. 1 (1996).
11. K. Siangchaew, Libera, M. , *Microscopy and Microanalysis*, **3**, p. 530 (1997).
12. D. Williams, Carter, C., *Transmission electron microscopy*, Plenum Press, New York, USA (1996).
13. D. Arayasantiparb, S. McKnight and M. Libera, *Journal of Adhesion*, **76**, p. 353 (2001).
14. O. Lunder, J. C. Walmsley, P. Mack and K. Nisancioglu, *Corrosion Science*, **47**, p. 1604 (2005).
15. J. H. Nordlien, J. C. Walmsley, H. Osterberg and K. Nisancioglu, *Surface and Coatings Technology*, **153**, p. 72 (2002).
16. F. Andreatta, A. Turco, I. de Graeve, H. Terryn, J. H. W. de Wit and L. Fedrizzi, *Surface and Coatings Technology*, **201**, p. 7668 (2007).
17. A. Pizzi, Mittal, K.L., *Handbook of adhesive technology*, CRC Press, New York, USA (2003).
18. A. J. Kinloch, *Adhesion and Adhesives: Science and Technology,*, Chapman and Hall, London (1990).
19. W. Brockmann, O. D. Hennemann and H. Kollek, *International Journal of Adhesion and Adhesives*, **2**, p. 33 (1982).
20. C. Scheuerlein and M. Taborelli, *Applied Surface Science*, **252**, p. 4279 (2006).
21. J. E. Castle and A. M. Salvi, *Journal of Electron Spectroscopy and Related Phenomena*, **114-116**, p. 1103 (2001).
22. Chastain, J., *Handbook of X-ray photoelectron spectroscopy : a reference book of standard spectra for identification and interpretation of XPS data*, Perkin-Elmer, Eden Prairie, Minnesota USA, p. 254 (1992).
23. D. Gonbeau, C. Guimon, G. Pfister-Guillouzo, A. Levasseur, G. Meunier and R. Dormoy, *Surface Science*, **254**, p. 81 (1991).
24. J. Zhao, L. Xia, A. Sehgal, D. Lu, R. L. McCreery and G. S. Frankel, *Surface and Coatings Technology*, **140**, p. 51 (2001).
25. J. V. Kloet, W. Schmidt, A. W. Hassel and M. Stratmann, *Electrochimica Acta*, **49**, p. 1675 (2004).
26. T. Marinova, A. Tsanev and D. Stoychev, *Materials Science and Engineering: B*, **130**, p. 1 (2006).

27. R. Comrie, PhD Thesis, in *Department of Pure and Applied Chemistry*, University of Strathclyde, Glasgow, UK (1998).
28. A. A. Roche, J. Bouchet and S. Bentadjine, *International Journal of Adhesion and Adhesives*, **22**, p. 431 (2002).

Appendix A

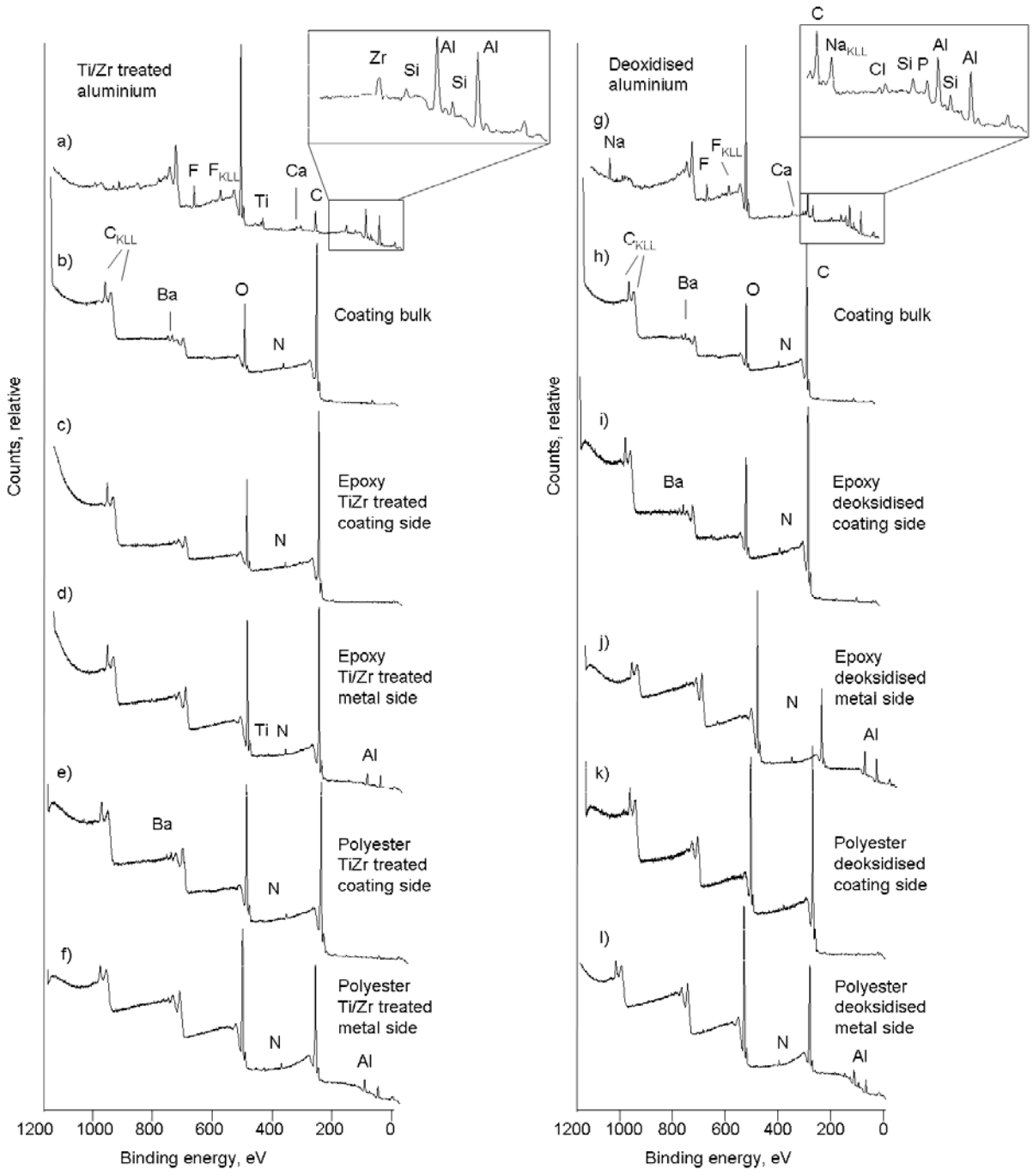

Figure A1. XPS spectra for deoxidised and Ti/Zr treated specimen surfaces after wedge test. Both sides of all 4 pre-treatment - coating combinations tested in XPS are shown. The pre-treated metal surfaces in a) and g) are sputtered for 20 seconds with argon to reduce the carbon contamination peak.

6. Effect of molybdate additions on adhesion of organic coatings on aluminium

Abstract

Application of organic coatings directly on metal surfaces without the use of surface pre-treatmentby conversion coatings poses advantages in cost reduction and eliminating the use of often toxic chemicals. In view of the stability of aluminium oxide in aqueous environment, the use of a slightly acidic coating is suggested. The compatibility of a polyester primid powder coating, pigmented with MoO_3, with an AA 6082-T6 aluminium substrate, was thus investigated. Commercial polyester TGIC and epoxy DICY powder coatings were also tested for comparison purposes. The pre-treatmentwas limited to alkaline degreasing and an acidic deoxidising process. Wet adhesion properties of the coating and the corrosion resistance of the coated surfaces were tested by use of a modified Boeing wedge test and EN 3665 filiform corrosion test, respectively. The wedge test procedure was adapted from the fracture-mechanical methodology commonly used in evaluating the durability of adhesively bonded metal surfaces. The adhesion properties of the MoO_3-pigmented coating were superior to the commercial coatings, whereas the corrosion properties were only slightly improved. It was demonstrated that organic coatings with improved compatibility with the aluminium surface can be developed by introducing simple modifications to the existing commercial coating systems.

6.1. Introduction

In order to enhance adhesion and protect against corrosion, conversion coatings are used on aluminium before applying organic coatings. Chromating [1-5], chromic acid anodising [6] and chromate pigmented polymeric coatings [7] have been widely used and proven both to enhance adhesion and prevent corrosion. However, the carcinogenic effects restrict the use of chemicals containing chromium (VI) [8, 9], and there is a significant effort for finding alternative pretreatments [5, 10, 11]. Anodising, especially hot AC, is a promising alternative to chromating, producing a thin, porous aluminium oxide on the surface for added

improvement of adhesion [12, 13]. Titanium and zirconium based pretreatments are the chromate free alternatives with the fastest growing market volume at present [14-16]. However, the Ti/Zr treatments appear not to be as robust as chromating and hot AC anodising, and they need to be validated for specific alloy-coating combination prior to any new application [14].

In a comprehensive study of filiform corrosion susceptibility of painted copper-free rolled aluminium alloys, the coated substrate was claimed to be corrosion resistant to atmospheric exposure, as long as the substrate surface was properly cleaned before application of the organic coating, even without the need for conversion coatings [17]. It was thus concluded that conversion coatings may be necessary more for improved adhesion than improved corrosion resistance for the type of alloys tested [17].

Most of the organic coatings available on the market are developed for steel. The alkaline environment generated by the selection of pigments and fillers in these coatings is not optimal for the aluminium substrate, which is stable at an appreciably lower pH (4.5 – 8) compared to steel (≥ 9) [18]. These coatings usually do not provide the desirable adhesion and corrosion protection if applied directly to the aluminium surface, without any conversion coating. It is therefore not surprising that chromating is a robust conversion coating for aluminium alloys, since its oxides are stable in alkaline environment [18].

The purpose of this work is to investigate the alternative of eliminating the conversion coating by modifying the organic coating so as to make it more compatible with the properties of the aluminium substrate. The approach was to prepare powder coatings with moderately soluble acidic pigments. It was also desirable to mimic the self healing property of chromate [1, 7, 19]. The alternatives suggested for chromate in conversion coatings are trivalent chromium, molybdate, permanganate and cerate salts [20]. Incorporating these ionic species into the coating is limited by their solubility and colour. Permanganate, *e.g.*, is dark purple and cannot always be used for aesthetic reasons.

Molybdate was selected based on its acidic properties and moderate solubility [20]. Earlier results about its use in sol-gel coatings [20, 21] and the incorporation of molybdate in anodised oxide of aluminium [22] were also taken into consideration. MoO_3 is stable at pH below 3. At higher pH it

is either reduced to MoO_2 or dissolved as MoO_4^{2-} [18]. Reduction into MoO_2 suggests capability for oxide repair on aluminium in the manner suggested for chromate [6, 21, 23]. MoO_3 is however also toxic [24], but it is not absorbed in organisms to the same extent as chromium oxide, CrO_3, which is both mutagenic and carcinogenic [8]. The purpose of the present Chapter is, therefore, to investigate the effect of molybdenum on the adhesion and corrosion properties of model polyester primid powder coatings. Different concentrations of molybdenum were investigated, also in combination with other types of pigments.

The adhesion test methodology used is based on crack growth on bonded double cantilever beam type specimens (DCB) [25], so called Boeing wedge test. The wedge test method [25-30] is investigated because of its simplicity, which does not require a significant investment, *e.g.*, in relation to widely used fatigue test [25, 31]. Water must enter the substrate/coating interface to measure wet adhesion. Correlation to in service failure is desirable, which means that the test should imitate real stress and exposure as much as possible. The wedge test is reported to be a reliable method for measuring wet adhesion of adhesives, compared to the shear and peel tests [25], in terms of correlation with outdoor exposure [32]. This might be due to the slow crack opening under constant but low stress, which allows water to access the stressed interface during the test. The constant access of moisture to the stressed region thereby allows the effect of water to be measured. Another advantage of the wedge test is the inexpensive and simple equipment. Own experience with wedge and fatigue tests in this work (Chapters 3 and 4) also indicated a higher reliability for the wedge test in the assessment of wet adhesion of organic coatings on aluminium.

In addition to the wedge test for measurement of wet adhesion, an accelerated filiform corrosion test [33] was used since corrosion resistance also is an important parameter with respect to durability of painted surfaces. The selected filiform corrosion test is frequently used based on reports about satisfactory correspondence between the results obtained from this accelerated test and the field test data [34].

6.2. Experimental

6.2.1. Selection and preparation of model coatings.

The model powder coating used was based on a primide cured polyester binder. The basic ingredients and composition for all the model coatings were 570 grams Uralac P 865 (resin provided by DSM Resins, Zwolle, Holland), 30 grams Primid XL-552 (curing agent provided by EMS Chemie AG, Domat, Switzerland), 9 grams Resiflow PV 88 (flow agent provided by Worlee Chemie GmbH, Hamburg, Germany) and 2.5 grams benzoin, which inhibits pore formation. Pores trap water and degrade the coating properties [35, 36]. This formulation is based on a recipe suggested by the curing agent supplier EMS Chemie AG.

White titanium oxide (TiO_2 rutile) and barium sulphate (colourless $BaSO_4$) [37] were selected as fillers for the model coatings because they are frequently used in commercial powder coatings, *e.g.*, in the commercial coatings used as reference in the present work. Seven different model coating formulations were tested, as summarised in table 1. These are labelled according to their pigment content, and these designations are used throughout the paper. The commercial products used as reference were an epoxy with DICY curing agent and a polyester with TGIC curing agent. Further information about the composition of these coatings was not available. The commercial coatings will be referred to as "epoxy pigmented" and "polyester pigmented" since they are coloured and opaque. Three replicate specimens were used in testing the model coatings. Six replicates were used in testing the commercial coatings.

Table 1. Type and composition of pigments added in preparing the polyester primid model coatings. Numbers are in grams, total weight per coating is 2.8 kg.

Coating name	Titanium oxide	Barium sulphate	Molybdenum oxide
TiO_2	300		
$BaSO_4$		340	
$BaSO_4$/Mo 1%		340	28 (1%)
$BaSO_4$/Mo 2%		340	56 (2%)
$BaSO_4$/Mo 4%		340	112 (4%)
TiO_2/Mo 5%	180		140 (5%)
TiO_2/Mo 10%	70		280 (10%)

6.2.2. Surface pre-treatment.

The substrate used in all experiments was extruded aluminium AlMgSi alloy EN-AW 6082-T6. The samples were degreased in alkaline degreaser Neutrasel 5269 (Henkel, Dusseldorf, Germany), diluted to 60 g/l, for 10 minutes at 60 ºC. Deoxidising was performed in acidic 35 ml/l Alfideox 73 (CANDOR Sweden AB, Norrkoping, Sweden) for 4 minutes at ambient temperature. Approximately 0.5 μm of aluminium was removed from the surface during the surface cleaning. The organic coatings were applied without any further pre-treatment on the as deoxidized surfaces.

6.2.3. Preparation and testing of DCB specimens.

ASTM D 3762-03 wedge test [38] was used, as modified and investigated in Chapter 3 of this thesis, and applied to painted aluminium [39]. The metal beam dimensions for the DCB specimens were 5x20x180 mm. The bar thickness was selected with consideration of the adhesive strength of the coatings. The powders were sprayed on the bar pairs by an electrostatic spray gun and cured at about 180ºC for 20 minutes. The bar pairs, with the painted surfaces facing each other, were then glued together with the epoxy based structural adhesive Betamate XD4600. 100 μm thick spacers were placed at each end, as shown in Figure 1. Curing of the adhesive was performed in a hot press for 20 minutes at 180ºC. Teflon was used as the spacer at one end of the specimen to generate about 5 cm long crevices in the adhesive layer, as shown in Figure 1, into which the wedge was

inserted. This procedure included an important improvement relative to the earlier procedure described in Chapter 3, in which the surfaces of the specimens with melted powder were pressed directly together with the 100 μm spacers and then cured as above. A separate adhesive was not used for joining the cured painted surfaces in the earlier procedure. The new procedure significantly reduced trapped voids in the coating, formed by water release during curing. The results to be reported for the commercial coatings, available from the study in Chapter 3, were obtained by use of the earlier procedure, in which the cured coatings included a significant volume fraction of trapped voids.

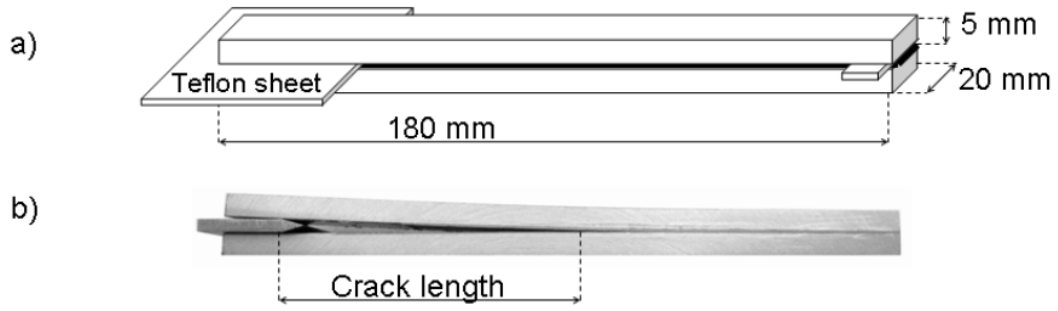

Figure 1. a) Sketch of the coated and glued double cantilever beam specimen with the Teflon spacer. b) Photograph of a DCB specimen after the wedge is inserted.

The wedge was inserted 20 mm into the crevice in the coating layer using a programmable drilling machine at a speed of 1 mm/s. After 24 hours of storage at ambient conditions, 3 to 6 replicates of each coating type were placed in a climate chamber maintained at 40°C and 82% RH for 1000 hours. The crack growth was determined by monitoring the crack length visible on the edge of the sample by use of a stereo microscope at predetermined time intervals until no further crack propagation was detectable. After the test was performed, the specimens were cracked apart and the mode of failure was established by visual inspection. The initial crack lengths obtained after 24 hours of stabilising at ambient conditions were used as a measure of dry adhesion properties, while the crack growth during wet exposure was used to evaluate the wet adhesion properties.

6.2.4. Corrosion testing.

Filiform corrosion testing was performed on four replicates of each coating according to EN 3665 [33]. A scribe was made through the coating to

expose a thin stripe of bare metal surface. Corrosion was initiated by adding droplets of 16 wt% hydrochloric acid in the scribe for ½ to 2 minutes, until corrosion reaction was visible. The excess hydrochloric acid was then carefully wiped off with tissue paper, and the samples were placed in a climate chamber for 1000 hours at 40 ºC and 82% RH. The number of filaments per unit length of scribe (filament density) and the length of longest filament of all the parallels were determined to assess susceptibility to filiform corrosion.

6.2.5. pH measurement.

The coating pH was measured by exposing free coating films in water. Cured free films were obtained by coating a Teflon plate and subsequent curing under the same conditions as specified above. The coating films peeled off the Teflon plate were cut into small pieces of about 0.1-0.3 cm^2. About 1g of coating pieces was subsequently immersed in 50 ml distilled, ion exchanged water for about one week. Water condensation during the exposure period was prevented by use of condensers attached to the flask openings. The pH change in the water, resulting from leaching of chemicals from the paint flakes, was then determined. Before pH measurement the water was purged with nitrogen for 1-2 hours in order to remove dissolved CO_2.

6.2.6. ICP-MS analysis.

The inorganic components of the commercial epoxy and polyester coatings were investigated by Inductively Coupled Plasma – Mass Spectroscopy, ICP-MS. The analysis was performed on the water used for the pH test described above, immediately after the pH measurement. The analysis was focused on the elements Ca, Ba, Zn, Cu, Mg and Ti in order to determine the presence of common fillers and pigments for organic coatings, such as TiO_2, $CaCO_3$, ZnO and $BaSO_4$.

6.3. Results and discussion

6.3.1. Adhesion test.

Figure 2 shows the dry crack lengths obtained after 24 hours of stabilization in ambient laboratory atmosphere after the insertion of the wedge. The Figure includes the values obtained both from readings along

the edge of the specimens and from the *post mortem* arrest marks on the crack surface of separated sample bars at the end of complete adhesion tests. In view of the scatter between the readings for the replicate specimens, the results obtained by the two methods were not too different, except for the fact that the edge readings were in general slightly smaller than the *post mortem* readings, as also observed and discussed in Chapter 3. The Figure indicates that the TiO_2-containing coatings gave the best dry adhesion resistance independent of the molybdate content. Dry resistance of the $BaSO_4$-containing coatings decreased with increasing molybdate content to a level similar to the resistance of the commercial coatings.

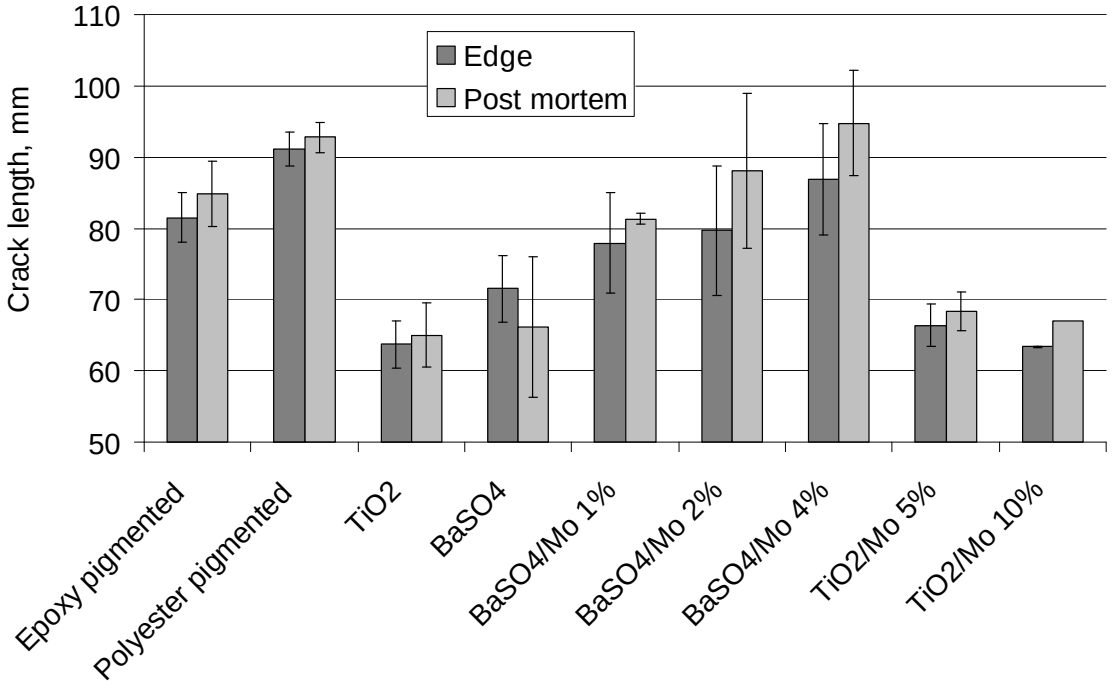

Figure 2. Dry adhesion results. Crack length data obtained under ambient conditions 24 hours after wedge insertion, comparing edge and *post mortem* measurements.

Figure 3 shows crack length data obtained during exposure in the climate chamber. The Figure illustrates the standard way of reporting crack growth data, *i.e.*, total crack length, found from the edge, is plotted as a function of time. As can be observed readily, the crack length data are essentially dominated by the initial dry growth obtained as a result of wedge insertion. The specimens, that were coated with commercial powder coatings, exhibited monotonic crack growth toward complete specimen failure, while

the crack lengths on other specimen variants more or less reached steady-state values after about 5 days of exposure.

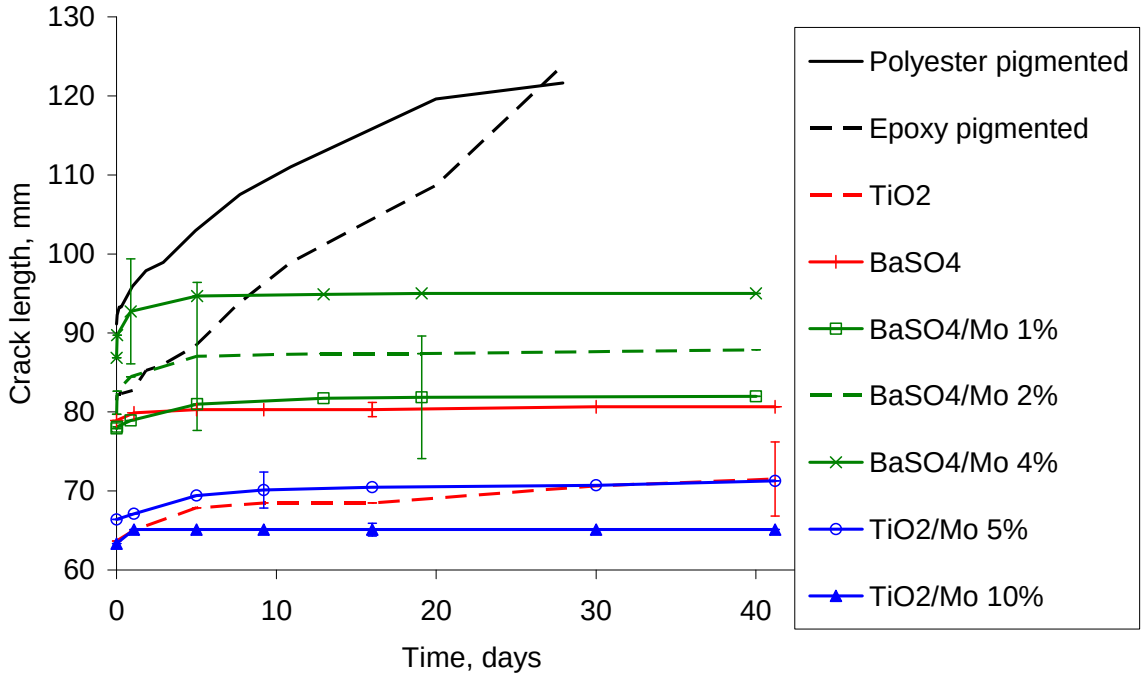

Figure 3. Average crack length vs. time obtained from the wedge test of all sample variants, as a result of exposure in the climate chamber. Typical error bars for the pretreatment-paint combinations are shown at different periods of measurement to avoid overlap. The crack lengths were measured at the specimen edge.

In order to obtain a more realistic idea about wet crack growth alone, the curves in Figure 3 were normalized by subtracting the initial dry crack lengths and replotted in Figure 4. This approach reduces the quantitative significance of the data for further fracture mechanical analysis, as discussed in Chapter 3. In view of significant scatter, it was still not possible to distinguish the role of molybdate in the model coatings. This is confirmed also by the steady-state length data shown in Figure 5, based on the edge measurements. However, the *post mortem* data, also included in Figure 5, exhibited a statistically clear reduction in the wet crack growth of the samples containing the molybdate. There was no observable effect of molybdate concentration in the range investigated.

The error in the crack lengths obtained by subtracting the dry lengths from the wet lengths based on edge measurements was probably amplified by

taking the difference of two large numbers, each of which was already associated with large uncertainty limit. The *post mortem* data, which were directly measured on the separated bare surfaces, were therefore much more reliable in reaching conclusions about wet adhesion based on the wedge test.

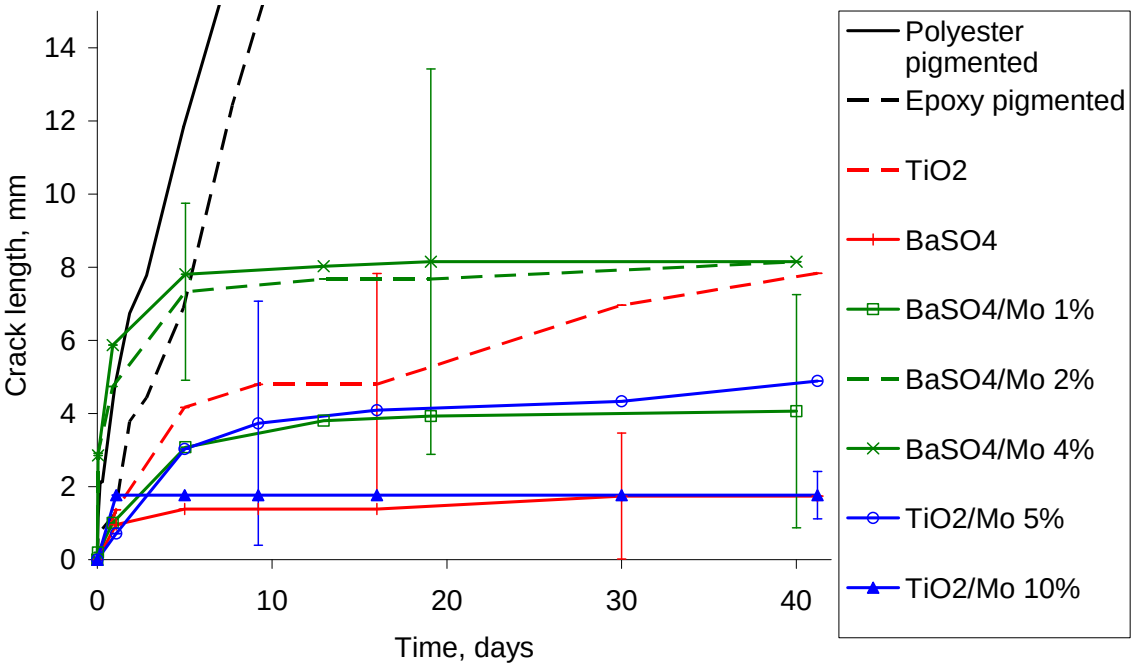

Figure 4. Average crack length vs time obtained from the wedge test of all sample variants, after the initial dry crack length is subtracted (wet growth). Typical error bars for the pretreatment-paint combinations are shown at different periods of measurement to avoid overlap. The error bars are based on data scatter in the replicate specimens of each variant only during crack growth in the climate chamber, *i.e.*, they exclude scatter from initial crack growth due to wedge insertion.

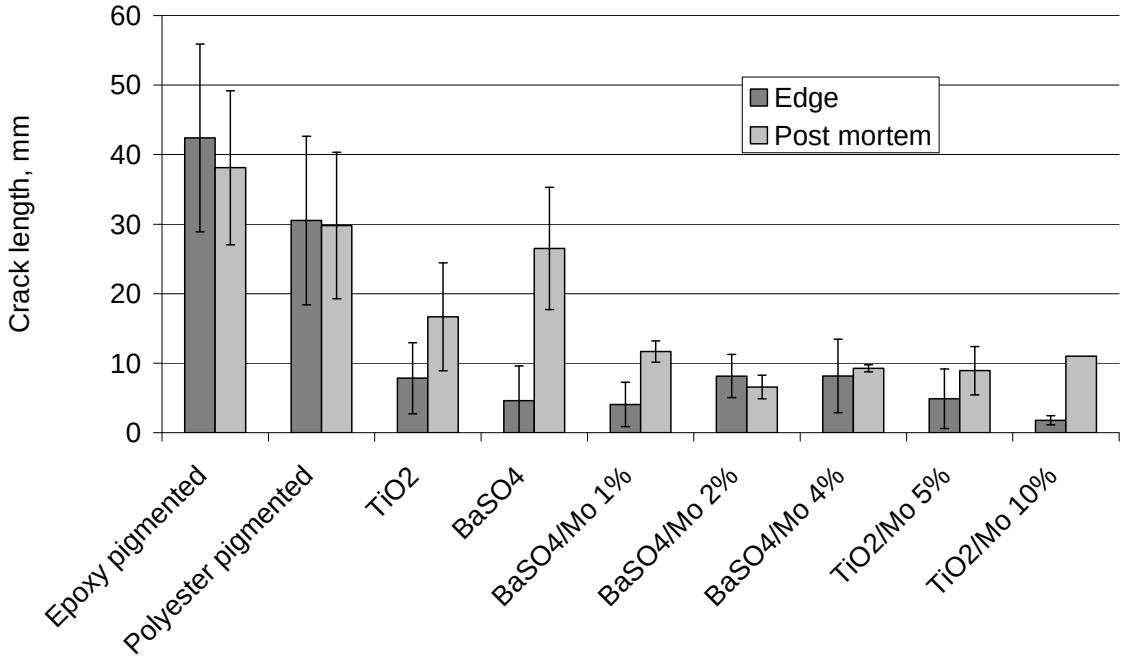

Figure 5. Steady-state crack length data as a result of exposure in the climate chamber (wet growth), determined by edge and *post mortem* measurements.

6.3.2. Failure mode.

Examples of images of crack surfaces on test specimens, which were split open mechanically after the climate chamber test, are shown in Figure 6. A significant length of most of the specimens was cracked initially by insertion of the wedge the first time, as discussed above. The typical fracture types observed can be classified as either adhesive (in the metal/polymer interface) or cohesive (inside the coating). The specimens, which were identified above as showing poor adhesion (commercial coatings and Mo-free $BaSO_4$ and TiO_2 model coatings) exhibited typical adhesive failure during climate chamber exposure (Figure 6a) and 6b), respectively), while molybdenum pigmented coatings exhibited mainly cohesive failure in the orange adhesive, as shown in Figure 6c.

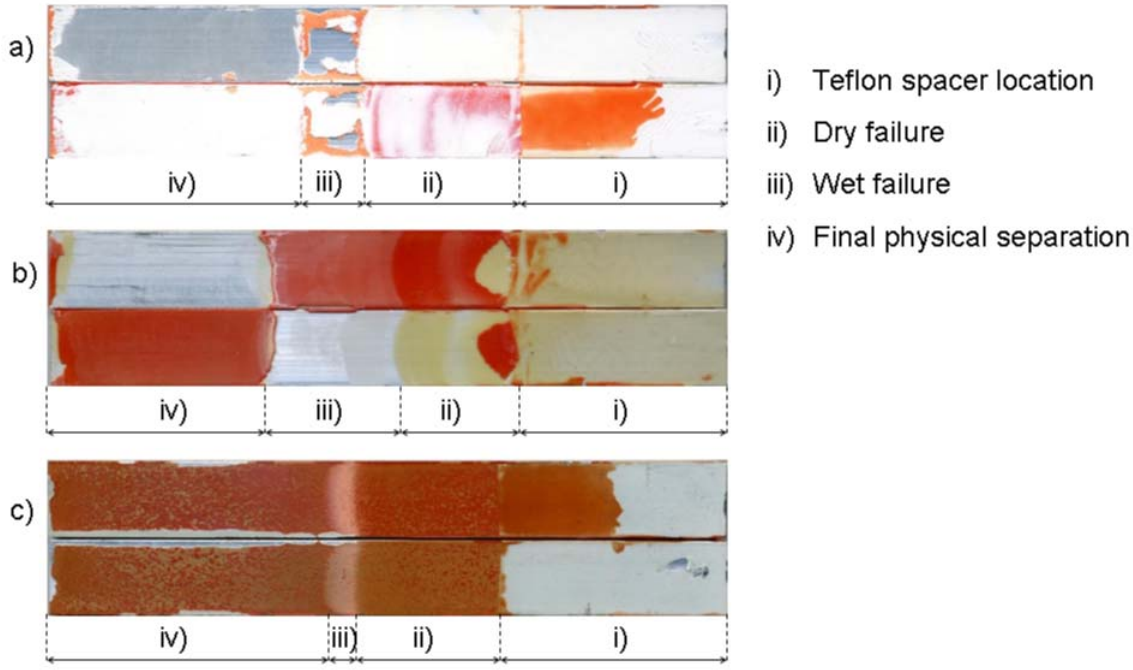

Figure 6. Images of coated aluminium specimen cracked apart after wedge test. a) Specimen with only TiO_2-pigmented coating (white), b) specimen with only $BaSO_4$-pigmented coating (yellow) and c) specimen with TiO_2/MoO_3 pigmented coating (grey). The Betamate adhesive is orange coloured. The grey colour in a) and b) is related to metallic aluminium.

Since most of the specimen variants exhibited more than one type of failure mode, fraction of failure mode for each variant was determined quantitatively by visual separation of the areas of different failure modes and manual area measurement. Figure 7 shows the average percentage of fracture modes for each pre-treatment-coating combination. The error bars indicate the average standard deviation of scatter among the replicate specimens. The results reconfirm that the initial dry growth phase was mainly cohesive for all specimens. Figure 7 verifies also that the molybdenum pigmented coatings exhibited mainly cohesive failure during the wet exposure phase. All coatings without molybdenum oxide showed a mode change from cohesive failure in dry conditions to adhesive failure in wet conditions, implying unfavourable adhesion properties. This finding along with the short crack growth during wet exposure may suggest that the positive effect of MoO_3 is promising for further work. The cohesive failure mode is commonly regarded as acceptable adhesion for practical purposes [32].

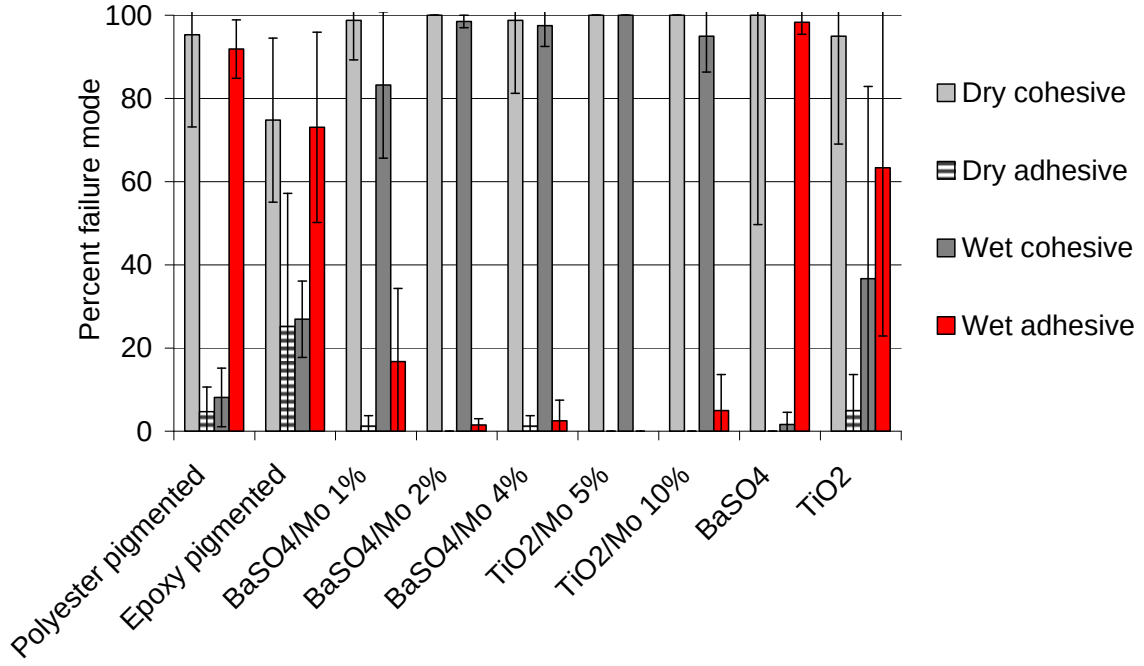

Figure 7. *Post mortem* evaluation of the fractured surfaces to determine the mode of failure during the wedge test, showing the percentage of crack growth mode in both dry and wet phases.

6.3.3. Corrosion test.

Corrosion test results, shown in Figure 8, indicate that all the model coatings, except for the TiO_2 pigmented one, showed filiform corrosion (FFC) attacks over 2 mm in length. The molybdenum oxide pigmented coatings did not give appreciable improvement against filiform corrosion, in contrast to the known behaviour of chromate pigmented coatings [7]. Thus, molybdate did not show evidence of the self-healing property of chromate in organic coatings [7, 40]. It is possible that the stability of MoO_3 in the acidic electrolyte of the FFC filament tip is a disadvantage in this case since the soluble MoO_4^{2-} needed for oxide repair on the metal cannot form. Reduction of a soluble Mo(VI) species such as MoO_4^{2-} is needed for oxidising the aluminium surface and/or precipitating a stable Mo(III) oxide to give the necessary protection. These processes are thermodynamically not possible [18]. However, FFC attacks were reduced slightly, compared to the commercial systems studied in this work, probably because of enhanced adhesion.

The present results demonstrated that improved adhesion is beneficial, but it does not necessarily result in significantly improved corrosion resistance.

The results also show that the adhesion and corrosion properties of coatings on an aluminium substrate can be distinguished to an appreciable extent and therefore can be investigated separately. The wedge test methodology used here appears to be well suited for investigating adhesion without significant interference from corrosion effects.

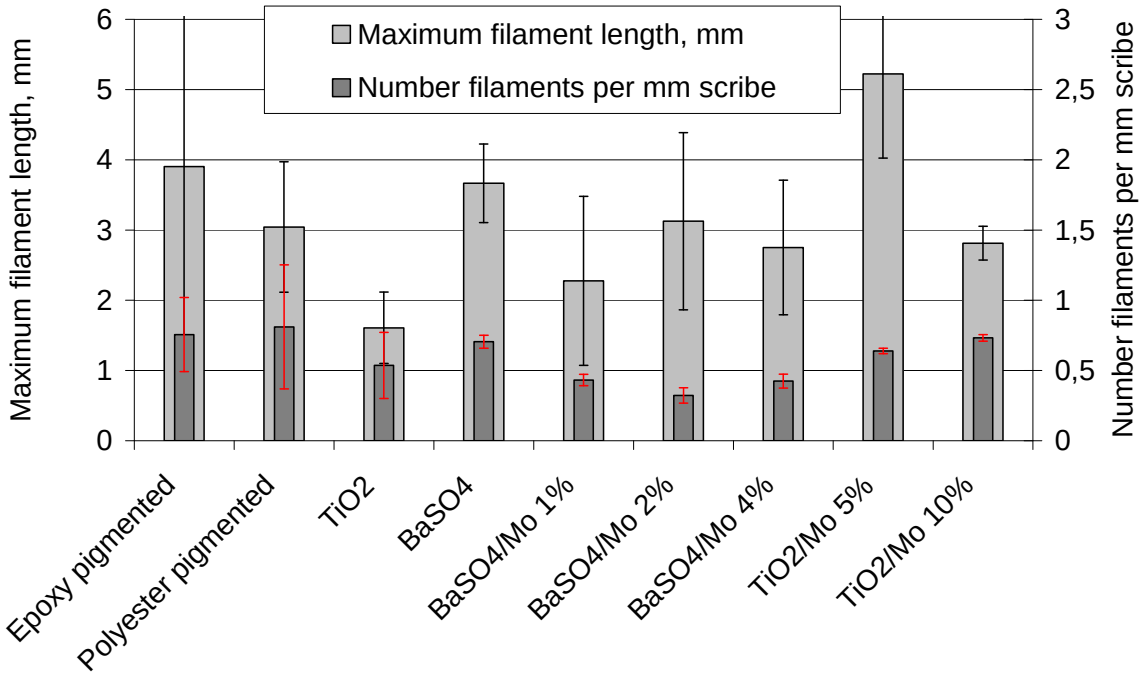

Figure 8. Results from the corrosion test in terms of filament density and maximum filament length. Maximum filament length longer than 2 mm was considered as a sign of significant susceptibility to filiform corrosion according to common procedure [10]. Error bars indicate the standard deviation in the data for 4 replicates of each coating/pre-treatment combination.

6.3.4. pH test.

The results shown in Figure 9 indicate that the water pH stabilized around 4-5 after 7 day immersion of the molybdate containing coatings. The other coatings gave pH around 8. It is clear, when compared to model coatings containing either TiO_2 or $BaSO_4$ alone, that the reduced pH was due to MoO_3. It can be concluded therefore that the role of the molybdate pigment in the reduction of the coating pH to a value at which the surface oxide is at its maximum thermodynamic stability is an important factor in improving the adhesion of the coating to the aluminium surface.

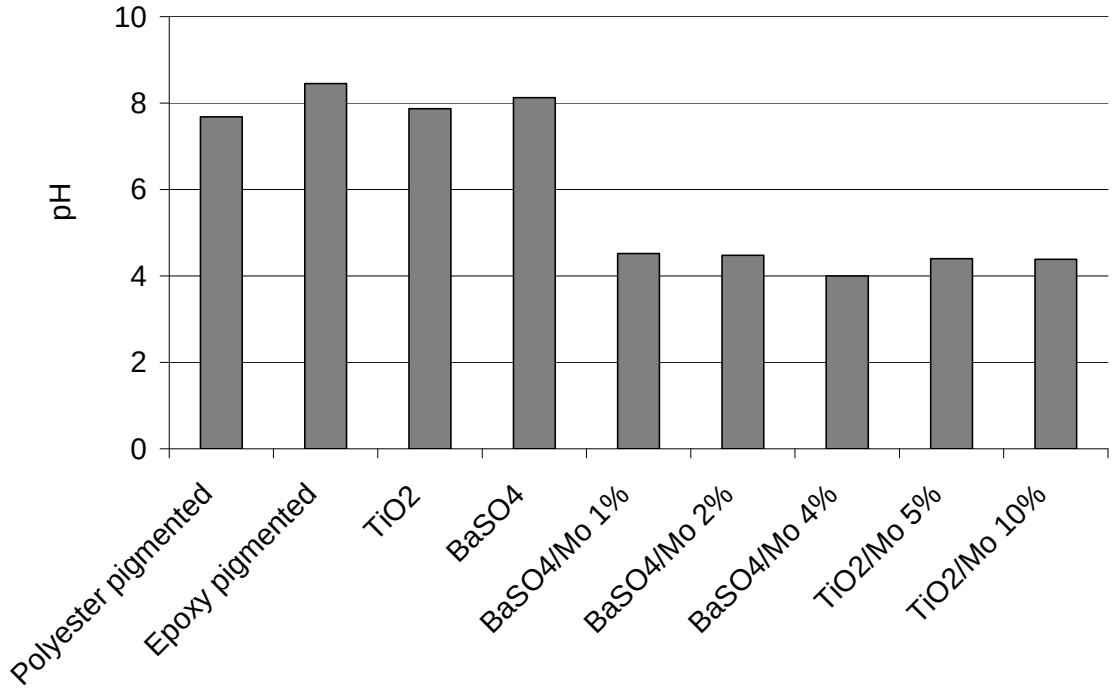

Figure 9. pH measured in CO_2-free water after exposure of free coating films for 7 days.

6.3.5. ICP-MS.

The results from ICP-MS measurements for the commercial coatings, summarised in Figure 10, showed that both $CaCO_3$ and $BaSO_4$ were present in both coatings. Mg was found in the red-pigmented coating, probably from the colour pigment. Large amount of Ti was present in the white polyester. These findings verified that the pigmented commercial coatings were produced with pigments that maintain alkaline pH.

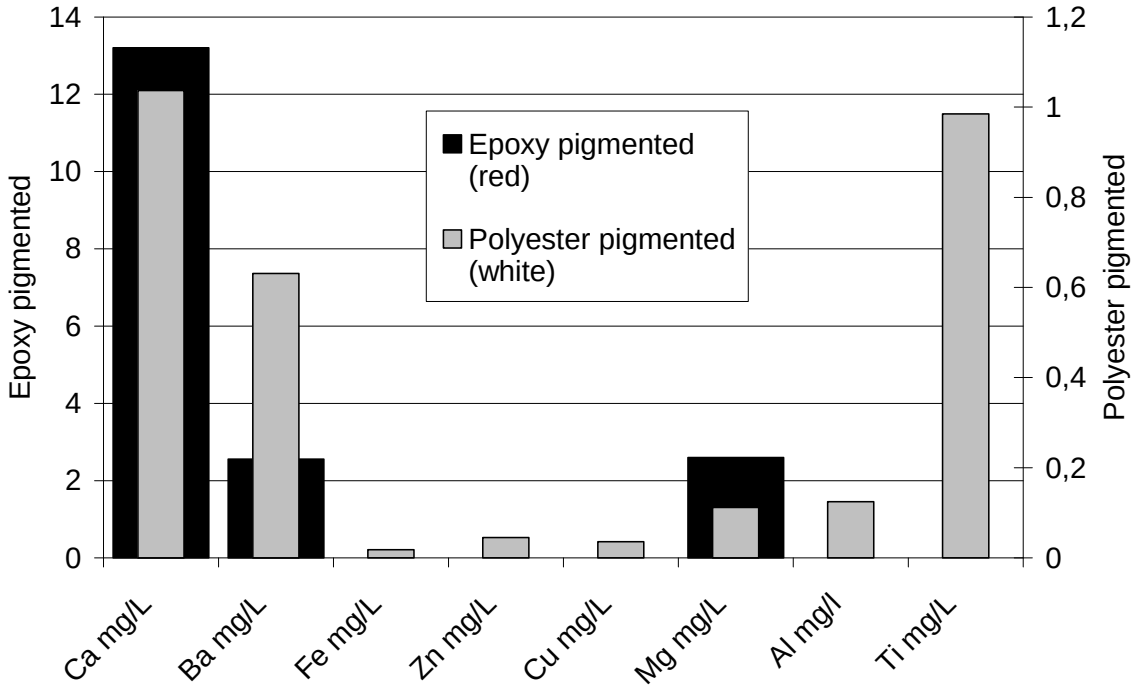

Figure 10. Composition of metallic elements expected in pigments in the commercial polymeric coatings measured by ICP.

6.4. Conclusions

- Acidic pigments, such as MoO_3 investigated in this work, can enhance the adhesion of coatings on deoxidised aluminium surface and eliminate the need for conversion coatings.
- Molybdate in the coating buffers the coating pH at a slightly acidic value, at which the naturally formed aluminium oxide has its maximum stability. This property is considered as an important factor in adhesion promotion.
- Commercial coatings produced for steel are not compatible with the aluminium surface because they include pigments which stabilize the coating pH at values higher than 8, at which aluminium oxide is unstable. This is not a beneficial condition for satisfactory adhesion of organic coatings on aluminium.
- Molybdate additions did not improve the filiform corrosion resistance of the model coatings investigated in relation to commercial powder coatings used as control cases.
- Enhanced adhesion of the coating to the aluminium substrate does not necessarily provide improved corrosion properties.

- Wedge test methodology developed in this work enables distinguishing the adhesion properties of the coating – aluminium substrate interface without significant interference from corrosion effects.

Acknowledgements

Nilufer Dibhil and Steve Kempes (Jotun Powder Coatings) contributed to the production and formulation of the model coatings. John Erik Lein and Nils-Inge Nilsen (SINTEF) assisted with the specimen preparations. This work was part of a research program entitled "Light Metal Surface Science", supported by The Norwegian Research Council, Hydro Aluminium, Jotun Powder Coatings AS and DuPont Powder Coatings.

6.5. References

1 O. Lunder, J. C. Walmsley, P. Mack and K. Nisancioglu, *Corrosion Science* **47**, p. 1604. (2005).
2 J. V. Kloet, W. Schmidt, A. W. Hassel and M. Stratmann, *Electrochimica Acta* **49**, p. 1675. (2004).
3 J. Zhao, L. Xia, A. Sehgal, D. Lu, R. L. McCreery and G. S. Frankel, *Surface and Coatings Technology* **140**, p. 51. (2001).
4 M. Kendig, S. Jeanjaquet, R. Addison and J. Waldrop, *Surface and Coatings Technology* **140**, p. 58. (2001).
5 G. W. Critchlow and D. M. Brewis, *International Journal of Adhesion and Adhesives* **16**, p. 255. (1996).
6 G. W. Critchlow, K. A. Yendall, D. Bahrani, A. Quinn and F. Andrews, *International Journal of Adhesion and Adhesives* **26**, p. 419. (2006).
7 T. Prosek and D. Thierry, *Progress in Organic Coatings* **49**, p. 209. (2004).
8 T.-C. Aw, *Regulatory Toxicology and Pharmacology* **26**, p. S8. (1997).
9 S. A. Katz and H. Salem, *The Science of The Total Environment* **86**, p. 53. (1989).
10 O. Ø. Knudsen, Bjørgum, A., Tanem, B.S., *ATB Metallurgie* **43**, p. 175. (2003).
11 K. Y. I. Oleinik S.V., *Protection of metals* **43**, p. 391. (2006).
12 O. O. Knudsen, B. S. Tanem, A. Bjorgum, J. Mardalen and M. Hallenstvet, *Corrosion Science* **46**, p. 2081. (2004).
13 A. Bjørgum, F. Lapique, J. Walmsley and K. Redford, *International Journal of Adhesion and Adhesives* **23**, p. 401. (2003).
14 B. D. Voevodin N., Balbyshev V., Khramov A., Johnson J., Mantz R., *Materials Performance (NACE Tri-Service Conference, Orlando, Florida, USA 2005)*, p. 48. (2006).

[15] O. Lunder, F. Lapique, B. Johnsen and K. Nisancioglu, *International Journal of Adhesion and Adhesives* **24**, p. 107. (2004).

[16] B. Tepe and B. Gunay, *Progress in Organic Coatings* **62**, p. 134. (2008).

[17] G. M. Scamans, Afseth, A., Remmers, U., van der Meer, W., Hallenstvet, M., Eschauzier, F., Katzgerman, L., Nisancioglu, K., *ECCA General Meeting, 27-30 May 2001*, edited by B. European Coil Coating Association, Belgium, Budapest, Hungary, 2001),c

[18] M. Pourbaix, *Atlas of electrochemical equilibria in aqueous solutions,* National Assocation of Corrosion Engineers, Houston Texas, USA, (1974).

[19] S. A. Kulinich, A. S. Akhtar, D. Susac, P. C. Wong, K. C. Wong and K. A. R. Mitchell, *Applied Surface Science* **253**, p. 3144. (2007).

[20] V. Moutarlier, B. Neveu and M. P. Gigandet, *Surface & Coatings Technology* **202**, p. 2052. (2008).

[21] A. S. Hamdy, *Progress in Organic Coatings* **56**, p. 146. (2006).

[22] V. Moutarlier, M. P. Gigandet, L. Ricq and J. Pagetti, *Applied Surface Science* **183**, p. 1. (2001).

[23] V. Moutarlier, M. P. Gigandet, J. Pagetti and L. Ricq, *Surface and Coatings Technology* **173**, p. 87. (2003).

[24] M7829: *Material Safety Data Sheet; Molybdenum-tri-oxide*. J.T. Baker (2006).

[25] A. J. Kinloch, *Adhesion and Adhesives: Science and Technology,* Chapman and Hall, London, (1990).

[26] K. B. Armstrong, *International Journal of Adhesion and Adhesives* **17**, p. 89. (1997).

[27] R. P. Digby and D. E. Packham, *Int. J. of Adhesion and Adhesives* **15**, p. 61. (1995).

[28] J. P. Sargent, *International Journal of Adhesion and Adhesives* **25**, p. 247. (2005).

[29] J. Cognard, *International Journal of Adhesion and Adhesives* **6**, p. 215. (1986).

[30] J. Cognard, *The Journal of Adhesion* **20**, p. 1. (1986).

[31] J. K. Jethwa and A. J. Kinloch, *The Journal of Adhesion* **61**, p. 71. (1997).

[32] J. A. Marceau, Y. Moji and J. C. McMillian, *Adhesives Age* **20**, p. 28. (1977).

[33] *European Standard EN 3665. Filiform corrosion resistance test on aluminium alloys*. (1997).

[34] H. Leth-Olsen, *Institute of materials science* (NTNU, Trondheim, Norway, 1996),c

[35] B. E. Maxwell, R. C. Wilson, H. A. Taylor, D. E. Williams, W. Farnham and J. Tria, *Progress in Organic Coatings* **43**, p. 158. (2001).

[36] S. Jahromi, B. Mostert, A. Derks and F. Koldijk, *Progress in Organic Coatings* **48**, p. 183. (2003).

[37] R. S. Lambourne, T.A., *Paint and surface coatings. Theory and practice* Woodhead Publishing Ltd, Cambridge, UK, (1999).

[38] ASTM 3762-03, *Standard Test Method for Adhesive-Bonded Surface Durability of Aluminum (Wedge Test)*, ASTM international, West Conshohocken, USA, (2008).

[39] O. Ø. Knudsen, Rodahl, S., Lein, J.E., *ATB Metallurgie* **45**. (2006).

[40] M. W. Kendig, A. J. Davenport and H. S. Isaacs, *Corrosion Science* **34**, p. 41. (1993).

7. Discussion

The purpose of this Chapter is to provide an overall discussion of the significance of the results presented in Chapters 3-6 in relation to the existing knowledge in the area of wet adhesion of organic coatings on aluminium and the objectives of the present work. Based on this discussion, it is intended to suggest possibilities for further development on the subject of coating adhesion testing, coating - pre-treatment compatibility and adhesion promoting pigmentation.

7.1. Adhesion tests

The original purpose of the thesis was to develop a fracture mechanical method capable of quantifying adhesion of coatings on aluminium in wet environments. The applicability of wedge and the fatigue tests, both originally developed for adhesives, were investigated. In the case of testing of adhesives, both tests, which use the double cantilever beam specimen, are known to correlate well with service exposure in humid environments due to the constant access of moisture at the crack front during the test [1, 2]. By initiating both tests under ambient conditions with subsequent exposure to moisture, the tests were intended to provide information on both the dry and wet adhesion of the coated specimen.

7.1.1. Wedge test

Quantifying adhesion by use of the wedge test proved difficult due to significant data scatter. The scatter was caused by

1. the insertion of the wedge, causing uncontrollable initial crack growth with large data scatter. The use of a Teflon spacer improved the reproducibility of duplicate test samples but still the scatter was significant.
2. pores in the polymer, which caused variable stresses in the coating and uneven crack growth. The pore density varied with coating formulation and curing mechanism. Porosity was reduced in the procedure used in Chapter 6, by complete curing of the coating before two identically coated surfaces were glued together by use of an adhesive.

3. the measurement of crack propagation by inspection using a microscope on the specimen edge. The exact location of the crack front was difficult to detect, which resulted in uncertainties in crack length measurements.

Improvement in crack length measurement was obtained by *post mortem* analysis. *Post mortem* data proved useful together with the edge readings obtained during the test. The original intention was to present the wedge test data in the same way that the fatigue data was presented, using a plot of strain energy release rate G against crack velocity. However, with the *post mortem* procedure, the crack velocity as a function of time could not be determined. Optical image correlation with displacement markers [3] can possibly used as an alternative method to monitor crack growth more accurately.

Post mortem results provided a clear distinction between dry and wet adhesion compared to evaluation based on crack lengths measured from the specimen edge. The failure region changed from cohesive in dry conditions to adhesive in wet conditions in the case of poor paint adhesion. For well adhering pre-treatment-coating systems, the cohesive failure mode continued to be observed also in the wet condition. However, the fracture surface was brighter than the dry fracture surface, possibly because the polymer was stretched more before it failed during the wet exposure. The only conclusion about the performance of such systems is then that the adhesion forces are larger than the cohesive forces in the coating. This result is satisfactory for many applications, provided that the coating cohesion is at an acceptable level.

The wedge test is a simple and reliable method for investigating coating performance, provided that the applied stress is not too high to cause specimen failure at a too early stage of the test. The test discriminates qualitatively between the poor and better performing specimens. Data scatter makes detection of smaller differences in the adhesion of pre-treatment-coating systems, as discussed above. Possible improvements are listed in section 7.5.

7.1.2. Fatigue test

The results from the fatigue test were expected to provide a similar ranking of the pre-treatment/coating combinations as tested for the wedge test.

However, the results were strikingly different. With the exception of the hot AC anodised specimens, no significant effect of moisture was detected on crack propagation. As a result most failures were cohesive in the paint. This suggests that the fatigue test frequency was too high to allow water penetration into the crack. This is further supported by the fact that crack lengths obtained for the deoxidised specimen were comparable under similar conditions to those for the specimen treated with conversion coatings. A similar result was obtained from the wedge test in dry conditions, supporting this conclusion.

The choice of frequency (6 Hz) used in this work was based on the value reported for fatigue testing of adhesives in the literature [4-8] and by Hydro Aluminium at Karmøy, where the experiments were performed [9]. The frequency used for adhesives is apparently not applicable for coatings. Total immersion of the specimen in water is probably necessary instead of climate chamber exposure as is the standard procedure in the work by Kinloch and coworkers [4, 8, 10]. The test frequency should also be reduced. The frequency used by that group is 5Hz. Even lower values may have to be considered for testing of organic coatings.

In short, it is believed that the fatigue test can be developed into a valuable quantitative test for organic coatings, in line with the fatigue test for adhesives, by introducing a few improvements, as will be discussed further below. Analogous to the fracture mechanical test for studying stress corrosion cracking and corrosion fatigue of metals, parallel application of improved constant strain/load and fatigue tests as wet adhesion tests for coated interfaces is believed to reveal different mechanisms and conditions of failure for a more comprehensive evaluation of wet adhesion.

7.2. Pre-treatment – coating compatibility

Ti/Zr based pre-treatments are technically and commercially promising alternatives to chromating [11]. The corrosion resistance of the combination Ti/Zr treatment and polyester coating was equivalent to those of hot AC anodised and chromated aluminium specimens discussed in Chapter 3. Ti/Zr treatment – epoxy combination performed as poorly as the deoxidised specimens. The compatibility between Ti/Zr treatment and polyester coating was attributed to the existence of strong bonding between the Ti/Zr coating and polyester as compared to that between Ti/Zr coating

and epoxy in Chapter 5. The results were, however, inconclusive for the Ti/Zr pre-treatment in view of the uncertainties with the characterisation data, as discussed in Chapter 5. In future work the role of hydration in wet adhesion failure should be investigated, in particular for the Ti/Zr treated surfaces [12]. Hydration resistance has been addressed as a reason for improved adhesion of organic coatings on Ti/Zr-pre-treated aluminium [13].

The adhesion properties of polyester and epoxy coatings on the hot AC oxidised surface were equally satisfactory according to the wedge test. The two coatings penetrated the pores of the oxide to the same degree, as shown in Chapter 5, which is one explanation of similar and superior adhesion properties. Another possible factor for the superiority of hot AC anodising is the effective removal of the noble intermetallic particles, which act as stress raisers for crack propagation and cathodic sites for filiform corrosion. In contrast, the intermetallics, which remain on the surface after Ti/Zr treatment, are coated with a thick layer of Ti/Zr oxides [11], which is probably brittle. The intermetallics acting as stress raisers and the brittle Ti/Zr oxide coating can be regarded as factors which would enhance adhesive crack initiation and growth on Ti/Zr-treated specimens.

The present result, that the hot AC anodised specimen was more susceptible to the fatigue test compared to the other pre-treatments, is difficult to explain, and it requires further study. Anodised aluminium should possibly be used with care in the presence of a cyclic load.

Despite the differences discussed above, all pre-treatments showed acceptable wet adhesion behaviour when compared to the unacceptable behaviour of the deoxidised specimens. The corrosion behaviour was really the criterion, which distinguished the performance of the pre-treatments under wet corrosive conditions (Section 7.3). However, all surface conditions, including deoxidised only, were found equally resistant to adhesion failure under dry conditions. For dry conditions it appears therefore that degreasing and deoxidising, without the need for a conversion coating, are sufficient, especially if the organic coating used is of acceptable quality.

7.3. Corrosion test

If the coated aluminium surface will be exposed to a corrosive environment in service, especially a chloride containing environment, this work indicates that a corrosion test is necessary in addition to a wet adhesion test. The filiform corrosion test (FFC) [14] used in this work is regarded as a reliable accelerated test since it correlates well with long term field tests in general. Based on the present results, it can be argued further that the filiform corrosion test is sufficient to qualify an alloy - pre-treatment - coating combinations for service in atmospheric exposure. It appeared that a given alloy - pre-treatment - coating combination, which was resistant to corrosion was also resistant to adhesive failure, as demonstrated by the AC-anodised and chromated specimens. The specimen, which were resistant to adhesion failure, could fail the corrosion test, such as the Ti/Zr-polyester combination and molybdate-pigmented coating. However, this conclusion is based on a limited selection of pre-treatment-coating combinations, and it is based on the wedge test results as the adhesion test. FICARP conclusions indicated, in contrast, that corrosion resistant surfaces were not necessarily resistant to adhesion failure and adhesion promoters may be necessary [15, 16].

7.4. Acidic pigments

This work demonstrated that coatings, which are essentially developed for the steel surface and contain alkaline pigments, are not compatible with the aluminium surface. It was demonstrated further that coatings with acidic pigments are more compatible as adhesion promoters for the aluminium surface. These findings indicate an important starting point for the development of coatings and pre-treatments, which are compatible with the aluminium surface. The molybdate pigments tested in Chapter 7 gave a significant improvement in the adhesion properties of polyester primid coating on aluminium. However, the corrosion protection expected, analogous to the corrosion-inhibitive protection provided by the chromate coating was not obtained. The causes need to be investigated further along with studies of other candidate oxides, such as vanadates, which are stable at higher pH than Al [17]. Oxo-compounds of both V and Mo can form stable poly-oxo-metallates with each other, phosphates or tungstates [17]. In combination with other metals these elements have proved to actively

inhibit corrosion of aluminium [17]. These materials should therefore be investigated further.

7.5. Further work

7.5.1. Adhesion testing

In preparing the specimens, we showed that (Chapter 6) complete curing of the coating before the beams are glued together with a suitable adhesive is a good measure to ensure low porosity of the coating, comparable to an actual coated product. Pores will act as stress raisers which can speed up crack growth rate.

One obvious improvement of the wedge test would be sensitive control of wedge insertion and thereby the initial cracking. Crack initiation by fatigue, as in the analogous stress corrosion cracking test [18, 19], is recommended. Instead of using a wedge for straining the DCB specimen, the use of bolts, or even better, a tensile stress instrument, equipped with a load cell, would give significant improvements.

Crack length measurement can be improved by use of *post mortem* analysis, optical image correlation with zero displacement markers [3] or other suitable methods. The failure mode should always be determined.

In the fatigue test, the dry test should be performed for longer time periods, before moisture is introduced, for distinguishing the effect of water more easily. Dry and wet tests can also be separated completely by using separate specimens for each [8, 20]. The humidity level should be increased, or samples should be immersed in water, as discussed above [4, 8, 10]. The test frequency should be decreased and optimised for coatings in relation to the levels normally used for testing adhesives. Too low frequencies should however be avoided to prevent creep in the polymer [9, 21].

To obtain a more comprehensive validation of the wedge and fatigue test methods, a larger variety of pre-treatment - paint combinations should be tested.

7.5.2. Crack surface characterisation

In future work evidence of hydration or other detrimental effects of water should be investigated [12]. The location of the coating remnants should be mapped out in sufficient detail to understand the significance of localised adhesion. The effect of intermetallic particles in this respect need to be investigated further. Another relatively unknown subject is the changes postulated to occur in the coating structure and chemistry near the metal surface and its effect on the adhesion properties of the interface. Boundary layers, which are enriched in nitrogen, formed in the epoxy coating near the metal surface are known to cause cohesive failure close to the interface [22]. Concentration changes of adhesion promoters, such as phosphonates [23] and silanes [24], have also been observed in the coating approaching the metal surface. Characterisation of such layers can reveal interesting information about their formation as a result of interactions between the oxide and the polymer components and how the bonds at the polymer-metal interface weaken in presence of moisture.

7.6. References

1. B. B. Johnsen, PhD Thesis, in *Institute of Materials Science*, Norwegian University of Technology and Science (2004).
2. J. A. Marceau, Y. Moji and J. C. McMillian, *Adhesives Age*, **20**, p. 28 (1977).
3. J. P. Sargent, *International Journal of Adhesion and Adhesives*, **25**, p. 247 (2005).
4. A. J. Kinloch, M. S. G. Little and J. F. Watts, *Acta Materialia*, **48**, p. 4543 (2000).
5. I. A. Ashcroft and S. J. Shaw, *International Journal of Adhesion and Adhesives*, **22**, p. 151 (2002).
6. H. Hadavinia, A. J. Kinloch, M. S. G. Little and A. C. Taylor, *International Journal of Adhesion and Adhesives*, **23**, p. 449 (2003).
7. A. Pirondi and G. Nicoletto, *Engineering Fracture Mechanics*, **71**, p. 859 (2004).
8. J. K. Jethwa and A. J. Kinloch, *The Journal of Adhesion*, **61**, p. 71 (1997).
9. J. A. Harris and P. A. Fay, *International Journal of Adhesion and Adhesives*, **12**, p. 9 (1992).
10. D. J. Bland, A. J. Kinloch, V. Stolojan and J. F. Watts, *Surface and Interface Analysis*, **40**, p. 128 (2008).
11. O. Lunder, C. Simensen, Y. Yu and K. Nisancioglu, *Surface and Coatings Technology*, **184**, p. 278 (2004).

12. L. Fedrizzi, F. J. Rodriguez, S. Rossi, F. Deflorian and R. Di Maggio, *Electrochimica Acta*, **46**, p. 3715 (2001).
13. R. Comrie, PhD Thesis, in *Department of Pure and Applied Chemistry*, University of Strathclyde, Glasgow, UK (1998).
14. European Standard EN 3665. Filiform corrosion resistance test on aluminium alloys, in *Test methods for paints and varnishes* (1997).
15. G. M. Scamans, Afseth, A., Remmers, U., van der Meer, W., Hallenstvet, M., Eschauzier, F., Katzgerman, L., Nisancioglu, K., in *ECCA General Meeting, 27-30 May 2001*, B. European Coil Coating Association, Belgium Editor, Budapest, Hungary (2001).
16. A. Afseth, J. H. Nordlien, G. M. Scamans and K. Nisancioglu, *Corrosion Science*, **44**, p. 2491 (2002).
17. M. Kendig, Buchheit, R.G., *Corrosion*, **59**, p. 379 (2003).
18. A. K. Roy, D. L. Fleming, D. C. Freeman and B. Y. Lum, *Micron*, **30**, p. 649 (1999).
19. S. Mostovoy, H. R. Smith, R. G. Lingwall and E. J. Ripling, *Engineering Fracture Mechanics*, **3**, p. 291 (1971).
20. M. W. Rushforth, P. Bowen, E. McAlpine, X. Zhou and G. E. Thompson, *Journal of Materials Processing Technology*, **153-154**, p. 359 (2004).
21. D. Plausinis and J. K. Spelt, *International Journal of Adhesion and Adhesives*, **15**, p. 143 (1995).
22. S. J. Hinder, C. Lowe, J. T. Maxted, C. Perruchot and J. F. Watts, *Progress in Organic Coatings*, **54**, p. 20 (2005).
23. K. Wapner, M. Stratmann and G. Grundmeier, *International Journal of Adhesion and Adhesives*, **28**, p. 59 (2008).
24. M.-L. Abel, J. F. Watts and R. P. Digby, *International Journal of Adhesion and Adhesives*, **18**, p. 179 (1998).

8. Conclusions

- The necessity of using chromate-free pre-treatments will require a closer look at the specificity and durability of new pre-treatment - paint combinations, which will in turn require the availability of reliable test methods. The absence of robust pre-treatments to replace chromating, with the exception of hot-AC anodising, requires validation of the compatibility of the selected pre-treatments with both the selected organic coatings and the aluminium substrate in terms of wet adhesion and corrosion resistance.

- Wet adhesion of coated metal specimen can be assessed by use of fracture mechanical techniques developed for adhesives, with certain modifications introduced to compensate for the reduced cohesion and adhesion strengths compared to the adhesives. In present work, the adhesion properties could only be ranked qualitatively by the modified wedge test, because of significant data scatter. The data scatter in the modified fatigue test was also too significant to obtain reliable results. The test frequency has to be decreased below the level normally used for testing of adhesives to allow the effect of water to be detectable. For both tests improvement of the crack initiation and specimen preparation is needed to obtain more quantitative results. The selection of test methods should be made on the basis of the real life exposure conditions for the product in question.

- The adhesion promotion by Ti/Zr treated aluminium depended on the type of organic coating used. Together with polyester coatings the treatment was satisfactory, while adhesion of the epoxy coatings was not satisfactory. Cohesive failure of the polyester coated specimen, in contrast to the adhesive failure of the epoxy, suggested stronger adhesion between polyester coating and the Ti/Zr treated aluminium specimen.

- Both the polyester and epoxy coatings effectively penetrated the pores of the hot AC anodised surface. A very large area made available for adhesive bonding by nearly complete pore filling and optimal mechanical interlocking effect gave excellent adhesion properties to the AC-anodised layer – organic coating interface.

- Most organic coatings on the market, developed for steel substrates, are not compatible with the aluminium surface because they contain alkaline pigments, which are detrimental for the stability of aluminium oxide. Coatings with acidic pigments are required for aluminium, as demonstrated by a MoO_3-pigmented coating in this study.